Identification of ribosomal proteins that are necessary for fully activating the protein kinase Gcn2

A thesis presented in partial fulfilment of the requirements for the degree of Master of Science

in Biochemistry

at Massey University, Albany, New Zealand

Viviane Aleta Jochmann

2014

Abstract

The environment in which cells grow often changes rapidly and in order to survive, cells need to adjust their metabolic pathway to these changes. Vitally important for all organisms is the constant availability of amino acids as they are building blocks for proteins. Proteins are essential molecules involved in most biological processes in a cell. Yeast and mammals overcome amino acid limitation by switching on a signalling pathway named General Amino Acid Control (**GAAC**), which triggers a decrease in general protein synthesis by inhibiting translation initiation while upregulating the transcription of stress-response genes.

For sensing starvation in yeast, the GAAC requires the kinase Gcn2 and its effector protein Gcn1. Gcn2 phosphorylates the α-subunit of the eukaryotic initiation factor 2 (**eIF2α**), which ultimately induces the selective expression of stress-response genes, leading to the *de novo* synthesis of all amino acids. In order to recognize the deacylated tRNA as an immediate signal for starvation, Gcn1 and Gcn2 need to be in direct contact and associated with the translating ribosome. The current model for sensing starvation by Gcn2 suggests that deacylated tRNA enters the ribosomal A-site and Gcn1 concomitantly transfers the starvation signal to Gcn2. However, the molecular details of this process are still unclear. Deletion analysis of *GCN1,* suggested that Gcn1 has multiple contact points with the ribosome. We therefore aim to uncover ribosomal proteins that are required to fully activate Gcn2 in order to better understand the starvation recognition process. The fact that Gcn1 has many ribosomal contact points implies that the deletion of one contact point will not remove Gcn1 from the ribosome and therefore maintains Gcn2 activation. This allows us to identify Gcn1-ribosome interaction points which are not only required to position Gcn1on the ribosome but also facilitate in Gcn1 mediated Gcn2 activation per se.

Genetic studies conducted in this thesis reveal that ribosomal proteins rps18, rps26, rps28, rpl21 and rpl34 are necessary for full Gcn2 activation. The deletion of their genes resulted in an impaired growth on starvation media and in a reduction in eIF2α phosphorylation. With these results we are able to create a first map of Gcn1 contact points of the ribosome that are necessary to promote Gcn2 activation. Two ribosomal

proteins that are necessary for fully activated Gcn2 are located on the large ribosomal subunit. Three others are located on the ribosomal head region of the small ribosomal subunit in proximity to the A-site region. Considering that Gcn1 is a large protein, our results support the idea that Gcn1 has multiple contact points with the ribosome and that some important contact points for Gcn2 activation are located near the ribosomal A-site.

Acknowledgements

In this space I would like to sincerely thank all the people who contributed to this work.

I would like to begin with my supervisor Dr. Evelyn Sattlegger for taking me as a master student under her supervision and therefore giving me the chance to undertake my master degree in New Zealand. Her guidance throughout my studies and her availability for critical feedback on my research project, gave me the opportunity to rise to my potential as a researcher.

Let me further extend thanks to my laboratory colleagues of my research group, Renuka Shanmugam, Michael Bolech, Rashmi Ramesh and Su Jung Lee who did not only become a family substitution but also helped with scientific discussions and applied laboratory work.

I am thanking especially people outside of my research group: Richard Cardoso da Silva, Daniela Quintana James as well as my good friends Natalia Lopez and Damien Luciano Venuto. You guys were such as big help in proof reading my thesis and to make sure that my sentence structure is not too typical German.

My special thanks goes to my family who has not just supported me financially but also encouraged me to fulfil a degree overseas and who have always been there for me from afar.

Last but not least I would like to thank my partner Marcelo. Your love and support during the last year of my studies and especially while writing up my thesis has given me power and courage to come to a good end in happy forecast of a time off with you.

I also want to thank collaborators as well as colleagues from the Sattlegger group to share unpublished data and to give me the chance to include those into my thesis.

- Yeast-two-hybrid data (Sattlegger group)
- rps10 trial study data (S.J.Lee and E.Sattlegger)
- Co-Immunoprecipitation data (R. Shanmugam and E.Sattlegger)
- Cryo-EM data (T. Budkevich and C.M. Spahn)

Table of contents

List of Figures

List of Tables

Abbreviations

In addition to the Système international d' unites (SI), the following abbreviations are used:

ABC	ATP-binding cassette
ALS	**A**ceto**l**acetate **S**ynthase
A-site	**A**cceptor-site
ATF4	**A**ctivating **T**ranscription **F**actor **4**
BSA	**B**ovine **S**erum **A**lbumin
c	**C**oncentration
Co-IP	**Co**-**I**mmuno**p**recipitation
cryo-EM	**Cryo**-**E**lectron **M**icroscopy
DMSO	Dimethylsulfoxide
EDTA	**E**thylene **D**iamine **T**etra acetic **A**cid
eEF3	**E**ukaryotic **E**longation **F**actor 3
eIF2	**E**ukaryotic **I**nitiation **F**actor 2
eIF2α-P	**E**ukaryotic **I**nitiation **F**actor 2 phosphorylated alpha subunit
eIF2B	Guanine nucleotide exchange factor
EtBr	**Et**hidium **Br**omide
E-site	**E**xit-site
GAAC	**G**eneral **A**mino **A**cid **C**ontrol
Gcn1	**G**eneral **c**ontrol **n**on-derepressible **1**
Gcn2	**G**eneral **c**ontrol **n**on-derepressible **2**
Gcn4	**G**eneral **c**ontrol **n**on-derepressible **4**
His	Histidin
HisRS	Histidyl-tRNA synthetase
kDa	Kilo Dalton
LB	**L**uria- **B**ertani
Met-tRNA$_i$	Methionyl initiator tRNA
mRNA	Messenger ribonucleic acid
NaCl	Sodium Cloride
NaOH	Sodium hydroxide
OD	**O**ptical **D**ensity
ORF	**O**pen **R**eading **F**rame

p	**P**lasmid
PAGE	**P**olyacryl**a**mide **G**el **E**lectrophoresis
PEG	**P**oly**e**thylene **g**lycol
Pgk1	3-Phosphoglycerate kinase
P-site	Peptidyl donor site
PVDF	**P**oly**v**inylidine **Dif**luoride
RNase	Ribonuclease
Rp(s/l)	**R**ibosomal **p**rotein (small/large)
rpm	**R**evolutions **p**er **m**inute
RT	**R**oom **T**emperature
SC	**S**ynthetic **C**omplete
SD	**S**ynthetic Dropout
SDS	**S**odium **D**odecyl **S**ulphate
SM	**S**ulfometuron **M**ethyl
SM^S	Sensitivity to sulfometuron methyl
Slg^-	**Sl**ow **g**rowth
TAE	**T**ris-**A**cetate **E**DTA
TBS	**T**ris-**B**uffered **S**aline
TBS-T	TBS-Tween
TC	**T**ertiary **C**omplex
TEMED	N,N,N, N- Tetramethylethylenediamine
WCE	**W**hole **C**ell **E**xtract
Y2H	**Y**east **Two H**ybrid
YPD	**Y**east extract **P**eptone **D**extrose
YPG	**Y**east extract **P**eptone **G**lycerol

1. Introduction

1.1 The General Amino Acid Control (GAAC)

Cells of all organisms are exposed to physiological and environmental stresses and need to adjust their biochemical response in order to survive. A constant availability of amino acids is vital, as they are the building blocks of proteins, essential molecules, involved in most biological processes in any cell. Yeast and mammals overcome amino acid limitation by switching on a conserved signalling pathway. Even when a single amino acid is lacking, it results in the *de novo* synthesis of all essential amino acids, in a process defined as 'General Amino Acid Control' (**GAAC**) pathway (Delforge, Messenguy, & Wiame, 1975). To activate the GAAC pathway and to overcome amino acid starvation the cell requires a stress sensor, which monitors conditions within the cell. In eukaryotes, this job is performed by the protein kinase General control non-derepressible 2**, Gcn2**, which senses uncharged tRNA (Dong, Qiu, Garcia-Barrio, Anderson, & Hinnebusch, 2000) (S. A. Wek, Zhu, & Wek, 1995) as an immediate signal of amino acid deprivation. Once it has recognised the amino acid limitation, it activates the stress response by phosphorylating the α-subunit of the eukaryotic initiation factor 2, **eIF2** (Dever et al., 1992). This in turn leads to the decrease of general protein synthesis, while increasing the expression of stress-response genes (D Tzamarias & Thireos, 1988) (Hinnebusch, 2005) including *GCN4* in yeast. General control non-derepressible 4**, Gcn4** and its mammalian homolog Activating Transcription Factor 4 **ATF4** are transcriptional activator that ensure cell viability during amino acid starvation.

1.2 Global translational arrest is caused by eIF2α phosphorylation

The GAAC pathway enables cells to immediately react to amino acid starvation. The reason for this rapid response is due to the involvement of post-translational regulation followed by an adjacent reprogramming of the cell's gene expression profile.

Under amino acid replete conditions, translation requires the formation of the ternary complex (**TC**) consisting of eIF2, GTP and the methionyl initiator-tRNA (**Met-tRNA$_i$**). The TC binds to the 40S ribosomal subunit forming the 43S-pre-initiation complex. This complex then binds to and scans the mRNA for start codons (AUG). Once the AUG codon is recognised, eIF2-GTP hydrolyses and eIF2-GDP is released. The 60S ribosomal subunit then joins in for 80S ribosome formation. With assembly of the 80S ribosome, translation is initiated (Figure 1). For another translational cycle to start, eIF2-GDP needs to be recycled into its GTP bound form by the guanine nucleotide exchange factor, **eIF2B**.

Under starvation conditions, when the GAAC is switched on, the phosphorylation of the eIF2α subunit by Gcn2 transforms eIF2 into an inhibitor of eIF2B, causing a recycling arrest of eIF2-GDP into the GTP-bound form (Pavitt, Ramaiah, Kimball, & Hinnebusch, 1998) (Figure 1). Since eIF2 is present in excess over eIF2B, the phosphorylation of a fraction of eIF2α is sufficient for drastically decreasing global protein synthesis thus reducing the consumption of amino acids.

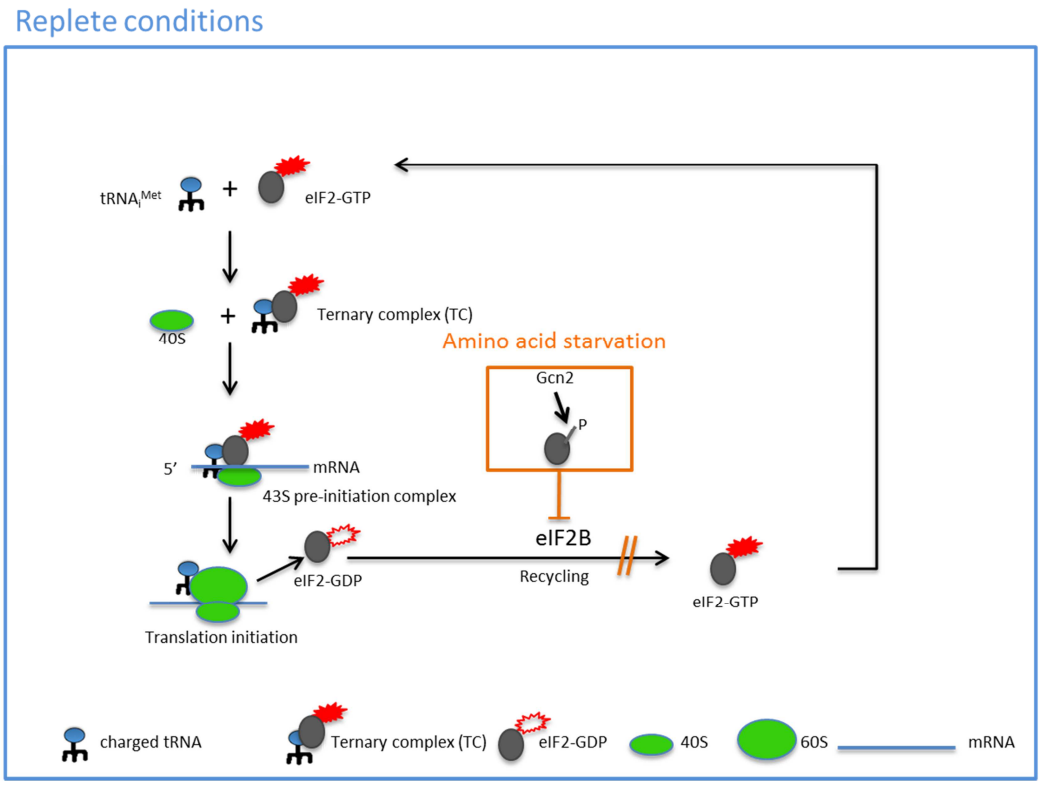

Figure 1: Translation initiation and recycling of eIF2 under amino acid replete conditions and the recycling arrest of eIF2 under amino acid starvation.

Translation depends on the formation of the ternary complex by Met-tRNAi, GTP and eIF2. This complex binds to the 40S subunit, where it builds the 43S pre-initiation complex. At the start codon of the mRNA, eIF2-GDP is released and the 60S subunit joins with the 40S complex resulting in the translating 80S ribosome. After translation is initiated, eIF2-GDP needs to be recycled by eIF2B for another initiation process. Under amino acid starvation however, this recycling comes to an arrest due to the phosphorylation of eIF2α, which impairs the recycling function of eIF2B and as a consequence decreases translation initiation and therefore global protein synthesis.

1.3 Selective translation of transcription activators that induce expression of stress-response genes

While global translation is downregulated when cells are starving, the translation of mRNA encoding for the transcriptional activator Gcn4 in yeast is upregulated. Gcn4 activates the transcription of stress-response genes (D. Tzamarias, Roussou, & Thireos, 1989) (Hinnebusch & Natarajan, 2002), some of which encode for enzymes involved in the *de novo* synthesis of amino acids. Genome wide analysis revealed that Gcn4 induces expression of nearly 1/10 of the yeast genome in amino acid

starved cells (Hinnebusch, 2005). Gcn4 selective translation under amino acid starvation is due to four unique upstream Open Reading Frames (**uORF**) in its mRNA leader sequence (D. Tzamarias et al., 1989) (Hinnebusch & Natarajan, 2002) that under replete conditions ensure low translation of *GCN4* mRNA.

Under replete conditions, the 43S pre-initiation complex scans the mRNA of *GCN4* downstream until it reaches the start codon of ORF1. The TC hydrolyses now into its eIF2-GDP form. The 60S subunit subsequently unites with the small subunit to create the 80S translating ribosome. After translation at the first ORF, the 80S ribosome separates into its two subunits and only the 40S scans down the mRNA (Hinnebusch, 2005). Due to the high abundance of TCs, most 40S subunits rebind with TCs before reaching the start codon of ORF 2, 3 or 4 where they reinitiate the translation. The ribosomes translating at ORF 2, 3 and 4 dissociate from the mRNA after translation and fail to reach the downstream start codon of *GCN4* mRNA. As a consequence Gcn4 translation is low. This state of *GCN4* expression is called "repressed".

This process differs under amino acid starvation because a lower abundance of ternary complexes results in reduced probability of 40S subunits to be reloaded with a TC when travelling downstream of ORF1. Consequently, this leads to 40S subunits bypassing ORF2, 3 and 4 (Abastado, Miller, Jackson, & Hinnebusch, 1991)(Figure 2). Since there is a long stretch of RNA between ORF4 and the downstream start codon of *GCN4*, the chance to rebind a TC and to reinitiate translation at the AUG of *GCN4* is higher. In fact, it has been shown that under amino acid starvation, 50% of all the 40S ribosomes from ORF1 bypass ORF 2, 3 and 4 and reach *GCN4* start codon (Hinnebusch, 2005). Overcoming the inhibitory effect of the uORF therefore leads to increased synthesis of Gcn4. Under these conditions *GCN4* is said to be "derepressed". In other words, the reduced level of TC, due to the phosphorylation of eIF2α, decreases 43S formation and leads to the bypass of inhibitory ORF 2, 3 and 4. This control mechanism of *GCN4* translation allows the cell to rapidly respond and to overcome amino acid deprivation.

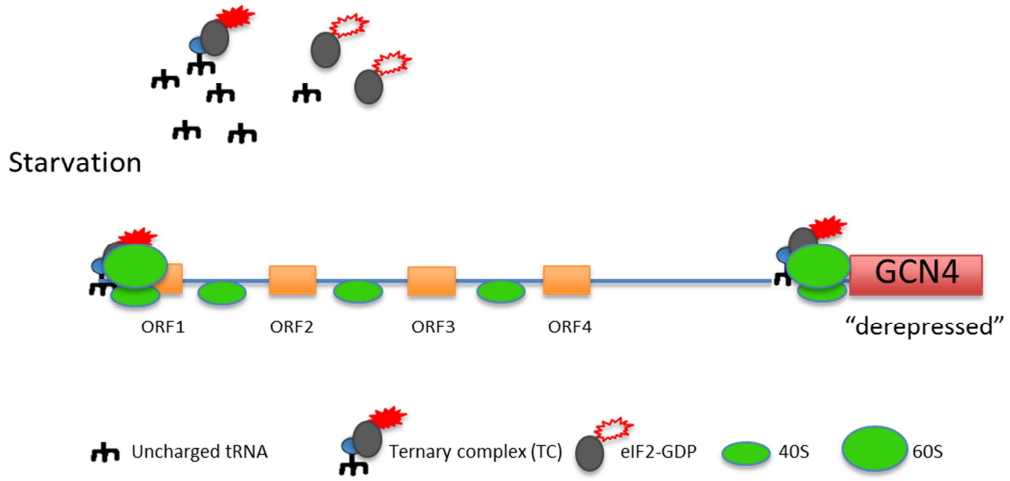

Figure 2: Schematic presentation of the selective Gcn4 translation.
Under amino acid starvation, reduced levels of ternary complexes allow scanning ribosomes to bypass ORF2, 3 and 4 and reinitiate at the start codon of *GCN4* leading to its translation. Figure 2 was modified from (Hinnebusch, 2005).

1.4 The eukaryotic eIF2α kinases

The Gcn2 kinase regulates translation in response to starvation by phosphorylating the α subunit of eIF2. However, global translation is not only reduced under amino acid starvation but also during most conditions of stress. Regulated by different stress stimuli, eIF2α can be phosphorylated by four different eIF2α kinases in mammals (De Haro, Mendez, & Santoyo, 1996; Hinnebusch, 2005):

- **H**eme **R**egulated **I**nhibitor (**HRI**), activated under heme deficient conditions (De Haro et al., 1996)
- Double strand **R**NA dependent **P**rotein **K**inase (**PKR**) activated by viral infection (Berlanga et al., 2006)
- **P**KR like **E**ndoplasmatic **R**eticulum **K**inase (**PERK**) activated by unfolded proteins in the endoplasmatic reticulum (Shi et al., 1998)
- **G**eneral **C**ontrol **N**on-derepressible-**2** (**Gcn2**) activated by amino acid starvation (Berlanga, Santoyo, & de Haro, 1999) (Dever et al., 1992), UV irradiation (Deng et al., 2002) and RNA viruses (Berlanga et al., 2006)

These four kinases have a conserved kinase domain in common, with sequences characteristic of an eIF2α protein kinase, but differ in the other domains (Hinnebusch, 2005). These unique domains, enables each kinase to specifically react to different type of stresses while resulting in the same downstream effect: the phosphorylation of eIF2α and consequently *GCN4* translation.

1.4.1 The kinase Gcn2

Gcn2 is the only eIF2α kinase that is present in all eukaryotes and its ubiquitous function is to sense amino acid starvation. Under amino acid replete conditions Gcn2 is present as an inactive dimer. In amino acid starved cells uncharged tRNA accumulates and hereby activates Gcn2 by binding to its regulatory domain, called HisRS domain as it resembles histidyl- tRNA synthetase (S. A. Wek et al., 1995). This domain is identified to bind uncharged tRNA (Dong et al., 2000) with a higher affinity than charged tRNA (Dong et al., 2000). Binding of the uncharged tRNA to HisRS-like domain induces a conformational change within Gcn2 (Dong et al., 2000). This stimulates its kinase domain and evokes auto-phosphorylation of the adjacent kinase domain (KD), subsequently leading to the phosphorylation of eIF2α (Hinnebusch, 2005). Upstream of its kinase domain, Gcn2 accommodates another domain containing kinase motifs but lacking certain characteristically sequences of kinases; hence, it is enzymatically inactive and is therefore called pseudo kinase domain (ΨKD). The function of this incomplete kinase domain is not yet completely understood but was shown to be crucial *in vivo* for Gcn2 activation (R. C. Wek, Ramirez, Jackson, & Hinnebusch, 1990). In yeast, it has been shown that Gcn2 associates with ribosomes and polyribosomes and that this binding is crucial for its activation (Sattlegger & Hinnebusch, 2005). This interaction *in vivo* requires the C-terminal fragment of Gcn2 (Figure 3) (Ramirez, Wek, & Hinnebusch, 1991) which also contains the dimerization determinants. Gcn2 N-terminal domain is highly conserved and recognized to be required for an interaction with a protein called General control non-derepressible 1 (**Gcn1**) (Garcia-Barrio, Dong, Ufano, & Hinnebusch, 2000)**,** which resides in a complex with the protein, General control

non-derepressible 20 (**Gcn20**) (de Aldana, Marton, & Hinnebusch, 1995). The interaction between Gcn2 and Gcn1 is required for Gcn2 function *in vivo* (Sattlegger & Hinnebusch, 2000).

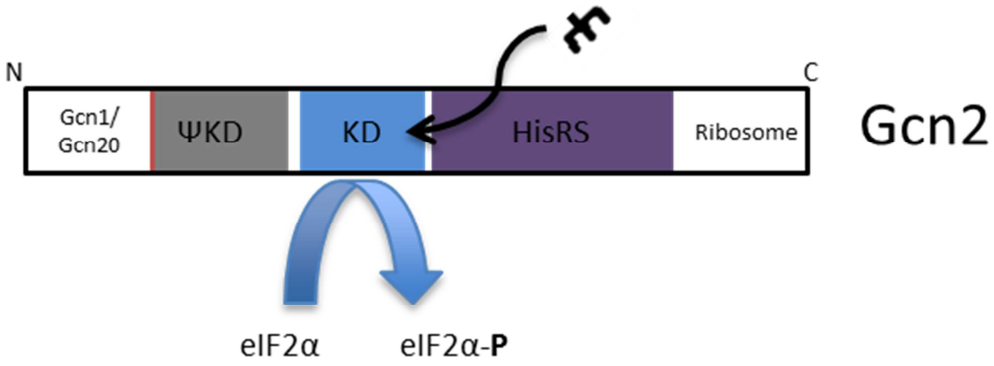

Figure 3: Schematic representation of Gcn2 domains.
As indicated, uncharged tRNA binds to the HisRS-like domain and results in the activation of the Gcn2 kinase domain (KD). This activation subsequently leads to the phosphorylation of eIF2α. Picture modified from (Hinnebusch, 2005)

1.5 Gcn1/Gcn20 complex

Yeast *GCN1* and *GCN2* are not essential to the cell under replete conditions. Under amino acid starvation, however, they are required for wild type growth (M. Marton, Crouch, & Hinnebusch, 1993) (Dever et al., 1992), suggesting that they are crucial for the cell to overcome amino acid starvation.

Gcn1 is a very large protein of 297 kDa which has been shown to reside in a complex with Gcn20. Gcn1 is present in all eukaryotes suggesting a conserved role of the protein within the GAAC. *GCN1* C-terminal region containing amino acids 2052-2428 are sufficient to bind Gcn2 (Sattlegger & Hinnebusch, 2000). Its middle region that binds Gcn20 also contains characteristic repeats which were first found in four proteins that developed the acronym **HEAT**: **H**untingtin, e**E**F3, protein phosphatase 2**A**(PP2A) and **T**OR1 (Andrade & Bork, 1995). Proteins that contain HEAT repeats are large proteins that interact with different types of proteins. They are often found in protein complexes and can function as scaffold proteins (Andrade

& Bork, 1995). These characteristics of Gcn1 suggest that it might function as a scaffold protein on the ribosome, placing Gcn2 in position to detect the uncharged tRNA. The first 2052 amino acids, comprising approximately 77 % of the protein are involved in ribosomal binding, indicating that Gcn1 has multiple contact points on the ribosome (Sattlegger & Hinnebusch, 2000).

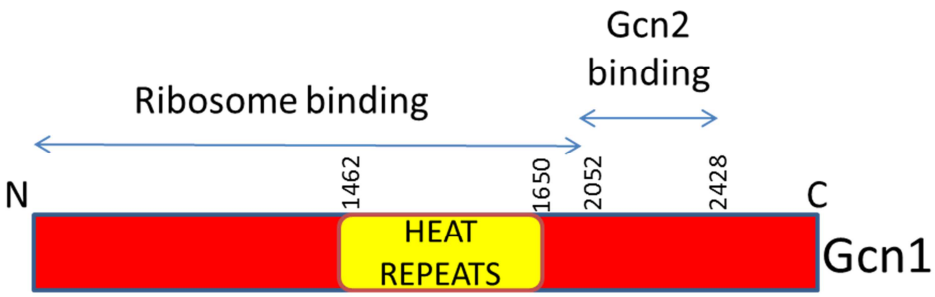

Figure 4: Representation of Gcn1 segments.
As indicated, almost three quarter of the protein is involved in ribosomal binding while only amino acids 2051-2428 are binding Gcn2.

In conjunction with the idea that Gcn1 has several ribosomal contact points, point mutations in two distinct conserved non-contiguous segments of *GCN1* ribosome binding region (M1 and M7) each led to a decrease in polyribosome binding and simultaneously reduced eIF2α phosphorylation while Gcn1-Gcn20 interaction remained unaffected. This effect was exacerbated when both mutations occurred simultanously (Sattlegger & Hinnebusch, 2005). Today there are studies in which potential ribosomal contact points of Gcn1 have been identified in a genome wide protein interaction screen (Gavin et al., 2006) of *Saccharomyces cerevisiae*. In an attempt to comprehensively find all Gcn1 binding ribosomal proteins the Sattlegger group conducted Yeast-two-hybrid (**Y2H**) screen and Co-immunoprecipitation (**Co-IP)** assays (Sattlegger et al., unpublished). So far it is unknown which of the identified ribosomal proteins are necessary for Gcn1 function rather than just being a redundant ribosomal binding site. This is, however, important to know as *GCN1* is critically required for Gcn2 activation (M. Marton, Crouch, & Hinnebusch, 1993). This is evidenced in the event that the absence of Gcn1 abolishes phosphorylation of Gcn2 substrate, eIF2α (M. Marton, Crouch, & Hinnebusch, 1993). Hence *gcn1*Δ is unable to grow on medium causing amino acid starvation. This phenotype is called a

Gcn$^-$ phenotype. Is Gcn1 present but Gcn20 absent, the phosphorylation rate of eIF2α is reduced (de Aldana et al., 1995). These results clearly showed that Gcn1 is more critically required for Gcn2 activation than Gcn20. Gcn1 nor Gcn20 are required for Gcn2 expression nor for its kinase activity (M. Marton et al., 1993), suggesting that they must be involved in the signal transduction that activates Gcn2. Due to the requirement of Gcn1 and Gcn20 for Gcn2 activation, they are regarded as Gcn2 effector proteins.

Gcn20 is a protein of 85 kDa and belongs to the ATP Binding Cassette (**ABC**) family (de Aldana et al., 1995). 15-20% of its N-terminus is essential to cooperate with the middle region of Gcn1 (M. J. Marton, de Aldana, Qiu, Chakraburtty, & Hinnebusch, 1997). Its C-terminal region contains two characteristic ABC cassettes. However, it has been shown that Gcn20 is rather related to other proteins that function in other processes than to the ABC family that is generally involved in active substrate transport and utilize ATP as an energy source to cross membranes (Kerr, 2004). Although Gcn20 only binds the ribosome weakly, it seems to contribute to Gcn1/Gcn20-ribosome interaction as demonstrated in their enhanced interaction in the presence of abundant ATP (M. J. Marton et al., 1997), which was attributed to Gcn20 ATP binding cassette. In contrast, 84% of Gcn20, containing its ABC regions are not required for Gcn1 complex formation (M. J. Marton et al., 1997), leaving the detail about Gcn20 function unclear.

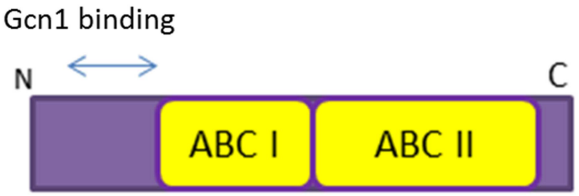

Figure 5: Representation of Gcn20 domains.
Its N-terminal domain is required for Gcn1 binding. Gcn20 harbours two ABC domains.

Interestingly Gcn1 HEAT repeats and Gcn20 ABC binding cassettes are found to be homologous to the domains in the eukaryotic elongation factor 3.

1.6 Gcn1/Gcn20 homology to eEF3

eEF3 is a (116 kDa) protein unique to fungus and belongs to the same ATP-binding cassette family (ABC) as Gcn20 (Kerr, 2004). eEF3 consists of several different domains of which one is the ABC domain and another the HEAT repeat domain. eEF3 binds the ribosome close to the E-site (Andersen et al., 2006). Some of its ribosomal binding partner are known today and comprise of proteins from the small and large ribosomal subunit. eEF3 stimulates binding of eEF1A-GTP-charged tRNA complex to the A-site of the yeast ribosome and at the same time facilitates the release of uncharged tRNA from the E-site (Andersen et al., 2006; Trianaalonso, Chakraburtty, & Nierhaus, 1995).

The Gcn1 middle region containing the HEAT repeats together with the C-terminus of Gcn20 consisting of ABC binding cassettes, show homology to the entire eEF3 molecule (Figure 6). Based on this homology, it is suggested that the Gcn1/Gcn20 complex has similar function to eEF3 and releases tRNA from the ribosomal A-site instead of the E-site (M. Marton et al., 1993).

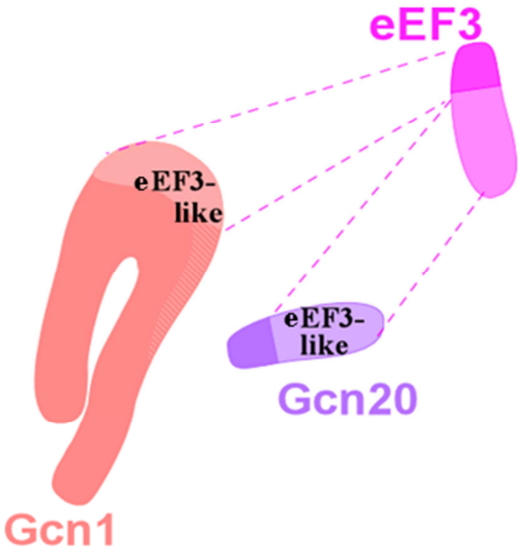

Figure 6: Domain homology between eEF3 and Gcn1/Gcn20.
Gcn1 middle portion has homology to the N-terminal HEAT repeat domain of eukaryotic translation elongation factor 3 (eEF3). Gcn20 C-terminus has homology to the eEF3 C-terminus including the ATP binding (ABC) cassettes. Together those homolog sequences make up a whole eEF3 molecule. This suggests that the Gcn1/Gcn20 complex may also have a function similar to eEF3. Picture received from (E. Sattlegger, unpublished)

1.7 Sensing amino acid starvation

In prokaryotes the sensing of amino acid starvation has been best studied so far. Here it was discovered that under amino acid starvation conditions, deacylated tRNA binds in the A-site and leads to the activation of (p)ppGpp synthetase RelA (Goldman & Jakubowski, 1990). Upon recognition of the deacylated tRNA at the ribosomal A-site, RelA converts ATP and GDP into (p)ppGpp (Goldman & Jakubowski, 1990), a small messenger molecule that binds to RNA polymerase. This results in the downregulation of rRNA and tRNA transcription. At the same time it leads to the upregulation of mRNAs coding for enzymes involved in amino acid biosynthesis (Knutsson Jenvert & Holmberg Schiavone, 2005). RelA enzymatic activity does not affect the amount of uncharged tRNA bound to the A-site, suggesting that RelA does not remove tRNA from the A-site. It has therefore been proposed that uncharged tRNA gets chased away by charged tRNA in complex with EF-Tu-GTP (Wendrich, Blaha, Wilson, Marahiel, & Nierhaus, 2002).

In analogy to prokaryotes, it has been suggested that also in eukaryotes uncharged

tRNA enters the A-site under amino acid starvation. Gcn1 location was accordingly proposed to be close to the A-site in yeast and mammals. In conjunction with this hypothesis it was evidenced that uncharged tRNA also enters the A-site in a codon specific manner in eukaryotes (Murchie & Leader, 1978), suggesting that the mechanism of the starvation signal occurring in the A-site is conserved from prokaryotes to eukaryotes. Evidence suggesting that Gcn1 can affect the A-site was provided from the overexpression of Gcn1 which increased sensitivity to paromomycin, an A-site-binding drug that affects translational fidelity (Sattlegger & Hinnebusch, 2000).

Based on these findings, a model was proposed for Gcn2 activation mediated by Gcn1 under amino acid starvation (Marton et al.1997, as well as Hinnebusch and Sattlegger 2000). In this model Gcn1, Gcn20 and Gcn2 are tethered to the ribosome in a Gcn1/Gcn20/Gcn2 complex. Uncharged tRNA enters the ribosomal A-site and gets transferred to Gcn2, in a yet unknown mechanism that involves Gcn1. Gcn1 could possibly deliver the uncharged tRNA to the A-site and transfer the tRNA from the A-site to Gcn2 or position Gcn2 in a way to be able to detect the uncharged tRNA.

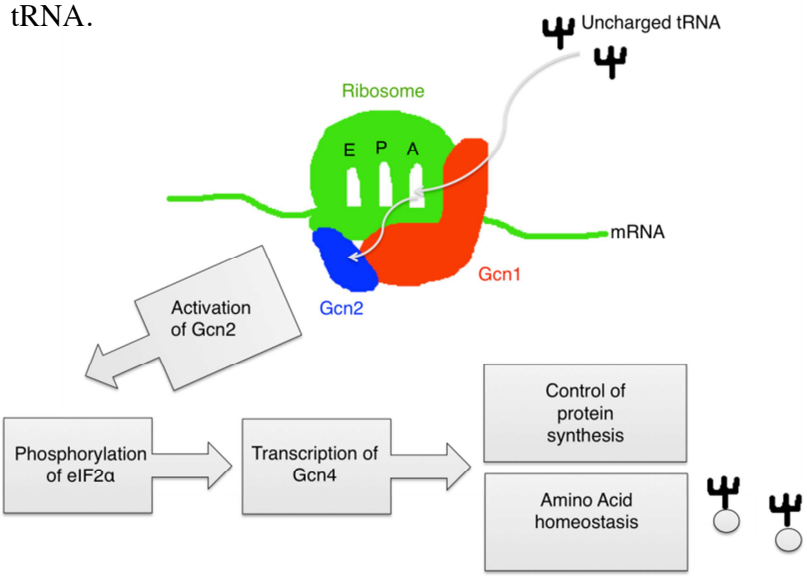

Figure 7: Hypothetical model of the sensing of amino acid starvation.
Deacylated tRNA is sensed on the ribosome by a complex formation of the trimeric complex, Gcn1/Gcn20/Gcn2. Uncharged tRNA enters the ribosomal A-site and gets transferred to Gcn2 by Gcn1. Gcn2 subsequently gets activated and phosphorylates the α subunit of eIF2. This phosphorylation leads to the expression of *GCN4*. This pathway, known as the GAAC allows the cell to overcome amino acid starvation by controlling general protein synthesis while inducing amino acid homeostasis. Reconstructed picture based on (Sattlegger & Hinnebusch, 2000)

1.8 The ribosome and its proteins

It is widely accepted that the starvation response occurs on the ribosome and most likely on translating ribosomes (M. J. Marton et al., 1997; Sattlegger & Hinnebusch, 2005). The ribosome is an essential macromolecular complex required for translation and is found throughout all kingdoms. The eukaryotic and prokaryotic ribosomes share core morphological features (Spahn et al., 2001). They consist of a small and a large ribosomal subunit which are composed of ribosomal RNA (**rRNA**) and ribosomal proteins (**rp**). Most ribosomal proteins are highly basic molecules that do interact with the rRNA to stabilize the formation of the ribosome (Spahn et al., 2001). Ribosomal proteins are incorporated into the ribosomal subunits, however, a number of them were found to have non-ribosomal functions (Lindström, 2009) (Ruggero & Pandolfi, 2003) (Zimmermann, 2003). The *Saccharomyces cerevisiae* 80S ribosome is 3.3 MDa in size and consists of the small 40S and large 60S subunit (Filipovska & Rackham, 2013) (Becker, 2005). Ribosomal proteins are given the suffix s (small) or l (large) according to their presence in the small and large ribosomal subunit. The 40S subunit consists of 32 small ribosomal proteins (**rps**) (T. Y. Kim, C. W. Ha, & W. K. Huh, 2009) and the 18S rRNA. The 60S subunit contains 46 large ribosomal proteins (**rpl**), the 25S, 5.8S and the 5S rRNA (T. Y. Kim et al., 2009). In yeast, 59 of all yeast ribosomal proteins are encoded by two paralogous genes (Kressler, Hurt, & Bassler, 2010; Planta & Mager, 1998; Wolfe & Shields, 1997) A and B, which only differ in some amino acids. Out of 19 singletons, 15 are essential. Remarkably 21 of 59 pairs encode identical proteins and the others are highly similar (Kristan K Steffen et al., 2012). Following the initial discovery of ribosomal gene duplicates, researchers showed that the overexpression of one paralogous gene can rescue the growth defect of the deletion of the other duplicate gene, suggesting that duplicated genes are functionally redundant (T. Y. Kim et al., 2009). Other studies, however, revealed a more complex situation of the duplicated genes, demonstrating that duplicated ribosomal proteins share no more phenotypes with each other than with any other ribosomal protein (Komili, Farny, Roth, & Silver, 2007).

1.9 Hypothesis and aim of research

The ribosome is an essential cellular component, which is found in all organisms. Apart from its principal role in the synthesis of polypeptides, it interacts with several non-ribosomal proteins such as the components of the GAAC. Here the ribosome is the recruiting platform for an interaction of three proteins, Gcn1/Gcn20 and Gcn2, which detect uncharged tRNA in the A-site. Studies suggest that Gcn1 has multiple contact points on the ribosome and potential ribosomal proteins for Gcn1 interaction have been identified (Sattlegger & Hinnebusch, 2005) (Gavin et al., 2006).

I hypothesize that some of these interactions only serve for recruitment of Gcn1 to the ribosome, while others are critically involved in Gcn1 function in transferring uncharged tRNA to Gcn2. Because Gcn1 is proposed to detect tRNA in the A-site (Sattlegger & Hinnebusch, 2000), I predict that ribosomal contact points necessary for Gcn1 function should be close to the ribosomal A-site.

I will test my hypothesis with the following aims:

- To screen strains, with genetically reduced levels of one ribosomal protein at a time, for their reduced ability to overcome starvation
- To verify whether Gcn2 function is affected in these strains
- To test the feasibility of an approach that validates whether Gcn1-ribosome binding was reduced
- To map Gcn1 “functional” binding sites on the ribosome based on the obtained results

1.10 Relevance

While the mechanism of the delivery of the charged tRNA to the ribosomal A-site as part of the translation process is very well understood, only little is known about the mechansim under which uncharged tRNA is detected in the A-site in amino acid starved cells. Finding ribosomal contact points of Gcn1 that are important for Gcn2 activation will give important details in order to resolve this ambiguity.

Besides its important role in allowing adaptation to amino acid deprivation in yeast, Gcn2 has been found to be crucial in a variety of other processes in mammals.

Gcn2, for example, is involved in controlling the regulation of the cell cycle (Grallert & Boye, 2007), aging (metabolic age-related diseases) and apoptosis (Almeida et al., 2009). It also plays an important role in the immune system (Munn et al., 2005) and memory formation (Costa-Mattioli et al., 2005; Costa-Mattioli et al., 2007).

One of the most significant and current discussion is the link between Gcn2 and cancer. The Gcn2-dependent pathway seems to be critical for tumour cell survival and Gcn2 inhibition has been shown to reduce proliferation of tumour cells. Interestingly solid tumour cells seem to have concomitantly activated Gcn2 and increased eIF2α phosphorylation as well as upregulated ATF4 target genes (Ye et al., 2010).

To date *GCN1* and *GCN2* have been found in all eukaryotes. This study will contribute to the understanding of the universal crucial function of sensing starvation. Generating a model of how Gcn1 binds to the ribosome and which ribosomal binding partner are necessary for Gcn1 to promote Gcn2 activation may be helpful to find an effective target in cancer research (Ye et al., 2010) to block Gcn2 activation.

2. Materials and Methods

2.1 Material

2.1.1 Biological materials

Gene knockdown strains:

Our strain collection was provided from the Buck Institute for research on aging and is a collection of *Saccharomyces cerevisiae* strains where one paralogous gene encoding a ribosomal protein at a time is replaced by a kanamycin resistance marker. The collection was newly generated in 2012 from the existing heterozygous diploid yeast *Saccharomyces cerevisiae* ORF deletion collection, where only one of the respective genes encoding a ribosomal protein was deleted (Kristan K Steffen et al., 2012)

Table 1: Yeast strains used in this study

Yeast	Genotype	Source
BY 4741	MATa *his3Δ1 leu2Δ0 met15Δ0 ura3Δ0*	Thermo Fisher
BY 4742	MATα *his3Δ1 leu2Δ0 lys2Δ0 ura3Δ0*	Thermo Fisher
*rpx*Δ	as BY 4741 but *rpx*Δ	(Kristan K Steffen et al., 2012)
*rpx*Δ	as BY 4742 but *rpx*Δ	(Kristan K Steffen et al., 2012)
*rpx*Δ	MATα *his3Δ1 leu2Δ0 ura3Δ0*	(Kristan K Steffen et al., 2012)
*rpx*Δ	MATα *his3Δ1 leu2Δ0 met15Δ0 lys2Δ0 ura3Δ0*	(Kristan K Steffen et al., 2012)
*gcn1*Δ	as BY 4741 but *gcn1Δ*	Thermo Fisher
*gcn2*Δ	as BY 4741 but *gcn2Δ*	Thermo Fisher

Table 2: Plasmids used in this study

Plasmid	Gene	Selectable marker	Vector	Source
p1834	*GCN1*-myc[b]	*URA3*, 2μ	pRS426	(Garcia-Barrio et al., 2000)
p630	*GCN2*	*URA3*, 2μ	YEp24	(R. C. Wek et al., 1990)
YPGM16k09	*RPS28B*	LEU2, Kan, 2μ	pGP564	OPEN BIOSYSTEMS
YPGM20a08	*RPS26B*	LEU2, Kan, 2μ	pGP564	OPEN BIOSYSTEMS
YPGM3a23	*RPS18A*	LEU2, Kan, 2μ	pGP564	OPEN BIOSYSTEMS

2.2 Media

Media for yeast and bacterial culture were prepared using Milli-Q® water and sterilized at 121°C and 15 psi for 20 minutes.

Carbon sources were autoclaved separately from the media and added to a final concentration of 2% (w/v) prior to use. Liquid media was cooled down to RT before supplements were added. The media was stored at RT if not mentioned otherwise.

Solid media was obtained by adding agar (Formedium) to a final concentration of 2 % (w/v) prior to sterilisation. Solid media was cooled down to 55°C before supplements were added or plates were poured. Plates were cooled down and stored at 4°C until usage.

All recipes are shown for the preparation of 1L if not mentioned otherwise.

Yeast-Peptone-Dextrose (YPD)

Bacto Yeast Extracts	10 g (Formedium)
Bacto Peptone	20 g (Formedium)
40 % Glucose	50 mL (Formedium)

Synthetic-Complete-Media (SC)

Yeast Nitrogen Base	1.9 g (Formedium)
Ammonium Sulphate	5 g (Ajax)
Amino acids (Kaisermix)	2 g (Formedium)
40 % Glucose	50 mL (Formedium)

Luria-Bertani Medium (LB)

Trypton	10 g (Oxoid)
Yeast Extract	5 g (Formedium)
NaCl	5 g (Ajax)

2.2.1 Media supplements

Solutions were prepared using Milli-Q® water and sterilized at 121°C and 15 psi for 20 minutes or filtered through 0.22 µm (milipore express® membrane filters).

Table 3: Synthetic Complete Amino Acid Drop out Supplements (Kaisermix, Formedium)

Amino acid	Solvent	Final concentration [mg/L]
Alanine	water	16
Cysteine	water	16
Aspartic acid	water	16
Glutamic acid	water	16
Phenylalanine	water	16
Glycine	water	16
Lysine	water	16
Methionine	water	16
Asparagine	water	16
Glutamine	water	16
Arginine	water	16
p-Aminobenzol	water	1.6
Inositol	water	16
Tyrosine	water	16
Threonine	water	16
Serine	water	16
Proline	water	16

Table 4: Amino Acid stock solution used (Formedium)

Amino acid	Solvent	Final concentration [g/mL]
Adenine	water	0.1351
Isoleucine	water	0.325
Leucine	water	1.31
Methionine	water	0.746
Tryptophan*	water	0.8
Histidine **	water	2.09
Valine	water	0.586
Uracil	water	0.224

*Tryptophan was filter sterilised and stored in a brown bottle, protected from light degradation at 4° C. **Histidine was autoclaved and store under the same conditions as Tryptophan.

Table 5: List of antibiotics and induction drugs used (Formedium)

Antibiotic	Solvent	Final concentration [µg/mL]
Ampicillin	water	50
Kanamycin	water	100
SM	DMSO	0.5-2

2.3 Methods

2.3.1 Measurement of optical density

The cell density of a culture was determined by measuring the OD at a wavelength of 600 nm with a Novaspec II (Pharmacia Biotech ^{TM}). Distilled water was used as calibration reference. If required, dilutions were made using distilled water.

2.3.2 Storage of cultures / Perming cells

Yeast strains were streaked on YPD plates and incubated for 2 days at 25°C. Single colonies were picked and permed in 30 % (v/v) glycerol. The strains were stored at -80°C. For a short period of time, the cells were stored at 4°C on solid YPD medium.

Glycerol Stock (30 %)

10 mL glycerol stock was generated by adding 3 mL glycerol 99.5 % (v/v), into 7 mL distilled H_20.

E.coli strains were streaked onto solid LB-selective Antibiotic and grown overnight at 37 °C. A single colony was picked and inoculated into 2 mL of sterile LB-Antibiotic media and grown overnight by shaking at 37°C until reaching an OD≈0.5. 500 µL of this culture was stored in 70 % (v/v) glycerol.

Glycerol Stock (70 %)

10 mL glycerol stock was generated by adding 7 mL glycerol 99.5 % (v/v), into 3 mL distilled H_20.

2.3.3 Preparation of Whole Cell Extract (Dirty Western)

Yeast deletion strains, derived from BY4741/BY4742 were grown to saturation at room temperature (RT) in 4 mL SC medium. Overnight cultures were inoculated into 25 mL starvation or non-starvation media and grown shaking at 120 rpm at 25°C to exponential phase (OD_{600} 1). In the exponential phase, the cells grown in starvation media were starved for 1h by adding SM to a concentration of 1 µg/mL. 6.6 g of crushed ice and 650 µL (1% final) were prepared in a 50 mL falcon tube. 25 mL of cell culture was subsequently poured into the tubes and left on ice for 30 minutes. After 30 minutes, the crosslinking process was stopped by adding 1.6 mL of 2.5 M glycine into the culture (0.1 M final). The cells were then harvested by centrifugation (5 min 4200 rpm). The pellets were stored at -80 °C until used or they were used to lyse the cells immediately.

2.3.3.1 Lysing cells

The thawed cells were resuspended in 100 µL water when stored at-80 °C. 100 µL of 0.2 M NaOH was added and the cells incubated on ice for 5 minutes. The sample was resuspended in loading dye and heated up for 3 minutes at 85 °C. The cells were pelleted by centrifugation (5 min. 4200 rpm) and the supernatant loaded on the gradient SDS PAGE gel.

2.3.3.2 Gradient Polyacrylamide-Gel Electrophoresis (SDS PAGE)

The discontinuous system is made out of a 4 % stacking gel and a 17 % separating gel. 1 % Agarose is first used to seal the bottom between the glass plates and the spacers.

20 mL of 4 % Premix and 20 mL of 17 % premix was added into the chambers of the gradient mixer followed by 200 µL of 10 % Aps and 20 µL TEMED each. The stocking gel was then casted within the glass plates and let dry for 1 h.

Once the gel was solidified, the comb was removed and the slots of the gel washed with sterile water. The samples were mixed with the loading dye and heated at 85 °C for 3 min. Between 5-10 µL of the sample were loaded onto the gel. Electrophoresis was then carried out at 250 V and 100 mA until the dye front reaches 9 cm distance to the gel pockets. The size of the proteins was compared with the SeeBlue®Plus ladder from Invitrogen.

4 % Premix (20 mL)

29:1 Acrylamide	2 mL
1.5 M Tris-HCl pH 8.8	5 mL
10 % SDS (w/v)	200 µL

17 % Premix (20 mL)

29:1 Acrylamide	8.5 mL
1.5 M Tris-HCl pH 8.8	5 mL
10 % SDS (w/v)	200 µL

Protein running buffer (2.5 L)

10 % SDS	25 mL
10X Tris-glycine	250 mL
10% SDS	10 mL

5X Laemmli loading dye (10mL)

Glycerol	1mL
10% SDS (w/v)	1 g
1% Bromophenol blue	1 mL
Tris HCl 0.5M pH 6.8	6.25 mL
B-Mercaptoethanol	2.5 mL

1M LiAc (100mL)

LiOAc	10.2g
10X TE	10 mL

The solution was filter sterilised.

10X Tris-Glycine

Tris	30.3g
EDTA	144 g

2.3.3.3 Western Blot

Once the proteins were separated via SDS-Page the proteins were transferred onto a polyvinylidene difluoride membrane (PVDF (Thermo Fisher)) with a pore size of 0.45 µm. The membrane was first soaked some minutes for activation in methanol for and subsequently equilibrated with transfer buffer. The transfer was carried out at 24 V and 1 A for 2.5-3 h. Membranes were then probed with polyclonal rabbit-anti eIF2α-P (1:5000) (Invitrogen).

The membrane was blocked with 3 % BSA in TBS-T buffer. Membranes were then probed with polyclonal eIF2α-P (1:5000). After 3 washing steps of 10 min each with TBS-T the membrane was immunoblotted with the secondary rabbit-anti eIF2α-P antibody. For the detection of eIF2α-P, a commercially available antibody was used (Invitrogen). The proteins were visualized by chemiluminescence detection. Equal amounts of loaded protein were confirmed with the abundant protein Pgk1 as a loading control. The antibodies were detected by enhanced chemiluminescence. The blots were subsequently quantified with the programs Fujifilm Science Lab 2005 Multigauge V3.1® or image J®.

Transfer buffer

1X Tris-glycine	100mL
Methanol	200 mL

10X Tris-Buffered-Saline (TBS)

NaCl	80 g
Tris	24 g

pH was adjusted to pH 7 by using HCl.

1X Tris-Buffered-Saline-Tween (TBS-T)

10X TBS	100 mL
Tween	1 mL

Detection mix A (200mL)

1M Tris pH 8.5	20 mL
Luminol	0.088 g
Coumaric acid	0.0131 g

Detection mix B (200mL)

1M Tris pH 8.5	20 mL
30% H2O2	134 µL

The solution was stored in a lightproof container at 4 °C.

Table 6: Primary antibodies and their dilutions.

Antibody	Dilution	Source	Secondary antibody
eIF2α-P	1:5000	Invitrogen	Anti-rabbit
Pgk1	1:5000	Invitrogen	Anti-mouse

Table 7: Secondary antibodies used in this study

Secondary	Dilution	Source
Anti-rabbit	1:100.000	Pierce
Anti-mouse	1:50.000	Pierce

2.3.3.4 Staining the PVDF membrane

After the protein transfer was performed the membrane was incubated and gently shaken with Ponceau stain for 10 min. and subsequently distained with 1 % acetic acid (v/v) until only the transferred bands were visible.

Ponceau Stain (1X) (500mL)

Ponceau S	0.5g
1% Acetic acid	5 mL

2.3.3.5 Quantification of the western blot signals

Example for a quantification of the western blot signals of Figure 14, C.

	eIF2-P		Pgk1		Calculation			
	Ratio of signal	Average of duplicates	Average of duplicates	Ratio of signal	eIF2-P/Pgk1	Average	Relative ratio	Std. Error
	[%]			[%]				
WT(4741) +	25.49	26.45	13.85	14.38	1.84	1.84	2.58	0.00
WT(4742) +	27.42		14.92		1.84			
WT(4741) -	7.97	8.79	9.94	12.65	0.80	0.71	1.00	0.12
WT(4742) -	9.61		15.37		0.63			
rps18AaΔ +	7.21	8.27	10.81	10.57	0.67	0.78	1.10	0.17
rps18AbΔ +	9.34		10.35		0.90			
rps18AaΔ -	7.62	6.49	15.36	12.39	0.50	0.53	0.75	0.05
rps18AaΔ -	5.37		9.42		0.57			

2.3.4 Plasmid isolation

The plasmids were isolated via alkaline lysis method. 5 mL of bacterial culture were grown for 9-15h in LB media + selection antibiotic. The culture was pelleted by centrifugation at 4 °C at 42000 for 2 minutes. After discarding the supernatant, the pellet was resuspendend in 200 µL of resuspension buffer + 2 µL RNase by vortexing. 400 µL of lysis buffer were added and the tubes quickly inverted. After incubating the samples on ice for 5 minutes, 300 µL of ice cold neutralisation buffer was added and the samples incubated on ice for 5 minutes. Cellular debris was pelleted by centrifugation at 42000 for 5 minutes and the supernatant transferred into new tubes. Equal amount of isopropanol was added and the samples left on ice for 2 minutes. The DNA was then pelleted by centrifugation (42000 for 5 minutes). The DNA pellet was washed with 70% ethanol and air-dried in a concentrator. The pellet was resuspended in 40 µL of sterile water and stored at -20 °C until used.

Resuspension buffer

Tris	6.06 g
EDTA	3.72 g

The pH was adjusted to pH 8 with HCl. Before usage 100 µg/mL RNase was added.

Neutralisation buffer

Potassium acetate	294.5 g

The pH was adjusted to pH 5.5 with glacial acetic acid prior to water.

Lysis buffer

NaOH	8.09 g
20 % SDS	50 mL

2.3.4.1 DNA verification

DNA was quantified on 1% (w/v) agarose gel against a known DNA marker (EcoRI/Hind III (Fermentas)).

2.3.4.2 Agarose Gel Electrophoresis (DNA Gel)

0.5 g agarose was dissolved into 50 mL 1X TAE buffer. 5 µL of EtBr has been added and the solution was poured into the gel apparatus and let to solidity for 20 minutes. 3 µL of DNA plasmid was loaded together with 5 µL of 6X loading dye. The gel was run for 30 min. at a constant voltage of 80 V. The Gel was visualized on a UV transilluminator the pictures analysed with Molecular Imager® Gel Doc™ system using Quantity One® analysis software (BioRad).

50X Tris –Acetate EDTA (TAE)

Tris	276 g
EDTA	18.6 g
Acetic Acid	57.1 mL

pH was adjusted to pH 8.5 using HCl.

DNA loading dye (6X)

Bromophenol blue	0.25mg
Glycerol	3mL
Water	7mL

2.3.5 Yeast transformation

2.3.5.1 Making yeast competent

An overnight culture of 5 mL yeast was used to inoculate 50 mL YPD media at OD=0.2. The culture was grown to OD= 1 at 25 °. The culture was spun down at 4000 rpm at 4 °C for 5 minutes and resuspended in 10 mL sterile dest. water and spun again at the same conditions. The pellet was subsequently resuspended in 500 µL Solution and stored at 4 °C overnight.

Solution 1 (10mL)

10 mM Tris-Cl	1 mL 10X TE, pH 7.4
1 mM EDTA	
100 mM LiOAc	1 mL 1M LiOAc

Made up to 10 mL with distilled H_20.

1M LiAc (100mL)

LiOAc	10.2g
10X TE	10 mL

The solution was filter sterilised.

2.3.5.2 Transformation

The cells were taken out of the fridge and were incubated 1 h at 25 °C. In the meantime the single stranded Herring sperm DNA was denatured at 95 °C for 5 min and subsequently cooled on ice for at least 3minutes. 5 µL of the sperm DNA, followed by 5 µL of plasmid, 300 µL of Solution 2 and 100 µL of cell culture was mixed by vortexing in an eppendorf tube. The tube was then incubated for 1.5 h at 25 °C while shaking.

The culture was heat shocked at 42 °C for 15 min and immediately put on ice for 2 - 5 min. The cells were spun down at 4000 rpm for 1 min and resuspended in 500 µL of sterile water and transferred onto SC selective plates. The cell suspension was spread by using glass beads and was incubated for 3 to 4 days at 25 °C.

Solution 2:

10 mM Tris-Cl	
1 mM EDTA	
100 mM LiOAc	1 mL 1M LiOAc
40 % PEG	9 mL PEG in 1X TE

44 % PEG (100 mL)

PEG	44 g
10X TE	10 mL

2.3.6 Semi-quantitative growth assay

Yeast strains were streaked for single colonies and their growth behaviour documented. Two single colonies were then selected from each strain and taken to prepare overnight cultures (4mL SC media). The overnight cultures were grown at RT until reaching saturation. The cultures were subjected to five 10 fold serial

dilutions. 5 µL of the dilutions together with the original undiluted culture were spotted onto solid starvation media made out of synthetic complete media containing three different SM concentrations: 0.5; 1; 2 µg/mL.

The cultures were additionally spotted onto solid media without SM (YPD, SC, YPG).

The growth of the investigated strains was monitored over 1-2 weeks and documented using a document scanner. Taking possible negative impacts of the ribosomal protein gene deletion on ribosome function into account, the strains were grown at reduced temperature. Setting the incubation temperature to 25°C ±2°C instead of 30°C, we avoided a fast accumulation of reversion mutations.

3. Identification of ribosomal binding sites of Gcn1 that are necessary to promote Gcn2 activity

As outlined in the introduction of this thesis, the GAAC pathway consists of a cascade of processes, beginning with the activation of Gcn2 that allows cells to overcome amino acid starvation. This activation is mediated by uncharged tRNA (deacylated tRNA) binding to Gcn2 (Dong et al., 2000) and to require the effector protein Gcn1 (M. Marton et al., 1993). Marton et al. (1997) as well as Hinnebusch and Sattlegger (2000) proposed a model of Gcn2 activation (chapter 1.7) wherein Gcn1 in complex with Gcn20 is suggested to be directly involved in the delivery or transfer of the deacylated tRNA to or from the A-site to Gcn2. The mechanism, by which the starvation recognition and the transfer of the starvation signal is carried out, still remains unclear. Mapping Gcn1 on the ribosome and hereby testing the model whether Gcn1 accesses the A-site, will help in understanding the molecular process of the starvation recognition in the GAAC.

Ribosomal proteins that are potentially contacted by Gcn1 have already been identified in Y2H screens and Co-IP assays performed in the Sattlegger group (E.Sattlegger, S.J.Lee, R.Shanmugam, unpublished) as well as in large scale interaction studies (Gavin et al., 2006). In this work we are interested in identifying which of these redundant ribosomal contact points are necessary for Gcn2 activation. In order to reveal these critical ribosomal binding sites of Gcn1 we took advantage of the fact that if such a ribosomal protein is missing, Gcn1 function in Gcn2 activation will be affected. This can easily be observed by the fact that strains unable to activate Gcn2 cannot grow under amino acid starvation. One caveat of this study was the fact that ribosomal proteins are essential and cannot be simply removed from the cell. However, this problem was overcome by the fact that *Saccharomyces cerevisiae* harbours two gene copies encoding for most ribosomal proteins. These ribosomal gene copies are referred to as paralogous genes and are named *RPX(A)* and *RPX(B)*. Deletion of only one of these two genes will just reduce i.e. knock down the protein level thereby still maintaining the cell's viability. For our studies we used a

collection of strains in which only one paralogous gene at a time is replaced by a kanamycin resistance marker. Those strains are referred to as *rpx*Δ strains. Ribosomal proteins from the small or large ribosomal subunit are given the suffix s (small) or l (large). The collection used in this study was newly generated in 2012 from the existing heterozygous diploid yeast collection in which reversion mutations already accumulated (Kristan K Steffen et al., 2012).

3.1 Screening of *rpx*Δ strains for sensitivity to sulfometuron methyl

In order to identify *rpx*Δ strains that are impaired in activating Gcn2 we benefit from the fact that Gcn2 function can be evaluated by scoring the growth of living cells on solid starvation media under which only those with active Gcn2 can grow. Performing those semi-quantitative growth assays allows us to analyse a large number of samples in a short time. A former PGDip student from the Sattlegger group (Tiena Liang) previously tested this procedure to show that the proposed method is feasible. As deletion cells with growth defect can accumulate compensatory mutations to revert the defect, it is important to remove such revertants by streaking for single colonies. After streaking the *rpx*Δ strains for single colonies, we picked two representative not reverted colonies as judged by similar size to most other colonies and used those for our studies.

Overnight cultures of the *rpx*Δ strains were prepared. Reaching saturation, the cultures were spotted in five tenfold dilutions onto solid rich media containing the drug sulfometuron methyl (**SM**). SM inhibits the function of the acetolacetate synthase which catalyses the first step in valine and second step in leucine and isoleucine biosynthesis (LaRossa & Schloss, 1984). SM therefore causes a branched chain amino acid starvation. In the interest of identifying strains with different degrees of sensitivity to SM, we used three different SM concentrations: 0.5; 1; 2 µg/mL.

The cultures were additionally spotted onto solid media without SM (**YPD** (Yeast-Peptone-Dextrose), **SC** (Synthetic complete), **YPG** (Yeast-Peptone- Glycerol)). As YPD and SC media represent a nutrient-rich (replete) condition, we were able to monitor the growth rate of the investigated strains under unstarved conditions. YPG

media represents a nutrient-rich media which contains glycerol instead of glucose. Spotting cell cultures onto this media helps to identify colonies with dysfunctional mitochondria. Glycerol is a carbon source that cannot be utilized by mitochondrial deficient colonies called petite. Petites form small colonies on glucose containing media and fail to grow on media containing glycerol. All presented results in this thesis are derived from non-petites.

The growth of the investigated strains was monitored over 1-2 weeks and documented using a document scanner. Taking possible negative impacts of the gene deletion on ribosomal function into account, which could lead to differences in growth rates, the strains were grown at reduced temperature i.e. 25°C ±2°C instead of 30°C.

Isogenic wild type (WT) strains with opposite mating type and a strain deleted for *GCN1 (gcn1*Δ) were chosen as control strains for this assay. WT parent strains were used as a positive control as they have the ability to overcome amino acid starvation and grow on SM plates. *gcn1*Δ strain was used as negative control as the strain cannot overcome amino acid starvation. In our assay, we expected that strains lacking the gene encoding a specific ribosomal protein required for Gcn2 activation to have a growth impairment compared to the WT under amino acid starvation conditions. If a *rpx*Δ strain grows worse than the WT in the presence of the starvation-inducing drug SM, this growth behaviour is called SM sensitivity phenotype (SM^S). *rps10A*Δ strain has previously been shown by the Sattlegger group to have a SM^S phenotype (Lee, Swanson & Sattlegger, Manuscript in preparation). The *rps10A*Δ strain was therefore included in our screen as a reference strain.

Out of 32 small ribosomal proteins (rps) and 46 large ribosomal proteins (rpl), 55 (23 rps and 32 rpl) viable *rpx*Δ strains were tested by the semi-quantitative growth assay. *rps12*Δ and *rpl17A*Δ strain caused a dramatic growth defect under nutrient replete conditions and therefore were not included in our assays.

Figure 8 and Figure 9 show scans of the growth assay of *rpx*Δ strains that resulted in a SM^S phenotype under amino acid starvation. Scans from all investigated *rpx*Δ strains can be found in the appendix (Section A) of this thesis.

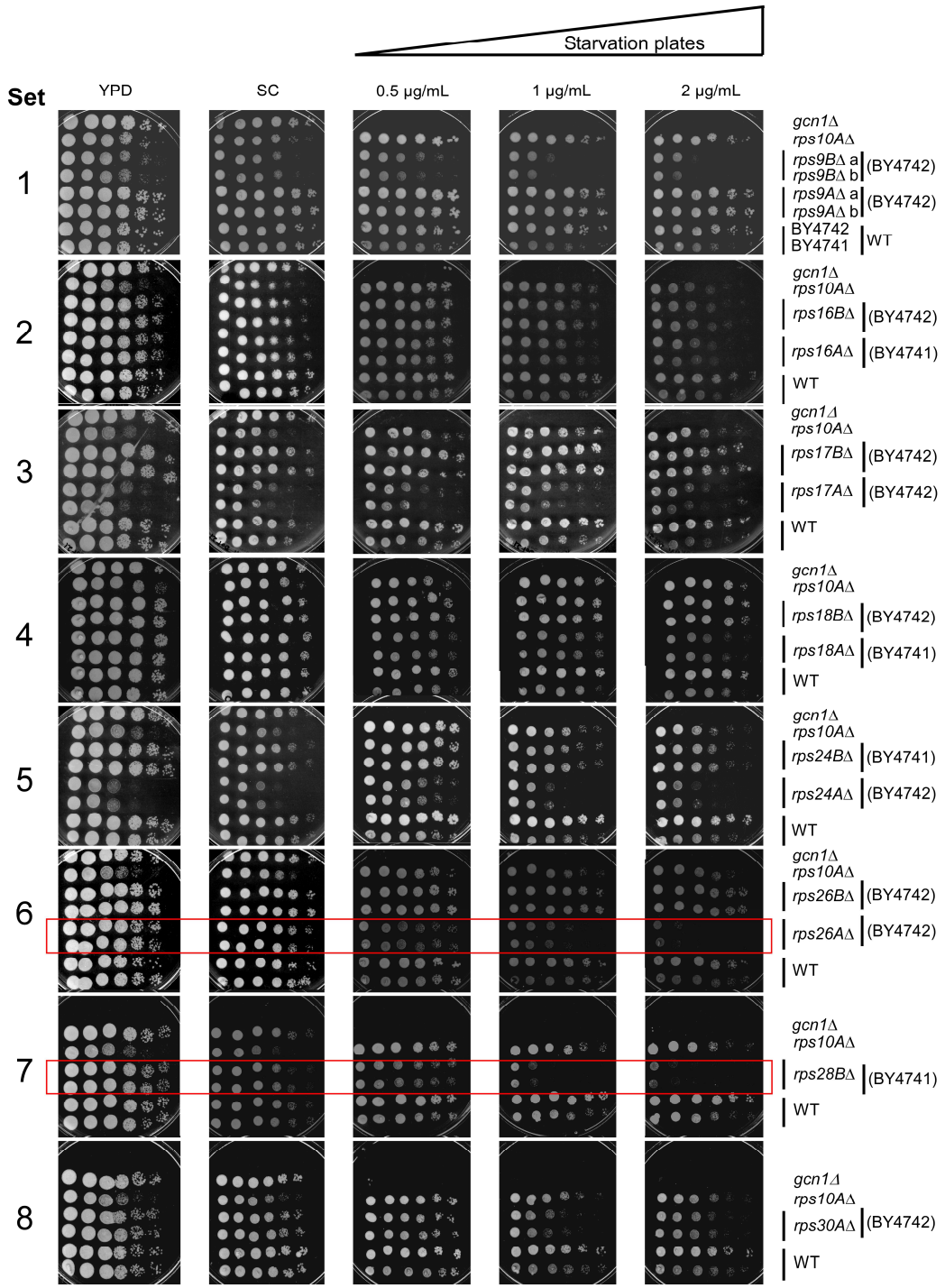

Figure 8: *rps*Δ strains show impaired growth under amino acid starvation.

Indicated strains were grown to saturation in liquid media. Cultures were subjected to five 10 fold serial dilutions and 5µL of each dilution together with the original undiluted culture was spotted onto solid media containing no drug (SC), the starvation inducing drug (SC+SM) at indicated concentrations (0.5-2 µg/mL) and on rich media (YPD). The plates were incubated at 25±2°C and the cell growth monitored and documented using a document scanner. Strains showing a strong SM sensitivity phenotype under amino acid starvation conditions are highlighted.

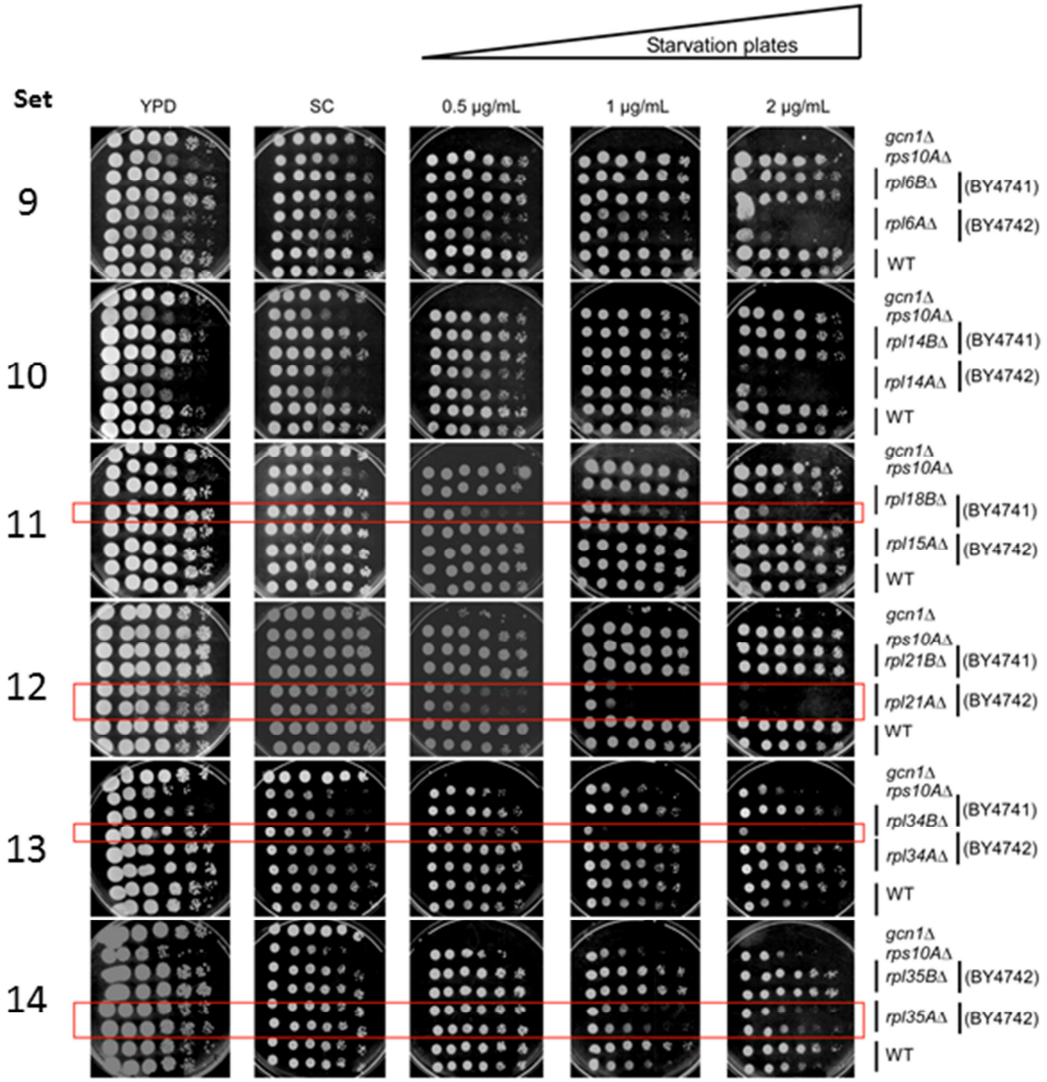

Figure 9: *rpl*Δ strains show impaired growth under amino acid starvation.
The experiment was conducted as outlined in Figure 8.

It can clearly be seen that both WT strains grew on the starvation plates, while the *gcn1*Δ strain did not (Example Figure 8, Set1). The expected growth behaviour of the *gcn1*Δ strain indicated that SM induced amino acid starvation. In most of our screens (Figure 8 & Figure 9) we observed that WT BY4741 (last row of each set) grew slower under amino acid starvation conditions, compared to the WT BY4742 (second to last row of each set). Both strains were tested on YPG plates and grew well. While the two WT strains share most of their auxotrophies, they differ in regards to lysine and methionine auxotrophy. While BY4741 is met-, BY4742 is lys-. Our collaborator, Mark

J. Swanson found that in this strain background methionine-auxotrophy leads to higher sensitivity to SM (M.J. Swanson, unpublished) which is in accordance with our observations and could explain the difference in growth of both WT strains under amino acid starvation.

In order to obtain more quantitative data from the growth assays, we numerically scored the growth of each strain on the three starvation and the SC control plate. Dilutions that led to full growth were given 2 points; half growth was given 1 point and so on (Figure 10). Due to limitation in our scoring system by eye, we could not distinguish scores below 0.5 points. In total a strain could reach a maximum score of 10 points for each plate (2 points for each of the five dilutions).

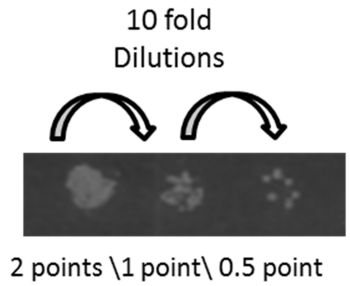

Figure 10: Example for the growth scoring of colonies in the semi-quantitative growth assay.
The three indicated dilutions would reach a final total score of 3.5.

Since the degree of SM sensitivity is dependent on methionine auxotrophy, we compared the investigated strains with their respective methionine auxotroph or prototrophic WT strain. Doing so, we observed that some of the *rpx*Δ strains in our screen were slow growing strains (Slg-). These strains *rps9B*Δ (Figure 8, Set1), *rps24A*Δ (Figure 8, Set5), *rpl6A*Δ (Figure 9, Set9) *and rpl14A*Δ (Figure 9, Set10) grew worse than their corresponding WT under replete conditions.

Scoring of the growth of *rpx*Δ strains from Figure 8 and Figure 9 are listed in Table 8 together with their corresponding WT as indicated by highlighted auxotrophy.

Table 8: Scoring the growth of *rps*Δ strains in the semi-quantitative growth assay from Figure 8 according to a numerical system that evaluates the growth of a colony by eye.

Colonies in dilutions that were entirely grown up reached a maximum score of 2. Having five dilutions for each strain the total maximum score of a strain on one plate was 10. Highlighted in red are ribosomal knockdown strains which growth was significantly impaired under amino acid starvation (SM sensitivity phenotype). Orange represents methionine auxotrophy (met). Yellow represents no auxotrophy to methionine.

Set	Auxotrophy	Strain	SC	SM (0.5)	SM (1)	SM (2)
1	MET,LYS	*rps9B*Δ	6.0	7.0	4.0	4.0
			6.0	7.0	4.0	4.0
	MET,lys	*rps9A*Δ	9.0	9.0	8.5	8.5
			9.0	9.0	8.5	8.5
	MET,lys	BY4742	8.0	8.5	8.5	7.0
	met,LYS	BY4741	8.5	8.5	8.0	6.5
2	MET,lys	*rps16B*Δ	8.0	9.5	8.0	6.0
			8.0	9.5	8.0	6.0
	MET,LYS	*rps16A*Δ	7.5	8.5	6.0	5.0
			7.5	8.5	6.0	5.0
	MET,lys	BY4742	9.0	9.0	9.5	8.0
	met,LYS	BY4741	8.5	8.5	7.0	5.0
3	MET,lys	*rps17B*Δ	8.0	9.0	9.0	6.6
			8.0	8.0	9.5	6.5
	MET,lys	*rps17A*Δ	5.0	4.0	5.0	3.0
			5.0	4.0	5.0	3.0
	MET,lys	BY4742	7.0	8.5	9.0	6.5
	met,LYS	BY4741	7.0	8.0	7.0	3.0
4	MET,lys	*rps18B*Δ	7.5	8.0	8.0	7.0
			7.5	7.5	8.0	7.0
	met,lys	*rps18A*Δ	8.0	7.0	7.0	5.0
			8.0	7.0	7.0	5.0
	MET,lys	BY4742	7.5	8.0	8.0	7.0
	met,LYS	BY4741	7.5	6.5	7.0	6.5
5	met,lys	rps24BΔ	8.0	9.0	8.5	7.0
			8.0	9.0	8.5	7.0
	MET,lys	rps24AΔ	4.0	7.0	5.0	3.0
			4.0	7.0	5.0	3.0
	MET,lys	BY4742	8.5	10.0	9.5	9.0
	met,LYS	BY4741	8.5	8.0	7.0	6.0
6	MET,lys	*rps26B*Δ	9.0	9.0	9.5	9.5
			9.5	9.5	10.0	10.0
	MET,lys	*rps26A*Δ	8.0	8.5	5.0	2.0
			7.5	9.0	5.0	2.0
	MET,lys	BY4742	7.0	8.5	8.5	8.0
	met,LYS	BY4741	8.5	8.5	8.0	8.5
7	met,lys	*rps28B*Δ	7.0	8.5	3.0	1.0
			7.0	8.5	3.0	1.0
	MET,lys	BY4742	8.0	9.5	9.0	8.5
	met,LYS	BY4741	8.0	8.5	8.0	7.0
8	MET,lys	*rps30A*Δ	8.5	8.0	4.5	5.0
			8.5	8.0	4.5	5.0
	MET,lys	BY4742	9.5	8.5	8.0	8.0
	met,LYS	BY4741	9.0	9.5	7.5	7.5

Table 9: Scoring of the semi-quantitative growth assay from Figure 9.

The scoring was performed as described for Table 8. Highlighted in red are ribosomal knockdown strains which growth was significantly impaired under amino acid starvation (SM sensitivity phenotype). Orange represents methionine auxotrophy (met). Yellow represents no auxotrophy to methionine.

Set	Auxotrophy	Strain	SC	SM (0.5)	SM (1)	SM (2)
9	met,lys	*rpl6BΔ*	8.5	9.0	9.0	7.5
			9.0	9.5	9.5	8.5
	MET,lys	*rpl6AΔ*	8.0	7.0	7.0	0.0
			7.0	7.0	7.0	0.0
	MET,lys	BY4742	10.0	10.0	10.0	9.0
	met,LYS	BY4741	9.5	10.0	10.0	8.5
10	met,lys	*rpl14BΔ*	9.0	9.0	8.5	7.5
			9.0	9.0	9.0	7.5
	MET,lys	*rpl14AΔ*	5.0	7.0	7.5	0.0
			5.0	7.0	7.0	0.0
	MET,lys	BY4742	8.0	9.0	9.0	8.0
	met,LYS	BY4741	8.0	9.0	8.0	7.0
11	met,LYS	*rpl18BΔ*	9.0	9.0	9.5	8.5
			8.0	5.0	4.0	1.0
	MET,lys	*rpl15AΔ*	8.5	9.0	9.5	9.0
			9.5	9.5	9.5	9.0
	MET,lys	BY4742	9.5	9.5	9.5	9.0
	met,LYS	BY4741	9.5	10.0	9.5	9.0
12	met,LYS	*rpl21BΔ*	10.0	10.0	10.0	9.0
			10.0	9.5	10.0	9.0
	MET,lys	*rpl21AΔ*	9.5	5.0	1.5	0.0
			9.5	5.0	1.5	0.0
	MET,lys	BY4742	10.0	10.0	10.0	9.5
	met,LYS	BY4741	9.5	9.0	9.5	8.0
13	MET,LYS	*rpl34BΔ*	5.0	8.0	8.5	8.0
			6.0	7.5	1.0	0.0
	MET,lys	*rpl34AΔ*	8.5	9.5	8.5	8.0
			8.5	8.5	8.0	8.5
	MET,lys	BY4742	8.0	8.5	8.5	8.0
	met,LYS	BY4741	8.0	8.0	8.0	5.0
14	MET,lys	*rpl35BΔ*	8.5	9.0	8.0	8.5
			9.0	9.5	8.0	9.0
	MET,lys	*rpl35AΔ*	8.5	9.0	4.0	3.0
			8.5	8.5	4.0	3.0
	MET,lys	BY4742	8.0	8.5	8.0	7.5
	met,LYS	BY4741	8.0	8.5	5.0	5.0

In order to identify *rpxΔ* strains with increased sensitivity to SM, and in order to take growth defects that were associated with the gene deletion encoding for ribosomal protein into account, the numerical scores of the SM plates were divided by that of the control plate. Considering that growth differences between experiments occurred, we also divided the ratio of the *rpxΔ* strains by that of the WT. This allowed us to compare the results of all experiments (calculations are shown in the appendix, Section C).

Among the strains tested, *rpl21A*Δ strain appeared to be the most SM sensitive strain (Figure 9, Set12). It showed reduced growth under all tested SM concentrations, with an expected tendency of developing a stronger growth defect under higher drug concentration. On the highest SM concentration (2 µg/mL) the strain failed to grow at all which means that Gcn2 activation was abolished (0 points) (Table 9, Set12). On the 1 µg/mL SM plate, *rpl21A*Δ strain was given a score of 1.5 points. As every column on the growth assay plates represents one dilution step and *rpl21A*Δ strain lacked the growth of four dilutions when compared to WT, this means that this strain grew 10,000 times (10^4) worse than the WT. Additional strong SM^S were found strains *rps26A*Δ, *rps28B*Δ, *rpl18B*Δ, *rpl34B*Δ and *rpl35A*Δ strain (highlighted in red in Table 8 & Table 9. *rps9B*Δ, *rps17A*Δ, *rps18A*Δ, *rps24A*Δ, *rps30A*Δ, *rpl6A*Δ and *rpl14A*Δ strain exhibited a weak SM^S phenotype in our assay. *rps18A*Δ strain for example was given the score of 5 points on the highest SM concentration (2 µg/mL)(Table 8,Set4). This suggests that the strain grows about 10 times worse than the WT. In the scoring system the WT reached 6.5 on the respective plate.

Contrary to our expectations, we saw a difference in the strength of SM^S for all investigated paralogous gene deletions. In the case of *rps9* for example, only *RPS9B* deletion led to SM^S phenotype, whereas the deletion of its paralogous gene *RPS9A* did not (Figure 8, Set1).

The growth of our reference, the *rps10A*Δ strain showed a significant variation in its SM^S phenotype between growth experiments (compare growth *rps10A*Δ strain in Figure 8 and Figure 9), suggesting that the strain already contained reversion mutations. Therefore we were not able to use this strain as a reference. In order to validate our results, we randomly retested three *rpx*Δ strains with SM^S phenotypes and four *rpx*Δ strains without SM^S in an independent experiment again and obtained the same results for all strains. This clearly showed the reproducibility of our findings and that the observed behaviour of rps10A was likely unique to the strain. The following graph (Figure 11) gives an overview of the SM^S results (after normalization to the WT) of all investigated *rps*Δ strains in the screen.

Figure 12 gives the overview for the *rpl*Δ strains tested.

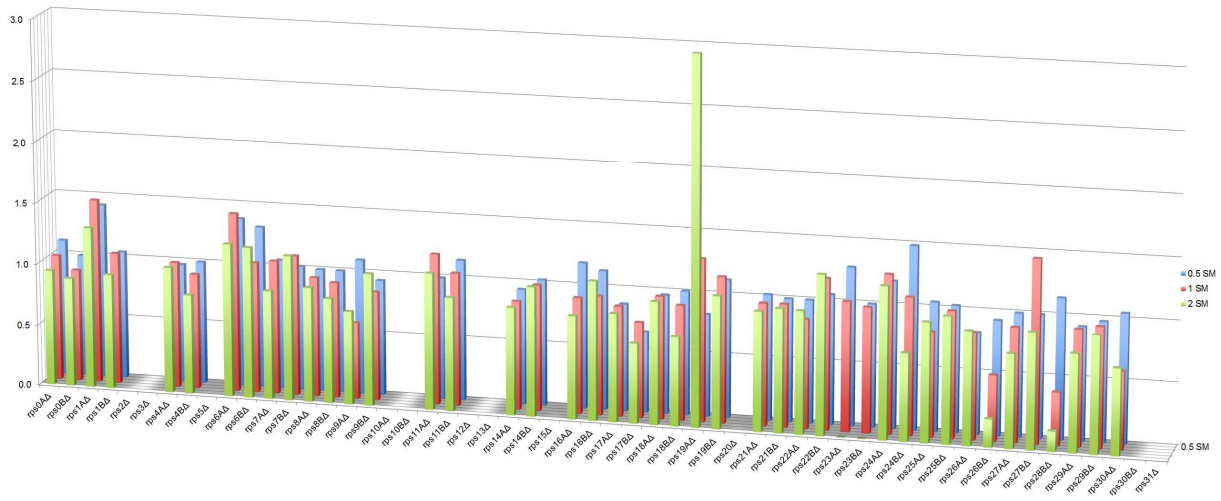

Figure 11: Bar graphs representing the results of the scoring of the SM sensitivity phenotypes of all investigated rpsΔ strains to three different concentrations of SM.

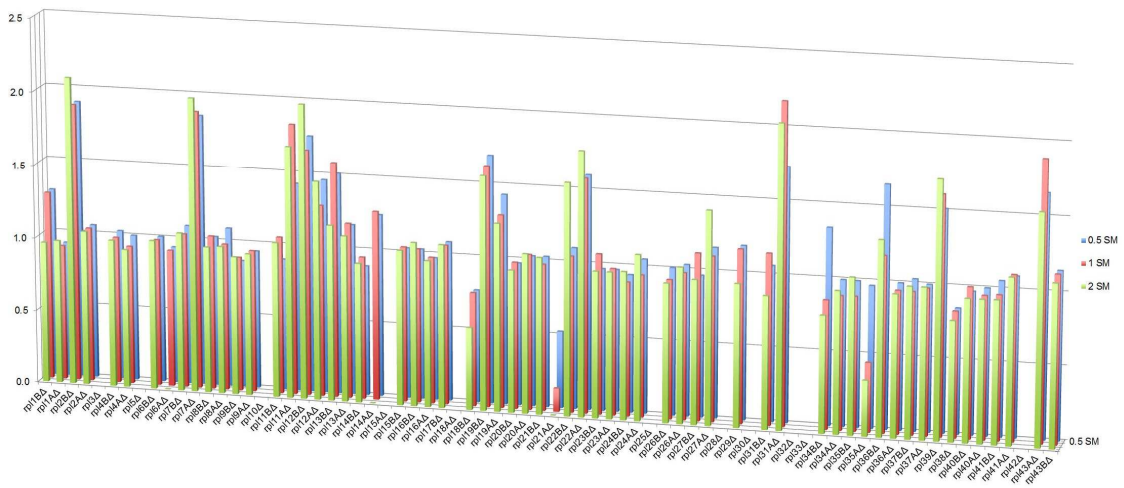

Figure 12: Bar graphs representing the results of the scoring of the SM sensitivity phenotypes of all investigated *rpl*Δ strains to three different concentrations of SM.

The bar graphs in Figure 11 & Figure 12 demonstrate the results of all investigated *rpxΔ* strains after they have been normalized to the correct met or MET WT. Most *rpx*Δ strains oscillate with their SM sensitivity around the value 1, which means that they grew similar to the WT. Strains that grew less than the WT in the presence of SM and therefore have SM sensitivity phenotype have values below 1. *rps26A*Δ, *rps28B*Δ, *rpl21A*Δ and *rpl35A*Δ strain show an ideal SM sensitivity phenotype increment with increasing SM concentration, whereas *rpl14A*Δ strain and *rpl6A*Δ strain for example only show severe SM sensitivity under the highest SM concentration but grow similar to WT under lower SM concentration (Figure 11 & Figure 12) suggesting that their SM^S is weak. As can be seen from Figure 11 & Figure 12 we did not only observe strains with SM^S but also strains that resulted in SM resistance (SM^R), indicative by the strains ability to grow better than the WT under amino acid starvation conditions. Strains with SM^R are: *rps19B*Δ, *rpl7A*Δ, *rpl11A*Δ, *rpl22A*Δ, *rpl31A*Δ and *rpl39*Δ strain. The images of their growth assays can be seen in Figure 13.

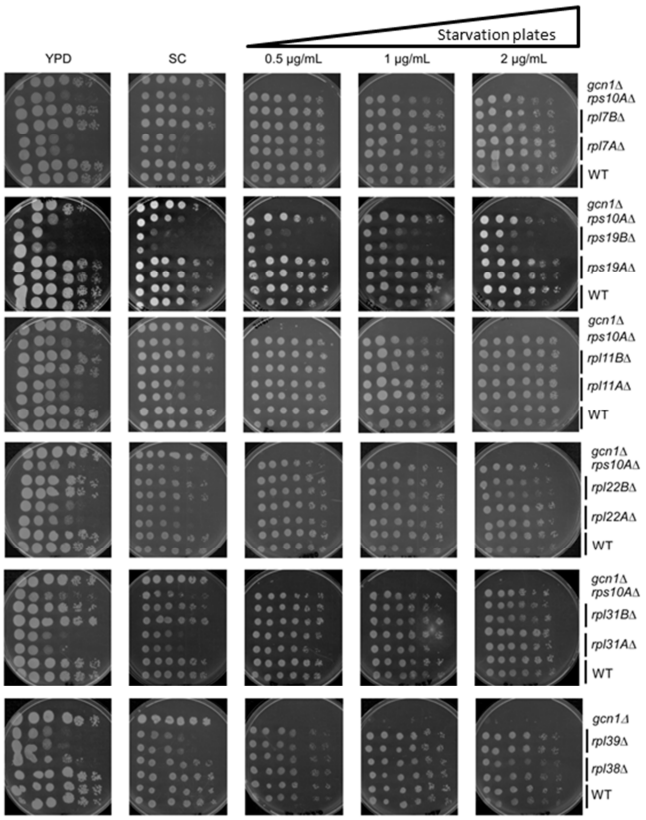

Figure 13: Semi-quantitative growth assays of strains with SM resistance.
The experiment was conducted as outlined in Figure 8.

Overall, the semi quantitative growth assay uncovered SM sensitivity of 14 *rpx*Δ strains, suggesting that these are important for mediating Gcn2 activation.

3.2 Screening *rpx*Δ strains with SM^S phenotype for those with impaired Gcn2 activation

The SM sensitivity observed for *rpx*Δ in the previous chapter may be indicative of their inability to activate Gcn2. However, it can also be due to an unrelated effect such as impaired protein synthesis or affected ribosome biogenesis. If the knockdown of a gene encoding for a ribosomal protein, affects Gcn1 function, then Gcn2 activation should be impaired and this can be detected by its reduced kinase activity. We therefore chose to monitor the phosphorylation levels of eIF2α (eIF2α-P) the substrate of Gcn2. If Gcn2 activation is diminished we expect to see a reduction in eIF2α-P levels.

Cell cultures of isogenic WT strains (BY4741&BY4742), *gcn2*Δ and *rpx*Δ strains were prepared for an overnight culture. Reaching saturation we inoculated two sets of new media using the overnight cultures. In the exponential phase, one set (starvation set) was starved for 1h by adding SM to a final concentration of 1 µg/mL, while the second set was not exposed to SM. The cultures were harvested and the whole cell extract generated and subjected to sodium dodecyl sulphate polyacrylamide gel electrophoresis (**SDS-PAGE**). The proteins were transferred onto a PVDF membrane and immunoblotted using antibodies against phosphorylated eIF2α (**eIF2α-P**) and phosphoglycerate kinase, **Pgk1**, as control for equal loading. The membrane was cut to allow simultaneous detection of eIF2α-P: 36 kDa and Pgk1: 45kDa. The signal quantification of eIF2α-P and Pgk1 was carried out with the V3.1 software from Multi Gauge (Fujifilm). The relative phosphorylation level was calculated for each strain by dividing the eIF2α-P signal by that of the loading control. Those values were then divided by the ratio of the WT under amino acid starvation to normalize the data (Calculation example can be found in chapter 2.3.3.5).

Isogenic WT strains were used as positive controls. As they have the ability to activate Gcn2, these strains are expected to show a distinctive increase in eIF2α-P under amino acid starvation compared to unstarved level. *gcn2*Δ strain was taken as a negative

control, expected not to show any eIF2α-P signal as the strain lacks Gcn2. We propose that strains with a deleted gene encoding a ribosomal protein important for Gcn2 activation to have a reduced eIF2α-P level. This phenotype is called a Gcn$^-$ phenotype.

Fourteen *rpx*Δ strains with weak and strong SM sensitivity have been subjected to this assay. Figure 14 presents the western blots for five *rpx*Δ, which showed a reduced eIF2α-P level when compared to WT level. All others can be seen in the appendix, Section D.

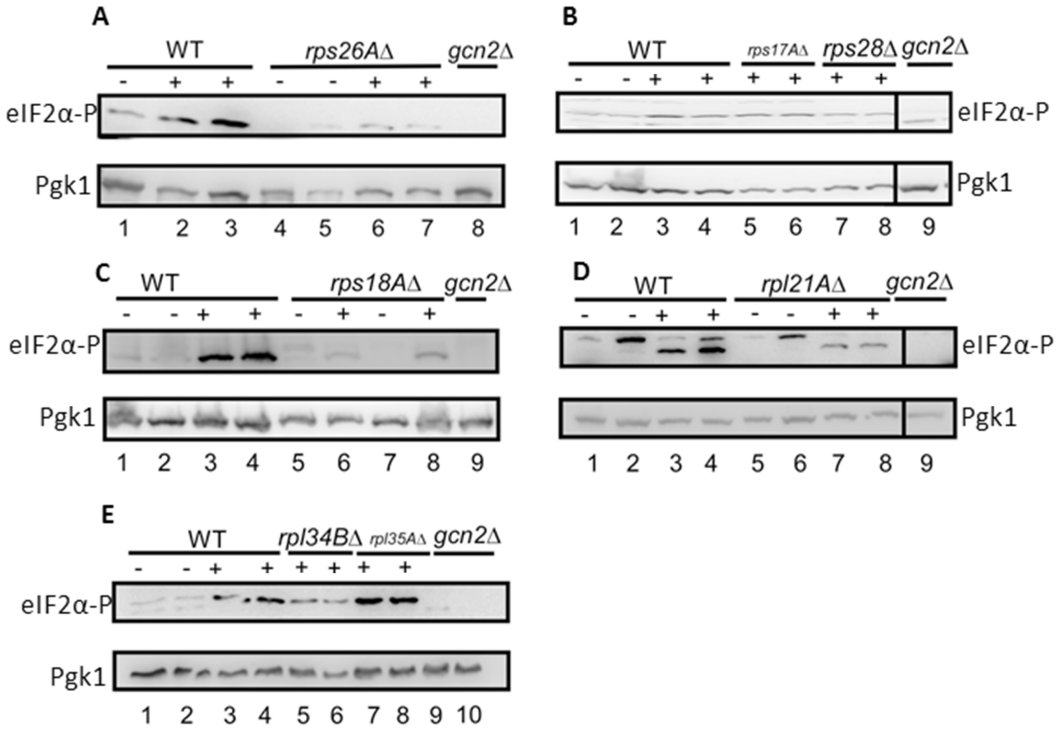

Figure 14: Five *rpx*Δ strains lead to reduced phosphorylation of eIF2α under amino acid starvation.
Immunoblot of phosphorylated eIF2α from indicated strains cultured in complete (-) and starvation media (+). The starvation was induced by the addition of SM to a final concentration of 1 µg/mL 1h before harvesting. The whole cell extract was subjected to SDS-PAGE and the proteins transferred onto a PVDF membrane. The membrane was probed with eIF2α-P specific antibodies (top row) and antibodies against Pgk1 (bottom row) as loading control. Immune complexes were visualized by enhanced chemiluminescence.

The presented western blots in Figure 14 showed the expected behaviour of the control strains. The increase in the basal level of phosphorylated eIF2α from the unstarved (-) to starved (+) WT indicated the effectiveness of the drug to induce amino acid starvation.

The negative control (*gcn2*Δ) strain showed no eIF2α phosphorylation under any condition. It was interesting to note, that the increase in phosphorylation of the BY4741 WT seemed to be slightly lower than that of the BY4742 WT (Figure 14,D lane 3 and 4). This is in accordance with the more severe SM sensitivity phenotype observed for BY4741.

Figure 15 shows the quantification of the western blots. The normalized eIF2α-P levels are illustrated relative to unstarved WT strain.

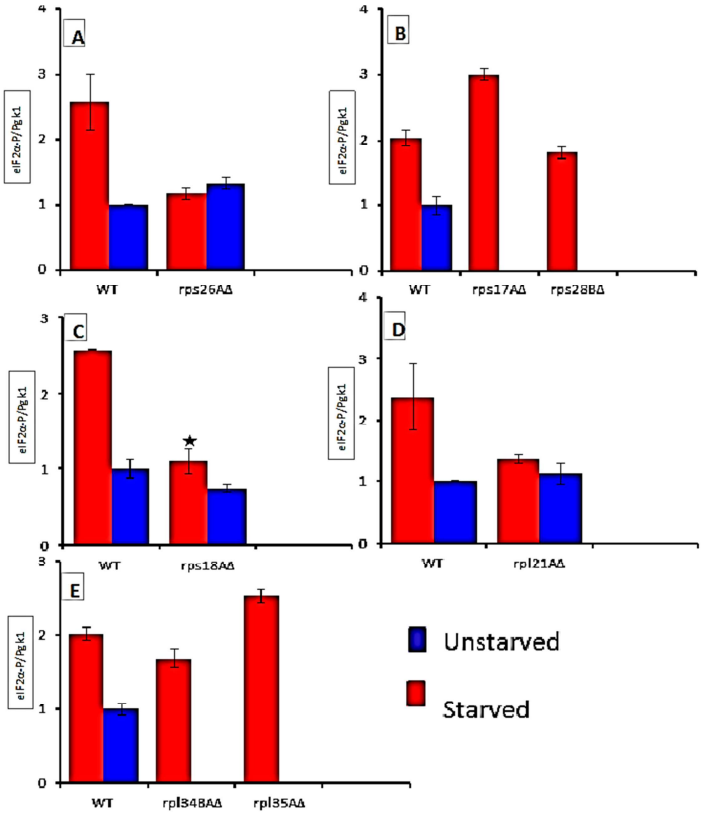

Figure 15: eIF2α phosphorylation levels of *rpx*Δ strains relative to WT.

The intensity of the eIF2α phosphorylation signal from Figure 14 was quantified by densitometry using the Multi Gauge V3.1 software (Fujifilm). eIF2α phosphorylation levels of unstarved (-, blue) samples and amino acid starved (+, red) is shown relative to that of the WT under unstarved conditions. The increase in phosphorylation level of the starved WT sample compared to unstarved WT sample indicates a proper starvation accomplishment. The standard error bars of two independent colonies are indicated. The star (★) illustrates statistically significant ($P<0.05$) difference between the values of starved cultures and starved WT when a two-tailed t-test was conducted.

Upon the tested strains, the deletion of *RPS18A* and *RPS26A* had highest effect on Gcn2 activation as judged by reduction in eIF2α phosphorylation under amino acid starvation.

*rps28B*Δ strain showed the least effect on Gcn2 activation, hence the deletion of *RPS28B*Δ resulted in the lowest decrease in eIF2α phosphorylation. For example *rps18A*Δ strain reached 50% of the phosphorylation level of eIF2α under amino acid starvation compared to the WT whereas *rps28B*Δ strain increased eIF2α-P to 90%. To determine whether the reduction in eIF2α-P is significant a two-tailed t-test was performed. Obtained p-values greater than 5 % (0.05), are considered with a probability of 95% to be insignificant. The t-test suggested that only *rps18A*Δ strain showed a significant decrease in eIF2α-P level when compared to the WT level. The outcome of the conducted t-tests can be explained with deviations in the results of the duplicate samples used for each strain. As the t-test requires a minimum of two data sets per sample for comparison we had to use results of two different WT strains and treated them incorrectly as duplicate samples. In order to be able to perform the t-test however that was the only possibility. For this reason it might be that from the five strains assayed more strains can have a significant reduction in eIF2α-P.

From the experiments above, it can be suggested that the five strains: *rps18A*Δ, *rps26A*Δ, *rps28B*Δ, *rpl21A*Δ and *rpl34B*Δ that have a reduction in eIF2α-P level ranking from 90 % to 50 % of that of the WT, had impaired Gcn2 activation. This indicates that rps18, rps26, rps28, rpl 21 and rpl34 are necessary for promoting Gcn2 activation.

3.3 Complementing *rpx*Δ strains with SM^S and impaired Gcn2

According to our studies, five *rpx*Δ strains did not only show SM^S but also decreased eIF2α-P levels. These findings suggested that these strains were impaired in activating Gcn2. However, the same phenotype could arise from a mutation in a gene other than the gene encoding for a ribosomal protein, such as *GCN1* or *GCN2* itself. If the SM sensitivity is truly due to the deletion of the gene encoding the ribosomal protein, reintroducing the gene should revert the SM sensitivity phenotype. Plasmid carrying the ribosomal protein genes were not available but instead the yeast genomic tiling collection. Due to time constraints, this collection consisting of a complete overlapping clone collection of the *Saccharomyces cerevisiae* genome allowed an initial complementation, to verify whether the SM sensitivity phenotype was due to the

deletion of the respective gene. To test this, we transformed five *rpx*Δ strains with the 2 micron-based LEU2 collection vector containing 10 kb inserts of genes of which one encodes for the respective ribosomal protein and conducted the same growth assay as in chapter 3.1.

In addition, we also transformed the strains with an empty vector as control. The same transformations were also carried out with the WT strain and the *gcn1*Δ strain. WT transformed with the tiling collection plasmid was used as control to verify that the transformation of the plasmid does not negatively influence the cell's fitness. In case of *gcn1*Δ the transformation was performed to test whether the introduced gene in itself can lead to a reversion of the SM sensitivity phenotype. As only *RPS26B* was available on the tiling plasmid of the collection, we used this paralogous gene to test for complementation. This is possible as ribosomal paralogous genes were shown to be functionally redundant (T. Y. Kim et al., 2009). However, we are aware of the fact that a complementation would require the reintroduction of the A version to complement *rps26A*Δ strain, nevertheless, for simplicity reason, we expand the term of complementation also for paralogous gene reintroduction.

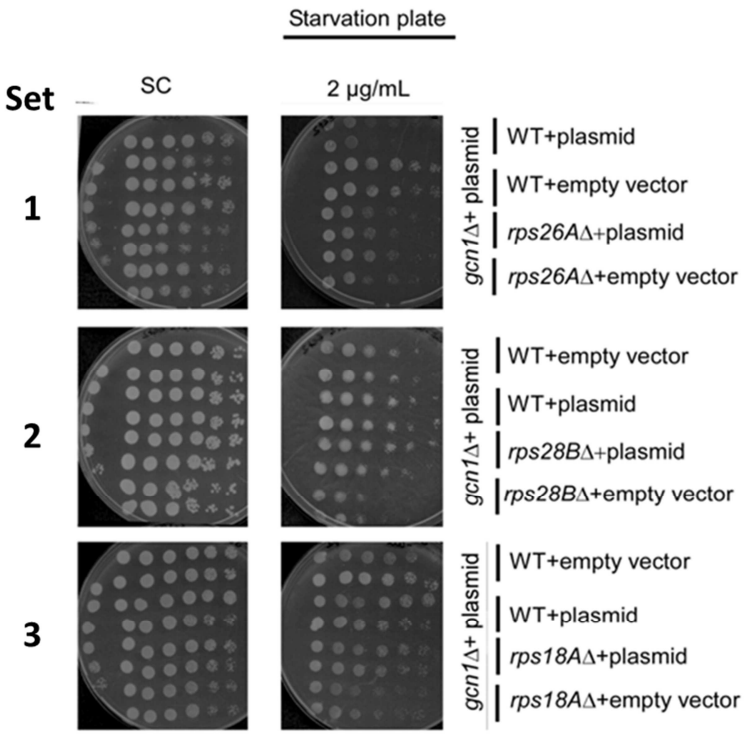

Figure 16: Complementation assay of *rpx*Δ strains.
Plasmids containing ribosomal genes were transformed into WT gcn1Δ and rpxΔ strains and subjected to semi-quantitative growth assays as described in chapter 2.3.6.

All transformed WT strains containing the collection plasmid grew similar to the WT strains transformed with empty vector under replete conditions (Figure 16), suggesting that the tiling collection plasmid does not affect the cell's fitness. The *gcn1Δ* strain with induced tiling collection plasmid did not grow on the starvation media but on plates without SM (SC), as expected. This verified that the drug did trigger the desired amino acid starvation and that the introduction of the plasmid in itself does not revert the SM sensitivity.

Curiously WT strain transformed with the tiling collection plasmid containing *RPS26B* grew worse than the WT strain transformed with empty vector under starvation conditions, suggesting that the transformation of the plasmid into WT strain affects the strains ability to overcome amino acid starvation (Figure 16, Set1). Equally we observed that the *rps26AΔ* strain containing the tiling plasmid (*rps26AΔ*+plasmid) grew similar to the strain containing the empty vector *rps26AΔ*+empty vector. As we expect this strain to have a SM sensitive phenotype, the above described result suggests that the fragment on the tiling plasmid transformed into *rps26AΔ* did not complement the phenotype of the strain. Regarding the fact that the plasmid affected WT growth under starvation conditions, we reason that a gene on the plasmid affects the stress response of the cell when expressed at higher levels. The tiling collection plasmid used for *rps26AΔ* strain complementation consisted of 7 genes of which one (YER130C) encodes a yet unknown protein in yeast. This protein has a homolog in *Candida albicans* (MNL1) and is here known to play a role in adaptation to acid–induced stress (Ramsdale et al., 2008). Based on this information we assume that the overexpression of this protein from the 2 micron collection plasmid interfered with the starvation response of the strain. For this reasons, the complementation of the *rps26AΔ* strain needs to be repeated. This can be done, by subcloning *RPS26B* into a plasmid and introduce this plasmid into the *rps26AΔ* strain. Due to time constraints this was not included in this study.

The growth of *rps28BΔ* strain transformed with the plasmid (*rps28BΔ*+plasmid) was similar to WT growth under amino acid starvation (Figure 16, Set2). The comparison of the growth of the transformed strain with tiling plasmid to the strain transformed with empty vector showed that the strain containing the plasmid grew better than the strain containing empty vector, suggesting that there is complementation. As a result, the SM sensitivity phenotype of the deletion strain was reverted. A similar result was observed

for *rps18A*Δ strain. The strain grew less when transformed with the empty vector alone as compared to the strain transformed with the tiling collection plasmid, hence the *rps18A*Δ strain was complemented (Figure 16, Set3). Overall we transformed five ribosomal deletion strains with their missing gene and were able to revert the SM^S phenotype of two strains.

3.4 Testing the feasibility of suppression assays using *rpx*Δ strains

The previously described screens investigated whether the ribosomal protein knockdown affects the activation of Gcn2 and therefore the cell's ability to overcome amino acid deprivation. We know that the direct contact of Gcn1 as well as Gcn2 to the ribosome is crucial for Gcn2 activation. As Gcn2 location on the ribosome is not fully known, it is possible that the observed SM sensitivity of some strains could result from the loss of ribosomal contact points of either Gcn1 or Gcn2. It was therefore necessary to uncover which of the ribosomal proteins contact Gcn1 or Gcn2. To address this task we aimed to overexpress Gcn1 or Gcn2 in the *rpx*Δ strains. We expected that the overexpression of Gcn1 or Gcn2 will strengthen the binding of Gcn1 or Gcn2 to the ribosome based on mass action. As a result the SM^S phenotype of the deletion strain would be rescued. If Gcn2 was able to rescue the phenotype when overexpressed in a *rpx*Δ strain, it would suggest that the deleted ribosomal protein was a binding site for Gcn2. The same is applicable for the overexpression of Gcn1.

For this purpose our aim was to subject the five *rpx*Δ strains, which had impaired Gcn2 activation as, judged by reduced eIF2α-P to a suppression assay. We therefore transformed the strains with a high copy (**hc**) plasmid expressing myc-tagged *GCN1* or *GCN2* from their own promoter. The same transformation was done with the control WT strains BY4741 and BY4742 and *gcn1*Δ strain. All strains have additionally been transformed with an empty vector control. The strains were then subjected to a semi-quantitative growth assay following the same procedure as in chapter 3. Due to time restrictions, we chose to test the feasibility of this approach with *rps18A*Δ and *rpl21*AΔ strain. We decided on transforming high copy *GCN1* into *rps18A*Δ strain and high copy *GCN2* into *rpl21*AΔ strain as we expected that rps18 will be a binding partner of Gcn1, due to its location on the 40S head region, whereas Gcn2 was shown to bind the 60S

subunit (Ramirez et al., 1991), hence it could possibly bind rpl21. If Gcn1 requires the binding of rps18 to activate Gcn2, then the overexpression of Gcn1 in *rps18A*Δ should rescue the SM sensitivity phenotype of the strain. If Gcn2 needs to bind rps21, then the overexpression of Gcn2 in *rpl21A*Δ should rescue the SM sensitivity phenotype of the strain.

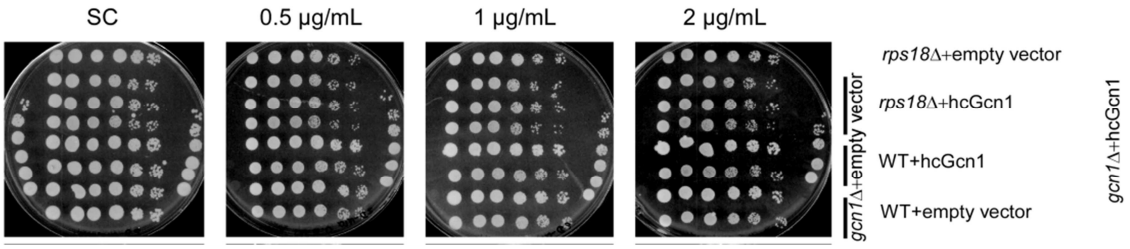

Figure 17: Suppression assay of *rps18A*Δ strain with high copy (hc) Gcn1.

As expected, the transformed WT strains did grow under all conditions and did not show a difference in growth between WT containing the plasmid or the empty vector (Figure 17). Our negative control *gcn1*Δ strain containing empty vector did not grow under amino acid starvation, but grew when it contained high copy *GCN1* instead, suggesting that the drug triggered the amino acid starvation and that high copy Gcn1 can rescue the Gcn$^-$ phenotype of the *gcn1*Δ strain. Furthermore it can be observed, that the *rps18A*Δ strain with empty vector still has a similar SM sensitivity phenotype as found in Figure 8. The strain containing high copy *GCN1* plasmid however grew similar to that containing empty vector under amino acid starvation, suggesting that the hcGcn1 plasmid was unable to rescue the weak SM sensitivity phenotype of the strain (Figure 17), for more see chapter 4.1.

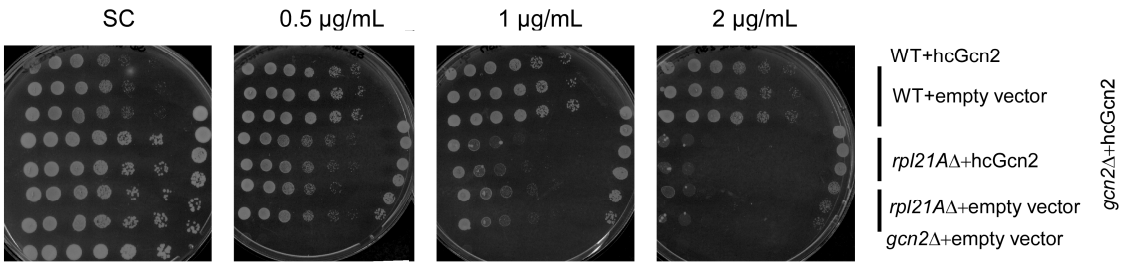

Figure 18: Suppression assay of *rpl21A*Δ strain with high copy (hc) Gcn2.

The control strains in Figure 18 showed expected behaviour. The WT strains did grow under all conditions and did not show a difference in growth between WT containing the plasmid or the empty vector. Also as expected, the *gcn2*Δ strain containing empty vector did not grow under amino acid starvation, but grew when it contained high copy *GCN2* instead, indicating that the starvation was induced and that high copy Gcn2 can rescue the phenotype of the strain. We observed, that the *rpl21A*Δ strain transformed with empty vector maintained its SM sensitivity phenotype (chapter 3.1, Figure 9) and that *rpl21A*Δ strain containing high copy *GCN2* showed a similar phenotype. This suggested that high copy number of Gcn2 cannot rescue the phenotype caused by *RPL21A* deletion.

4. Discussion

Parts of the results described in this chapter were presented in the following international and national conferences:

National conferences:

- QMB – **Q**ueenstown **M**olecular **B**iology conference 2013 " Mapping Gcn1 on the ribosome" by Viviane Jochmann (Poster presentation, won the best poster award)
- INMS – **I**nstitute of **N**atural and **M**athematical **S**ciences student conference 2013 " Mapping Gcn1 on the ribosome" by Viviane Jochmann (Poster presentation)
- YPD –**Y**east, **P**roducts, **D**iscovery Meeting 2013
  "Mapping Gcn1 on the ribosome" by Viviane Jochmann (Poster presentation)
- NZMS –**N**ew **Z**ealand **M**icrobiological **S**ociety conference 2013, New Zealand "Gcn1 binding to the 40S ribosome head region is essential for fully activating the ancient nutrient-sensor-kinase Gcn2". (Oral presentation by E. Sattlegger)

International conferences:

- EMBL – **E**uropean **M**olecular **B**iology **L**aboratory conference 2013, Germany. "Gcn1 binding to the 40S ribosome head region is essential for fully activating eIF2α kinase Gcn2" (Oral presentation by E. Sattlegger)

4.1 Ribosomal binding points of Gcn1 found to be necessary to promote Gcn2 activation

In case of amino acid deprivation it has been exceedingly described how the cell regulates the global translation and activates the expression of stress response genes in order to survive (Hinnebusch, 2005). The expression of the stress response genes is performed via a cascade of events in the GAAC, one of which is the activation of Gcn2 which requires the protein Gcn1 and its association with the ribosome. The purpose of this research project was to determine crucial ribosomal binding partners of Gcn1 for Gcn2 activation. Regarding this purpose, we performed genetic assays to look for impaired growth on SM plates as well as reduced eIF2α-P level in *rpx*Δ strains. We complemented some strains with their missing gene in a 10 kb fragment to see if their SM sensitivity phenotype was reverted.

In chapter 3.1, we showed the result of *rpx*Δ strains, which when grown under amino acid starvation caused a growth defect compared to the WT. We found six *rpx*Δ strains resulting in strong SM sensitivity and eight in weak SM sensitivity. However, as the location of the ribosomal proteins and whether they are clustered on the ribosome can influence the degree of their deletion phenotype, we cannot relate the strength of a phenotype to the cells ability to overcome amino acid starvation. A ribosomal protein reduced in a strain resulting in a weak SM sensitivity phenotype, might still be equally required for overcoming starvation as proteins whose knockdown led to a strong SM sensitivity phenotype.

Surprisingly, for all of the investigated *rpx*Δ strains, only one of the paralogous gene knockdowns resulted in the SM^S phenotype in our screen. This seems to be paradox as the majority of the ribosomal paralogous genes are 98 % identical in their amino acid sequence (T.-Y. Kim, C. W. Ha, & W.-K. Huh, 2009) (Pnueli & Arava, 2007) (K. K. Steffen et al., 2008). For this reason we expected to see a similar effect for the deletion of each of the paralogous genes. It needs to be pointed out, that paralogous genes show some severe differences in their untranslated regions, including the non-homology in their promoter sequences (Komili et al., 2007). Based on this knowledge we suggested that the differences in SM^S phenotypes of paralogous genes knockdowns, was due to

different expression levels of those genes. To aim for more transparency, we compared the published expression levels of both paralogous genes with our SM sensitivity screen results. The expression levels of each ribosomal paralogous gene were taken from the yeast genome database and derived from a global protein expression analysis in yeast by S. Ghaemmaghami (Table 10) (Ghaemmaghami et al., 2003)

For the *rps9*Δ strain for example, the SM sensitivity phenotype (Figure 8, Set1) correlated with the corresponding gene expression level. The expression level of *RPS9B* for example is six times higher than for *RPS9A* and therefore the *rps9B*Δ has stronger sensitivity to SM. The same behaviour was observed for rpl14Δ strain. These observations are in accordance with the ribosome insufficiency model that theorizes that the severity of a phenotype correlates with the expression level of its corresponding gene (Horiguchi, Van Lijsebettens, Candela, Micol, & Tsukaya, 2012).

Table 10: Ribosomal gene expression levels as known and stated by the yeast genome data base. Data derived from a global protein expression analysis in yeast by S. Ghaemmaghami et al. 2003.

Ribosomal protein (rp)	Expression level for gene A	Expression level for gene B
rps9	10600	63300
rps16	33800	unknown
rps17	30900	30500
rps18	48100	112000
rps24	unknown	6160
rps26	16300	503000
rps28	inviable	8600
rps30	37600	inviable
rpl6	37100	38400
rpl14	45300	35100
rpl18	unknown	63700
rpl21	unknown	66400
rpl34	23600	21000
rpl35	unknown	19100

Many *rpx*Δ strains that have SM sensitivity, however, arose from the deletion of the paralogous gene, which is expressed less. For example rps26B is 30 times more abundant in the cell than rps26A (Table 10). Based on this, we expected to see a stronger phenotype for the *rps26B*Δ strain than for *rps26A*Δ. However, we saw the

opposite. The same discrepancy was found for *rps18*Δ and *rpl34*Δ. The expression levels of both paralogous genes of *RPS17* and *RPL6* are almost identical, but a SM sensitivity phenotype was only seen for one of the paralogous gene deletions. A possible explanation for this phenomenon would be that only the proteins expressed from one of the paralogous gene play the predominant role in stress response. This means that in case of *rps26*, *rps18* and *rpl34*, proteins from the lower expressed gene seem to be more important in the stress response than their higher expressed protein counterpart. However, we have to take into account that the global protein expression study of S. Ghaemmaghami does not necessarily reflect the correct amount of proteins per cell, as the ribosomal proteins were GFP tagged and this large tag could have interfered with the proteins incorporation into the ribosome and therefore could have led to the proteins degradation.

The difference in phenotype in our screen might therefore be due to different functions of the ribosomal paralogs or due to ribosomal paralogs that are incorporated under different specific conditions into the ribosome. Different functions of ribosomal paralogs have already been suggested by Kim (2009) who found that rpl7A is localised in the cytoplasm but its paralog rpl7B is additionally localised in the nucleus, indicating that the physiological roles of both identical proteins might be different (T. Y. Kim et al., 2009). Apart from different functions within the ribosome, such as assistance in ribosome assembly and stabilization of the ribosome (Pnueli & Arava, 2007), single ribosomal proteins were found to function outside of the ribosome, including processes like DNA repair and auto regulation of ribosomal protein synthesis (Shenoy et al., 2012). Assumedly only the higher expressed gene encodes the protein with non-ribosomal function and therefore the knockdown of this protein has no effect on the GAAC. This might also explain why we only saw SM sensitivity for the strain containing the knockdown of the lower expressed gene.

The deletion of a ribosomal protein can also affect the function of the ribosome. If the deletion of a ribosomal gene affects translation it should lead to a growth defect of the *rpx*Δ strain, a phenomenon that was reported before (K. K. Steffen et al., 2008). In our study, we found that some *rpx*Δ strains had a severe growth defect which made it impossible to score for SM^S. We have to consider that impaired ribosome function could somehow lead to Gcn2 activation, however, arguing against this scenario, not all

strains resulting in a growth defect under nutrient replete conditions also had SM^S (*rps1B*Δ, appendix, Section A, Test nr: 29). The lack of a ribosomal protein could also affect the inhibitory functions of the Gcn4 uORFs. Impaired Gcn4 expression would lead to a SM^S phenotype. Together, this raises the possibility that the observed SM^S phenotype is due to an effect unrelated to impaired Gcn2 activation. However, these strains can easily be identified since Gcn4 is downstream of Gcn2 activity. In this scenario one would therefore not expect to see a reduced eIF2α phosphorylation in these strains.

As much as the ribosomal protein knockdown can impair Gcn4 expression, it can also improve Gcn4 translation. In our semi-quantitative growth assay we observed that some strains did grow better than the WT strain and therefore showed a SM resistance (Figure 13). For example, the knockdown of a large ribosomal protein could lead to a decrease in 60S subunits. This in turn could lead to a bypass of the ORFs of Gcn4 by the 40S subunits as they have less 60S subunits to reinitiate with. Consequently this would increase the Gcn4 translation. This theory finds support in the results of rpl gene mutations that induced the expression of Gcn4 reporter (Martin-Marcos, Hinnebusch, & Tamame, 2007). Another possibility for SM resistance is increased transcription of selected genes that prevent import of SM into the cell, or increased expression of genes that counteract the effect of SM. Furthermore, Gcn2 activation could possibly increase by a mechanism that allows Gcn2 to get easier access to the uncharged tRNA in the ribosomal A-site. However, we are interested in finding ribosomal proteins that affect Gcn2 function rather than in events downstream of Gcn2.

In order to ensure that in fact Gcn2 function was impaired in a *rpxΔ* strain with SM^S, we scored for the phosphorylation of eIF2α. As eIF2α is the substrate of Gcn2, this assay directly informs us whether a ribosomal protein affects processes downstream or upstream of Gcn2. Based on results of our study this means that *rps9B*Δ, *rps16A*Δ, *rps17A*Δ, *rps24A*Δ, *rps30A*Δ and *rpl6A*Δ, *rpl14A*Δ, *rpl18B*Δ, *rpl35A*Δ strains, which showed impaired growth on SM but unchanged eIF2-P levels, affect a process downstream of Gcn2.
*rps18A*Δ, *rps26A*Δ, *rps28B*Δ and *rpl21A*Δ, *rpl28B*Δ strains, however, affect Gcn2 activation upstream of Gcn2. When comparing *rpx*Δ strains that appear to have affected GAAC upstream of Gcn2, some of them showed a more pronounced SM^S phenotype

when compared to the effect on eIF2α-P (*rps28B*Δ strain and *rpl34B*Δ strain), or vice versa (*rps18A*Δ strain). The former may be attributed to the ribosomal protein knockdown affecting the GAAC upstream, as well as downstream of Gcn2.

In order to distinguish whether Gcn2 is directly affected by the knockdown of a ribosomal protein or is indirectly affected by the impairment of Gcn1 due to the knockdown of a ribosomal binding partner of Gcn1, we tried to overexpress Gcn1 or Gcn2, in *rpxΔ* strains. If the interaction of a ribosomal protein is affected, then their overexpression should compensate for this defect by mass action, thereby rescuing the SM^S phenotype. *rps18A*Δ strain containing the high copy Gcn1 plasmid did not show a rescue of the weak SM sensitivity phenotype. Nevertheless based on the previous findings with this strain, we still trust in the protein interaction between rps18 and Gcn1 and reason, that the high copy plasmid did not lead to a high enough expression of Gcn1 to rescue the phenotype of the deletion strain. Supporting this idea, Cridge et al. 2013 found that the expression of low copy and high copy *GCN1* is lower than expected. To illustrate, the low copy Gcn1 levels only reached half of the endogenous Gcn1 level (Cridge, Visweswaraiah, Ramesh, & Sattlegger, 2014). Alternatively a suppression experiment could be repeated by using a plasmid in which the protein of interest is expressed from a strong galactose-induced promoter. However, this approach is not feasible for Gcn1, because such extreme Gcn1 expression leads to a SM sensitivity phenotype by itself (Sattlegger, unpublished).

Introduction of hcGcn2 into the *rpl21A*Δ strain did not rescue the SM sensitivity phenotype of this strain, suggesting that rpl21 is likely to bind to Gcn1 and not to Gcn2. However, physical interaction studies are necessary to verify this theory.

To find further support for our results, we decided to include other screening projects of Gcn1.

4.2 Ribosomal proteins that are necessary for Gcn2 activation were also found in other studies

Deletion studies in which mutations in different regions of *GCN1* led to reduced polyribosome binding of Gcn1 suggested that, Gcn1 has several ribosomal contact

points (Sattlegger & Hinnebusch, 2005). Taking this as a fact, the deletion of one contact point will not remove Gcn1 from the ribosome and therefore maintains Gcn2 activation (Sattlegger & Hinnebusch, 2005). Taking advantage of this phenomenon allowed us to study Gcn1-ribosome interaction that is not only involved in ribosome binding, but also important for Gcn1 function. If a ribosomal protein is necessary for a functional Gcn1-ribosomal interaction than this protein should also be found in other studies that uncovered possible Gcn1 interaction partners. Previously the Sattlegger group conducted a yeast-two-hybrid (**Y2H**) screen in order to uncover interactions between Gcn1 and small ribosomal proteins (S.J.Lee and E.Sattlegger). Within this screen, two fragments of Gcn1 encompassing amino acids [1-900] and [1067-1777] were chosen as pray and bait. Further research on Gcn1 binding partners was performed in the Sattlegger group by R. Shanmugam and E. Sattlegger in a Co-immunoprecipitation (**Co-IP**) study. Gcn1 was myc-tagged, and formaldehyde cross-linked or not, whole cell extracts subjected to co-IP using anti-myc antibodies. Using formaldehyde as a cross-linking agent prevented the loss of proteins during the experimental procedure that only weakly interact with each other. The co-precipitated proteins were identified via mass spectrometry. Apart from the Sattlegger lab, comprehensive studies from other research labs gave additional information about possible contact partner of Gcn1. Gavin et al. 2006 for example used TAP tagged Gcn1 to co-purify proteins and found ribosomal proteins in their approach (Gavin et al., 2006). Table 11 shows the findings of these approaches and compares them with the screens performed for this thesis.

Table 11: Result comparison of the Y2H interactome and Co-IP study with the results obtained in this study.

Ribosomal protein	Y2H		Growth assay	eIF2α-P reduction	Presence in Co-IP
	fragment(1-990)	fragment(1060-1777)			
rps0A	+ (AD)	++ (AD)		no	yes
rps1B					yes*
rps3			not determined	not determined	yes*
rps4A			(+)	not determined	yes
rps5	+ (AD)		not determined	not determined	yes
rps6A				no	yes
rps9A		(+) BD			no
rps9B			++	no	no
rps10A	+++ (BD)	+++ (BD) (+) AD	+	yes	yes
rps13		++ (AD)	not determined	not determined	no
rps14A			(+)	not determined	yes
rps15	++ (BD)	++ (BD) (+) AD	not determined	not determined	no
rps16A			(+)	not determined	yes
rps17A		+ (AD)	++	no	no
rps18A		+ (AD)	+	yes	yes
rps19A		++ (BD) +(AD)			no
rps23A		++ (BD)			no
rps24A			+	no	yes
rps25A	+++ (BD)	((+))(BD)			no
rps25B			(+)	yes (10%)	no
rps26A			+++	yes	no
rps28A		+ (BD)			no
rps28B			+++	yes	no
rps29A		+ (AD)			no
rps30A			++	no	no
rps31A		+ (BD)	not determined		no
rpl4B	not determined	not determined			yes*
rpl6A	not determined	not determined	++	no	no
rpl14A	not determined	not determined	++	no	no
rpl18B	not determined	not determined	++	no	no
rpl21A	not determined	not determined	+++	yes	yes
rpl34B	not determined	not determined	+++	yes	no
rpl35A	not determined	not determined	+++	no	no

found in 1 assay and has weak SM sensitivity

found in 1 assay and has medium to strong SM sensitivity

found in 2 assays and has medium SM sensitivity

weak SM sensitivity

medium SM sensitivity

strong SM sensitivity

very strong SM sensitivity

weak interaction

medium interaction

strong interaction

very strong interaction

* found by Gavin et al. (2006)

A trial study by S.J. Lee from the Sattlegger lab on rps10 did not only show Y2H interaction for rps10A but also SM^S for both paralogous gene deletions. Rps10 was additionally found in the Gcn1 Co-IP study (Table 11). Furthermore, *in vitro* studies confirmed that there is direct interaction between Gcn1 and rps10 (Lee, Swanson & Sattlegger, Manuscript in preparation). This study demonstrated that the genetic approach performed for this thesis was feasible for identifying interactions required for Gcn1 function.

When we compared results from our study with referenced studies, we found rps18A in the Y2H screen and in the Co-IP experiments, in addition to the SM sensitivity phenotype and reduced eIF2α-P level in our work. In our research rps28B had SM sensitivity and reduced eIF2α-P level and was previously found in the Y2H screen but with its paralog rps28A. However, rps28 was not detected in the Co-IP studies. This might be due to a weaker or transient interaction of rps28 with Gcn1 that did not withstand the experimental procedure of the Co-IP. It is also possible that due to insufficient amount of rps28, detection via mass spectrometry failed. rpl21A which in our experiments resulted in SM sensitivity and reduced eIF2α-P level was likewise found in Co-IP studies to interact with Gcn1.

Our results and compared with third party data, strongly suggest that rps18A, rps28B and rpl21A are crucial binding partners for Gcn1 and are necessary for Gcn2 activation under amino acid starvation.

The Y2H data and the Co-IP data do not show identical results, indicating that these approaches include false negative or positive data. The Y2H screen found interaction between Gcn1 and rps13, rps15, rps17A, rps19A, rps23A, rps29A and rps31A which were not found in the Co-IP. The reason might be false positive results in the Y2H screen, which occur when reporter activity is observed even though the two investigated proteins normally do not interact with each other. For example, forced interactions between proteins in Y2H assays can occur as the expression of the genes is under a high expression promoter. Another possibility for the absence of ribosomal proteins in the Co-IP data is the detection limitation of the mass spectrometer as discussed above.

Both Y2H as well as Co-IP do not give any information about whether the ribosomal protein found to interact with Gcn1, is additionally necessary for Gcn1 function in promoting Gcn2 activation which made the study of this thesis a crucial approach.

4.3 Gcn1 binding to small ribosomal proteins is necessary for full activation of Gcn2

In chapter 1.1 we proposed that uncharged tRNA, entering the ribosomal A-site, activates Gcn2 under amino acid starvation (Sattlegger & Hinnebusch, 2000). As we demonstrated, Gcn2 activation requires Gcn1 binding to the ribosome suggesting that Gcn1 is directly involved in the transfer of uncharged tRNA to Gcn2 (Sattlegger & Hinnebusch, 2000). If this is true then Gcn1 must bind close to the ribosomal A-site. This thesis produced results that suggest that three small ribosomal proteins are necessary for Gcn1 mediated Gcn2 activation. In order to check whether the location of these ribosomal proteins agrees with the above hypothesis we took advantage of the fact that the location of the ribosomal proteins of the 80S ribosome of *S. cerevisiae* has been published (Ben-Shem et al., 2011).

Of the strains assayed in our study, gene deletions of rps18A, rps26A and rps28B resulted in SM sensitivity and reduced eIF2α-P level, suggesting that the lack of those proteins affected Gcn1 binding and therefore Gcn2 activation. rps18 is a conserved ribosomal protein, located at the small ribosomal subunit. rps18 forms part of the ribosomal head region and so do rps28 (Malygin & Karpova, 2010) and rps26 which are direct neighbours of each other. Interestingly rps28 and rps26 are unique to eukaryotes, raising the possibility that both ribosomal proteins have evolved as docking sites of Gcn1. Contrary to our hypothesis, however, these ribosomal proteins are not in close proximity to the ribosomal A-site. The ribosomal A-site is located close to rps23 and is part of the intersubunit site (Wilson & Cate, 2012)(Figure 20). As rps23 was not found in the assays of this study, but in the Y2H screen Table 11, we consider rps23 to be a Gcn1 binding protein without any significance for Gcn1 function. This was rather unexpected, as Gcn1 was hypothesised to function at the ribosomal A-site. Considering our results, we can envision that the binding of Gcn1 to rps18, rps26 and rps28 could affect the conformation of the ribosomal A-site region, possibly leading to the release of uncharged tRNA.

It cannot be ruled out that there are essential ribosomal proteins that interact with Gcn1 and are equally required for Gcn1 function but were not identified in this study as they could not be investigated in our approach. Some of those proteins are particularly

destined to be tested for their importance for Gcn1 function, as they are closely located to the translation sites (A, P, E-site).

We would also like to refer to the findings of our collaborators, T.Budkevich who works on creating a cryo-electron microscopic (**cryo-EM**) image of Gcn1 on the ribosome. Figure 19 illustrates the first obtained cryo-EM image of the 80S ribosome in the presence and absence of the Gcn1/Gcn20 complex. In comparison with the empty ribosome, the 80S ribosome in complex with Gcn1/20 showed an additional density at the location of rps20 (T.Budkevich, Spahn lab, unpublished).

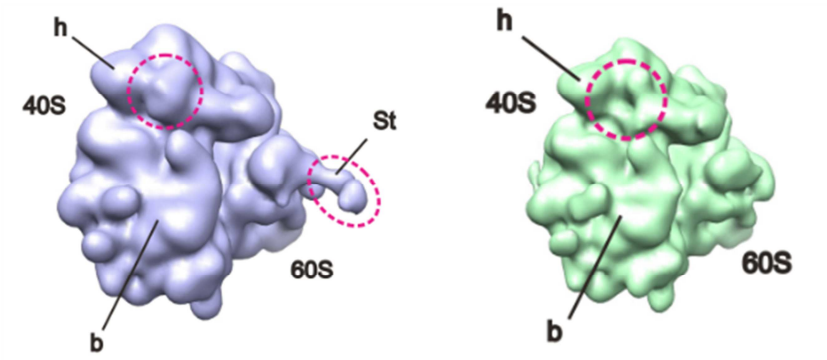

Figure 19: Density map of the 80S ribosome in complex with (left) and without (right) Gcn1.
Image was reconstructed by single particle cryo -EM. Specific regions are indicated as follow: h (head), b (body) and St (Stalk). Picture received from T.Budkevich & C.M. Spahn, unpublished Data.

Interestingly, rps20 is an essential ribosomal protein that is closely located to rps10 (Figure 20), which has already been evidenced to interact with Gcn1 (Lee, Swanson & Sattlegger, Manuscript in preparation). Between rps20 and rps10 lies another essential ribosomal protein, rps3 that was identified by Gavin et al. (2006) to possibly interact with Gcn1(Gavin et al., 2006). The cluster of those three proteins is also part of the ribosomal head region. Between these two groups of ribosomal proteins, are additional ribosomal proteins that form part of the ribosomal head region. Figure 20 shows the bird's-eye view and the A-site of the ribosomal head region, including the small ribosomal proteins, which were found to interact with Gcn1. As illustrated in Figure 20, rps18 is surrounded by rps15, rps25 and rps19. rps15 is essential and was therefore not part of our study. rps19A and rps25A were both found in the Y2H screen to interact with Gcn1. However, none of them had SM sensitivity in our screen, suggesting that they are not necessary for Gcn1 function.

In summary this chapter showed, that small ribosomal proteins, suggested as binding candidates of Gcn1, are located at the ribosomal head region. Furthermore it demonstrated that three of those proteins (rps18, rps26 and rps28) which are necessary for Gcn1 function are not located at the ribosomal A-site, as expected.

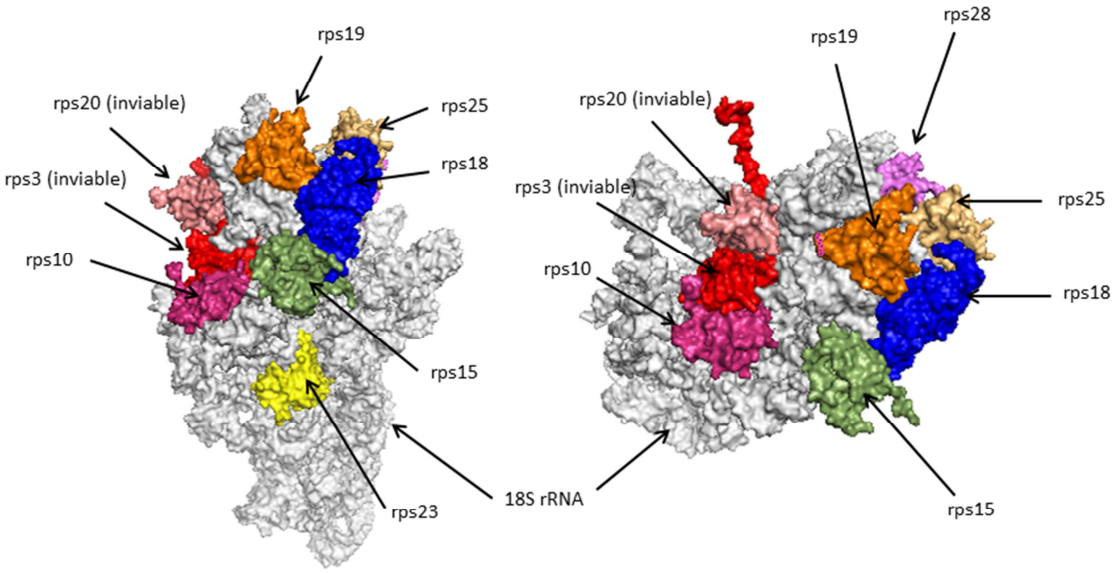

Figure 20: Surface presentation of the *S. cerevisiae* 40S ribosome, consisting of the 18S rRNA and certain ribosomal proteins.

The picture on the left shows the 40S subunit from the A-site view with highlighted ribosomal proteins of the head region. The picture on the right illustrates the ribosomal head region from above with highlighted ribosomal proteins on the head region. The ribosome was reconstructed from the 80S ribosomal data of A. Ben-Shem et al. 2011 3U5C& 3U5B (Ben-Shem et al., 2011) by using PyMOL 1.1 (DeLano Scientific LLC.)

4.4 Gcn1 binding to large ribosomal proteins is necessary for Gcn2 activation

Today we know that Gcn1 has multiple contact points with the ribosome (Sattlegger & Hinnebusch, 2005). As Gcn1 is proposed to function in the ribosomal A-site, we hypothesised, that ribosomal proteins, necessary for Gcn2 activation, will be close to that region. However, due to the size of Gcn1, which is about 1/10 of the ribosome size, it is possible, that Gcn1 also interacts with proteins on other parts of the ribosome and that those proteins are equally important for the performance of Gcn1 as an effector protein of Gcn2.

Deletion of genes as in *rps21A*Δ and *rpl34A*Δ strains resulted in SM sensitivity and reduced eIF2α-P levels in our study. These result suggested that rpl21 and rpl34 are potential binding candidates of Gcn1 and are necessary for Gcn2 activation.

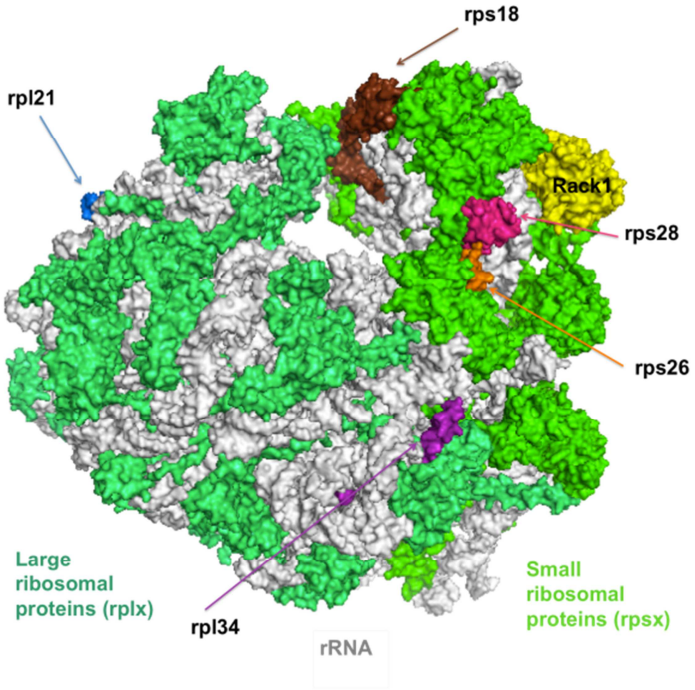

Figure 21: Surface presentation of the 80S ribosome of *S. cerevisiae* with highlighted ribosomal proteins that showed reduced eIF2α-P level in addition to SM sensitivity.
The ribosome was reconstructed from the 80S ribosomal data of A. Ben-Shem et al. 2011 3U5C& 3U5B (Ben-Shem et al., 2011) by using PyMOL 1.1 (DeLano Scientific LLC.)

rpl21 is a solvent exposed protein in the central protuberance of the large 60S subunit whereas rps34 is partially reaching into the intersubunit site but also has an exposed surface. rpl34 is located close to the small ribosomal subunit near to rps26 and rps28 (Figure 21).

Our findings suggest that Gcn1 binds to large and small ribosomal proteins and that ribosomal proteins from both subunits are necessary for Gcn2 activation. Our results are supported by the in house co-immunoprecipitation data of Gcn1 performed by R. Shanmugam and E.Sattlegger. Here rpl21 has been found to co-precipitate with Gcn1, suggesting that there is a physical interaction between rpl21 and Gcn1. As this binding point is necessary for Gcn2 activation we envision that Gcn1 interaction with proteins

from the large subunit is required for a conformational change to let the tRNA travel alongside the ribosome to Gcn2.

4.5 Gcn1 and eEF3 share the small ribosomal protein rps18 as a ribosomal contact point

As illustrated in Figure 4 *GCN1* contains HEAT repeats in its middle region similar to those in eEF3 (M. Marton et al., 1993). This eEF3-like region of Gcn1 is important for ribosomal binding and therefore promoting Gcn2 activation (Sattlegger & Hinnebusch, 2005). This and the finding that the overexpression of eEF3 impedes Gcn2 activation (Visweswaraiah, Lee, Hinnebusch, & Sattlegger, 2012) suggested that eEF3 and Gcn1 share ribosomal binding sites. Overexpression of eEF3 did not reduce the polysome-Gcn1 association, implying that Gcn1 and eEF3 could reside on the same ribosome but that eEF3 blocks Gcn1- regulatory function (Visweswaraiah et al., 2012).

The work of this thesis results in the theory that rps18 is a binding partner of Gcn1 and is necessary to stimulate Gcn2 kinase activity. As eEF3 was shown by cryo-EM to contact rps18 (Andersen et al., 2006) we propose that rps18 is the first shared ribosomal binding partner of Gcn1 and eEF3 to be found. This idea is further supported by the fact that the eEF3 fragments sufficient for inhibiting Gcn1 both have rps18 binding activity, suggesting that the overlap of ribosomal binding points of Gcn1 and eEF3 is with rps18 (Andersen et al., 2006).

If we include our results into the existing model of the starvation detection, we can envision the following: under amino acid starvation, when the cellular pool of uncharged tRNA increases, uncharged tRNA enters the ribosomal A-site. eEF3 not binding to the ribosome under amino acid starvation allows Gcn1 to form a productive interaction with the ribosome including its binding to rps18 and therefore to perform its purpose in the delivery of uncharged tRNA from the ribosomal A-site to Gcn2 (Visweswaraiah et al., 2012) Figure 22, B.

Under amino acid replete conditions, it has been proposed that Gcn1 cannot access all the ribosomal binding sites, as they are occupied by eEF3 which hinders Gcn1 function

(Visweswaraiah et al., 2012). We suggest that under replete conditions eEF3 binds rps18 which in turn blocks complete Gcn1 ribosome interaction resulting in Gcn2 inactivation Figure 22, A.

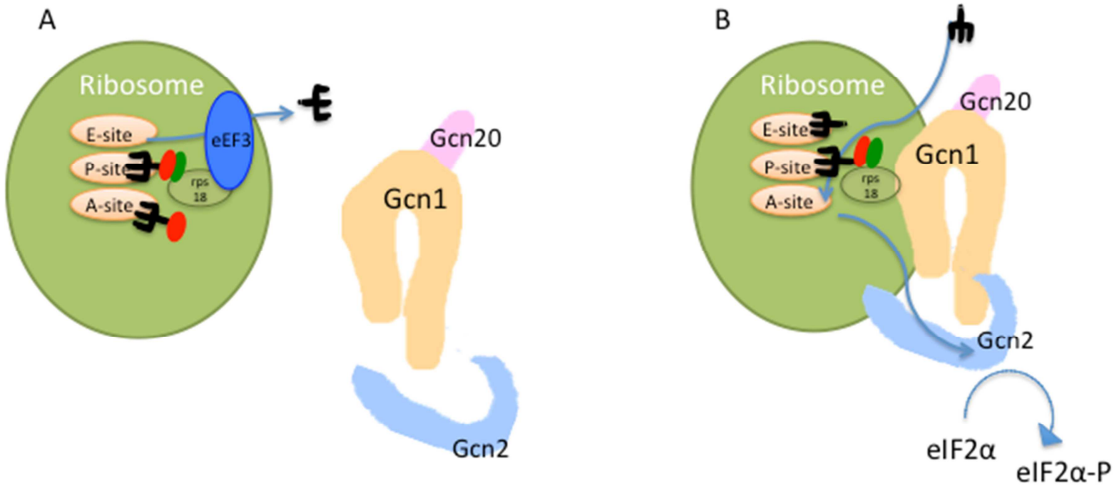

Figure 22: Model for eEF3 and Gcn1 function on the ribosome.
Under replete conditions (A), eEF3 functions in the ribosomal E-site where it releases the E-site bound uncharged tRNA and at the same time promotes the binding of charged tRNA to the A-site. One of eEF3 contact points is rps18. Under amino acid starvation conditions (B), Gcn1 and Gcn2 are both contacting the ribosome. Gcn1 is now binding to rps18. Uncharged tRNA binds the ribosomal A-site and gets transferred to Gcn2 via Gcn1. After overcoming amino acid starvation eEF3 will rebind to rps18 which renders Gcn1 in functional. The model was adapted from Sattlegger and Hinnebusch (2000).

Interestingly rps19, one of the neighbouring proteins of rps18 was also found to be a component that comprises the eEF3 binding sites on the ribosome (Armache et al., 2010). However, the knockdown of rps19 did not lead to any SM sensitivity phenotype in our assay when deleted for one of the two paralogous genes and was therefore not further investigated. It is still possible, that rps19 is another candidate for a shared binding site between eEF3 and Gcn1 but is not essential for Gcn1 function as its deletion did not affect Gcn2 function.

Another study published that eEF3 binds to is the essential ribosomal protein rps5 (Galkin et al., 2007). Remarkably, rps5 is in close proximity with rps28, one of our interesting candidates. rps5 has been found in the Y2H screen to interact with Gcn1 and was also found in the Co-IP screen (Table 11), suggesting that it might be another

shared ribosomal protein of Gcn1 and eEF3. Suggested overexpression of rps5 in the future will reveal whether it is also necessary for Gcn2 activation.

4.6 Stringent response and GAAC: A comparison

The hypothesis, that Gcn1 functions as a deacylated tRNA transporter at the ribosomal A-site, mainly developed from knowledge about the stringent response in prokaryotes. Today we know that both pathways, the stringent response in bacteria and the GAAC in eukaryotes, link amino acid stress with the transcriptional control of genes via the activation of stress sensors. It is possible that Gcn1 and RelA do not only both detect starvation on the ribosome but could also reside on similar ribosomal regions to receive deacylated tRNA to activate the response pathways.

However, up to date, little is known about the molecular basis for how RelA senses a stalled ribosome complexed with uncharged tRNA. Researchers found that its binding is primarily governed by mRNA. The synthesis of (p)ppGpp by RelA, however, strictly requires uncharged tRNA at the A-site and the presence of the large ribosomal protein L11 (Wendrich et al., 2002). L11 is an ortholog of rpl12 in yeast. rpl12 did not show any SM sensitivity in our screen nor was it found in Co-IP studies. Published cryo-EM reconstruction of the 70S ribosome-RelA complex showed densities close to the acceptor stem of the A-site tRNA in the decoding centre (Agirrezabala et al., 2013), indicating that RelA can access the A-site. Based on our studies and the Co-IP data from R. Shanmugam and E.Sattlegger, we propose that Gcn1 does not only bind close to the ribosomal A-site but also interacts with ribosomal proteins from the large subunit. Both Gcn1 and RelA occupy regions close to the A-site and our study suggests that Gcn1, similar to RelA binds ribosomal proteins from the large subunit and that their interactions is necessary for the activation of the stress response.

Interestingly, it has been found that RelA does not stay bound to the ribosome but dissociates from the ribosome after having synthesized (p)ppGpp (English et al., 2011). Based on this, it was predicted that RelA hops from ribosome to ribosome to detect the presence of uncharged tRNA (English et al., 2011) (Wendrich et al., 2002). In analogy to this, there are indications that Gcn1/Gcn2 complex hops on and off the ribosome (Ramirez et al., 1991) and thereby ensures that both proteins (Gcn1 and Gcn2) which

are highly outnumbered compared to the amount of ribosomes in the cell, reside at the same time on the same ribosome to sense starvation (Visweswaraiah et al., 2012).

In our studies we found that, four (rps26, rps28, rpl21, rpl34) out of five ribosomal proteins that are necessary for Gcn1 function, do not have an ortholog in bacteria. The only candidate that arose from our studies to be important for Gcn2 activation and to also exist in bacteria is rps18 (S13 in bacteria). This is worth to note, as this work suggests rps18 to be an overlapping binding site of eEF3 and Gcn1. The ATPase, RbbA from bacteria cross-reacts with anti-EF-3 antibody and has sequence similarity to the yeast eEF3 (Kiel, Aoki, & Ganoza, 1999), suggesting that RbbA has a similar function in bacteria as eEF3 in yeast. In yeast rpl11 was found to be a ribosomal binding candidate of eEF3 (Andersen et al., 2006) and that antisera from rpl11 does cross react with L11 from *E.coli* (Juan-Vidales, Sanchez Madrid, Saenz-Robles, & Ballesta, 1983). As mentioned earlier, L11 is required for (p)ppGpp synthesis by RelA. All this findings indicate that there are several links between both stress pathways.

It would be interesting to investigate whether the rps18 homolog in bacteria, S13, is also a shared ribosomal binding partner for RelA and RbbA. Our research will contribute to a better understanding about the ribosomal contact points of Gcn1 but might also give suggestions on the ribosomal binding sites of proteins involved in the stringent response in prokaryotes.

4.7 Conclusion and future work on this project

In order to shed more light on Gcn1 function to promote Gcn2 activation, we aimed to identify ribosomal binding partners of Gcn1 that are necessary for Gcn2 activation and to map Gcn1 “functional binding sites” on the ribosome. This study revealed five ribosomal proteins that are required for a fully activated Gcn2. Three of those are found in the ribosomal head region of the small ribosomal subunit and two form part of the large ribosomal subunit. These are important findings as they show that the Gcn1 binds ribosomal proteins that are not directly at the ribosomal A-site where Gcn1 function was expected to be. Our work on functional Gcn1-ribosome interaction is therefore an

important step in understanding the plethora of the mechanism of signal recognition by Gcn2. Next steps in this field should be to verify that Gcn1 in fact physically interacts with the five ribosomal proteins from this study, by conducting Co-IP studies. Furthermore it will be necessary to carry out an alternative approach for pinpointing Gcn1-ribosomal interaction with importance for Gcn2 function. The overexpression of the ribosomal proteins is an alternative method that allows investigating all ribosomal proteins including those that are essential. The idea is that the overexpressed protein masks the binding site in Gcn1 and thereby preventing it from binding to the same ribosomal protein that is incorporated into the ribosome. Similarly to the deletion screen done in this thesis, the overexpression should lead to SM^S phenotype if an interaction is important for Gcn2 function.

In analogy to RelA in bacteria which binds to rRNA, it would be interesting to map the rRNA sites involved in Gcn1 binding.

Getting the complete footprint of Gcn1 on the ribosome is a lot of work but it is fundamental for understanding Gcn2 activation. As Gcn2 is involved in several diseases, it is necessary to understand the mechanism of promoting Gcn2 activation. It can then be possible to develop drug targets to specifically impair Gcn2 function and cure Gcn2 associated disorders.

5. Appendix

5.1 Section A

Test #	Control plates	Starvation plates

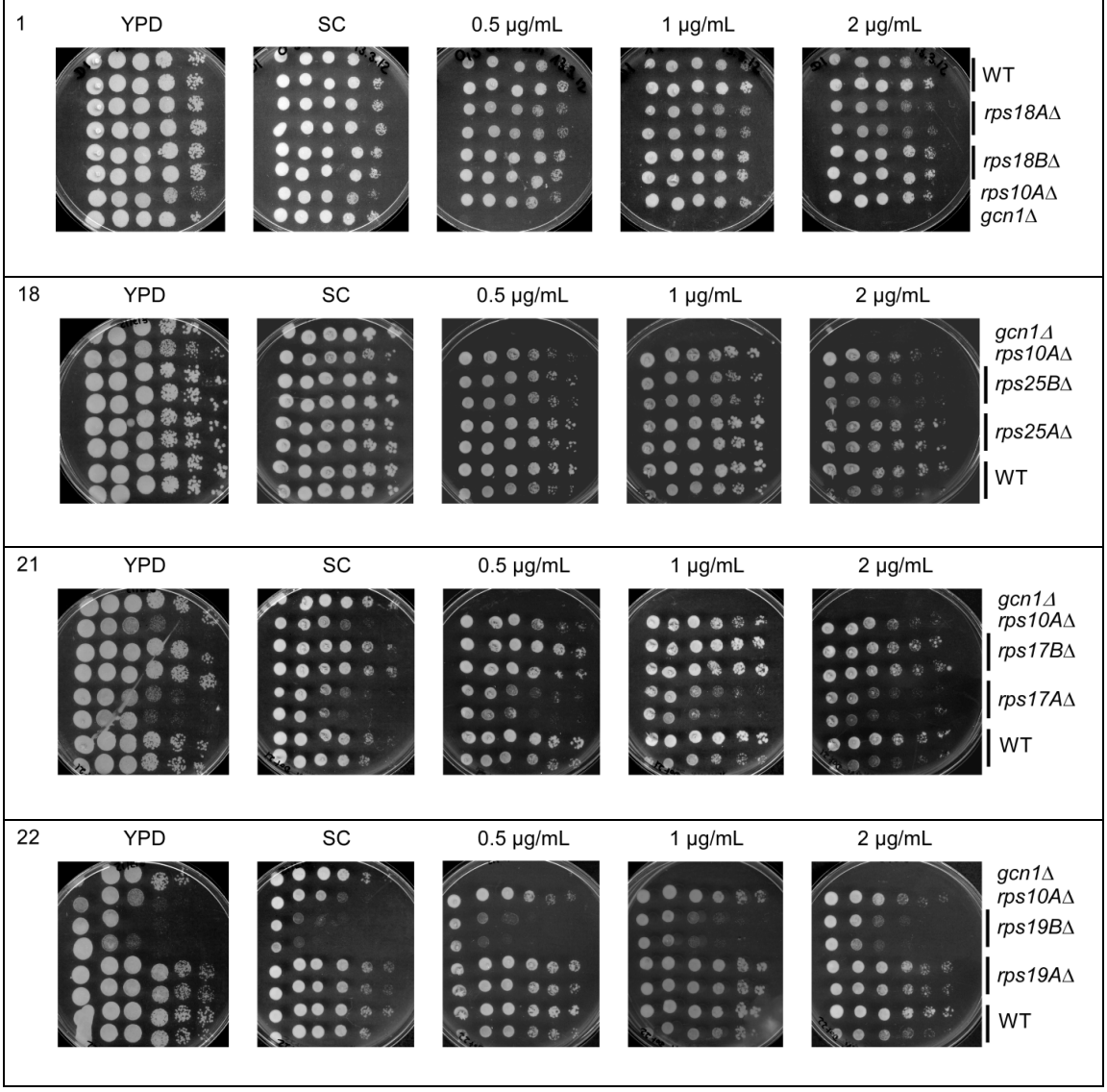

Test #	Control plates	Starvation plates

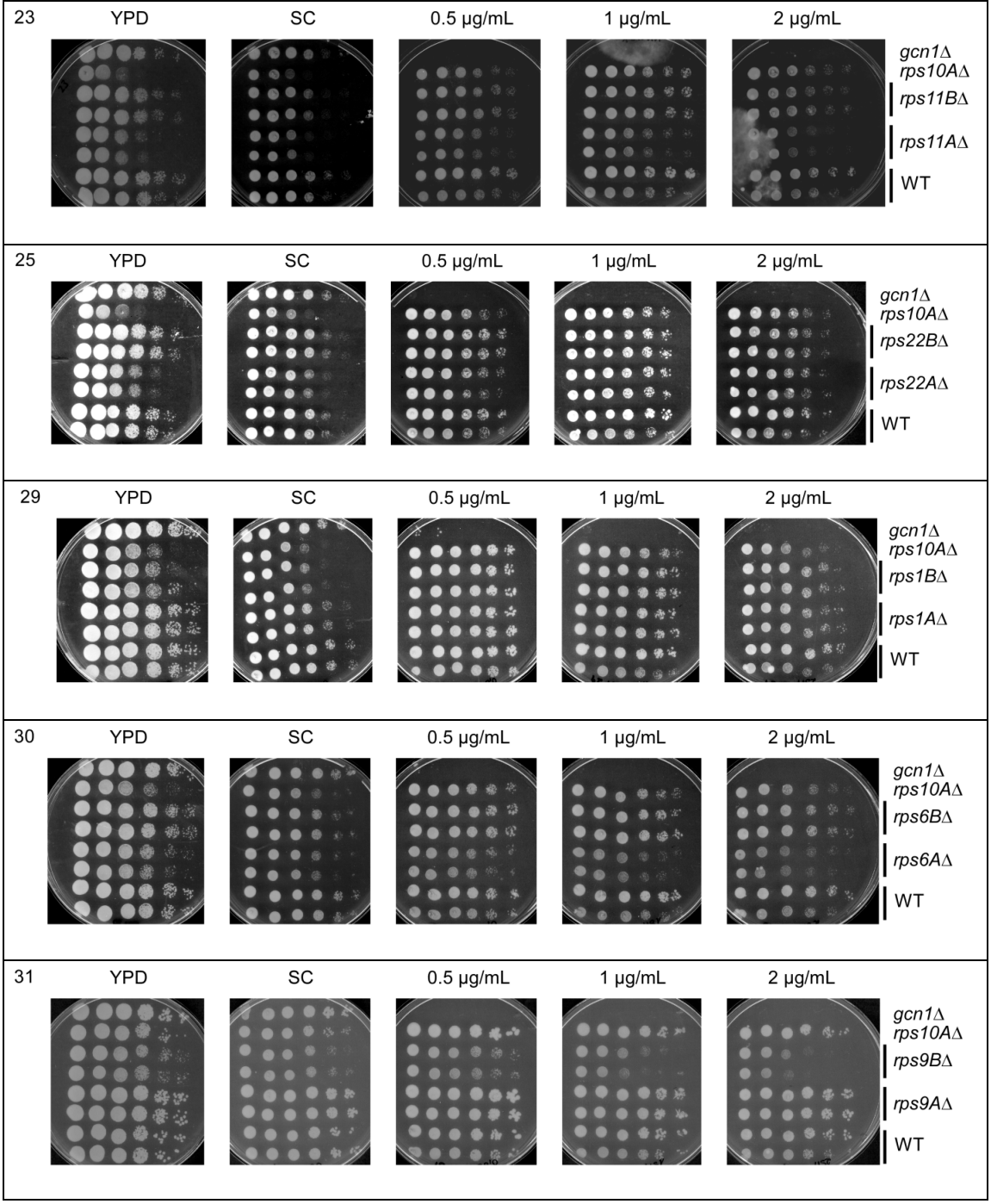

Test #	Control plates	Starvation plates

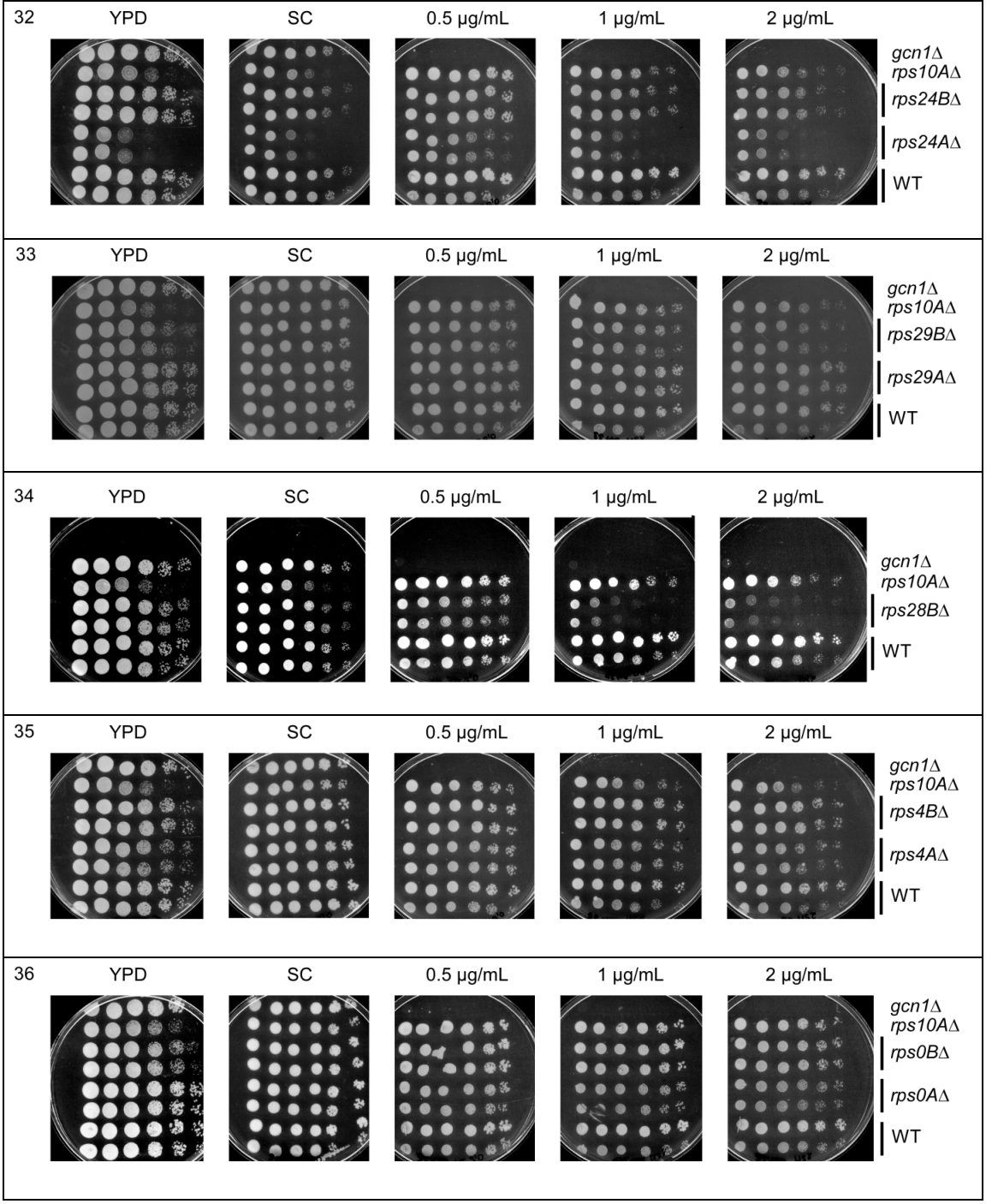

Test #	Control plates	Starvation plates

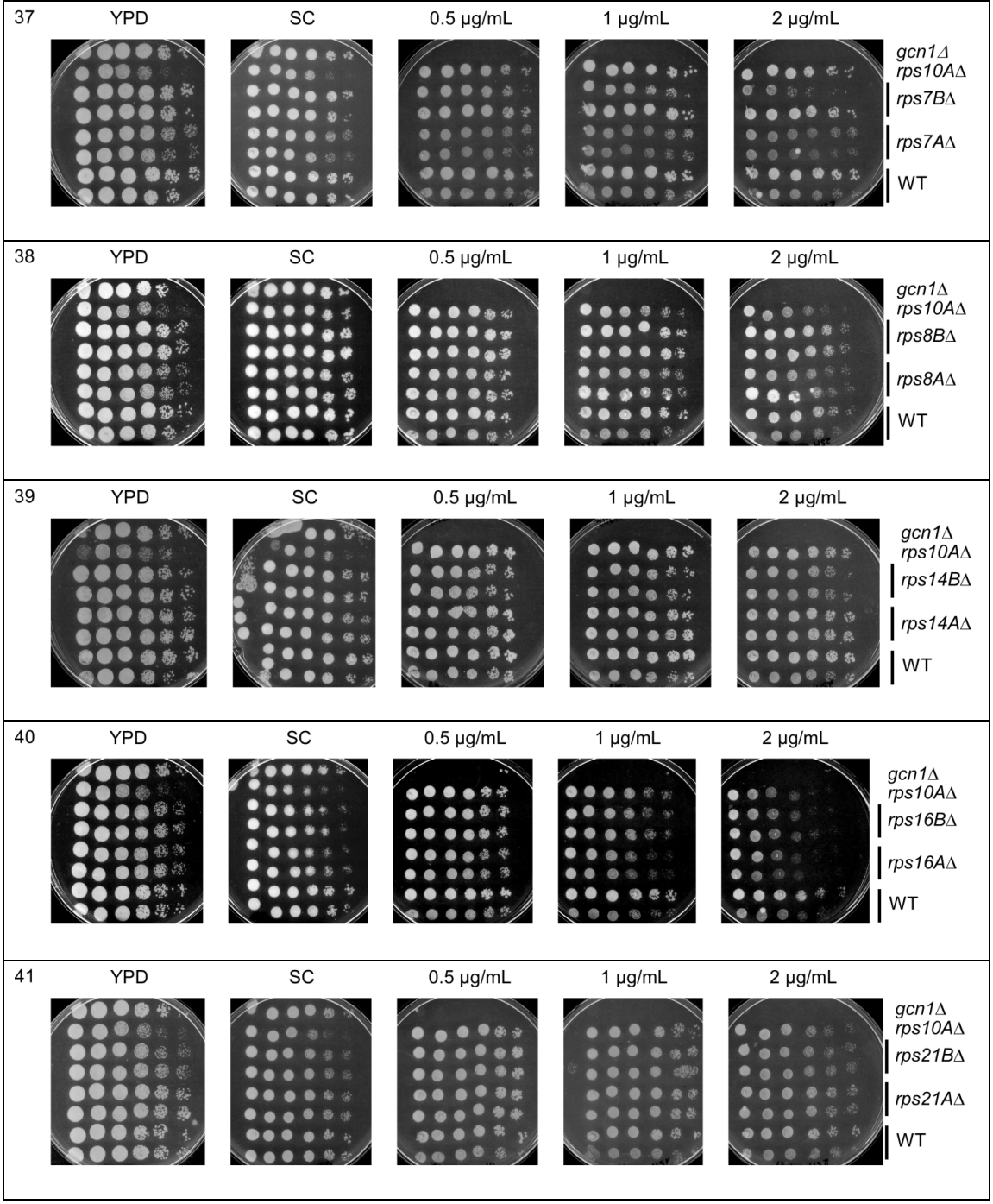

Test #	Control plates	Starvation plates

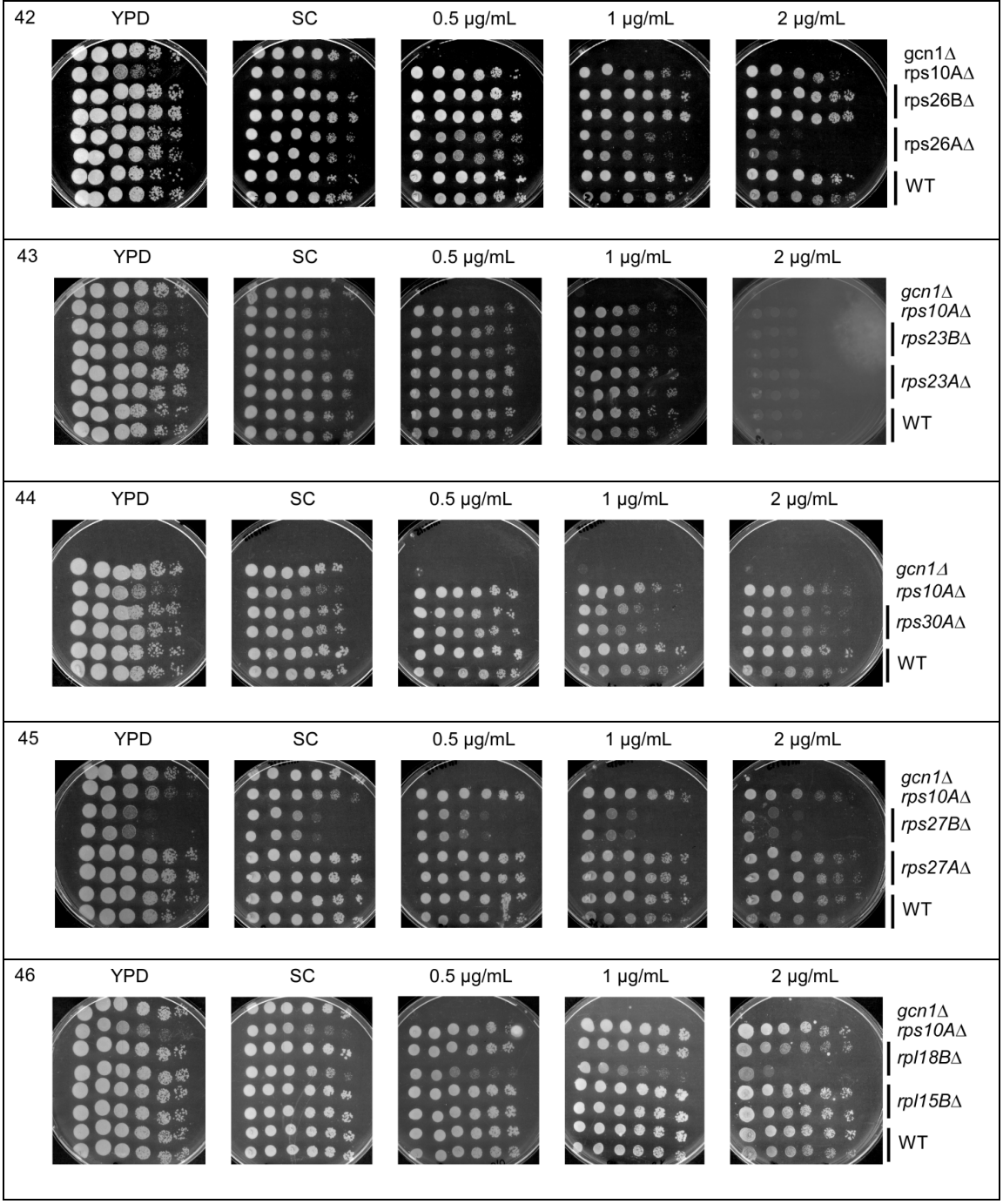

Test #	Control plates	Starvation plates

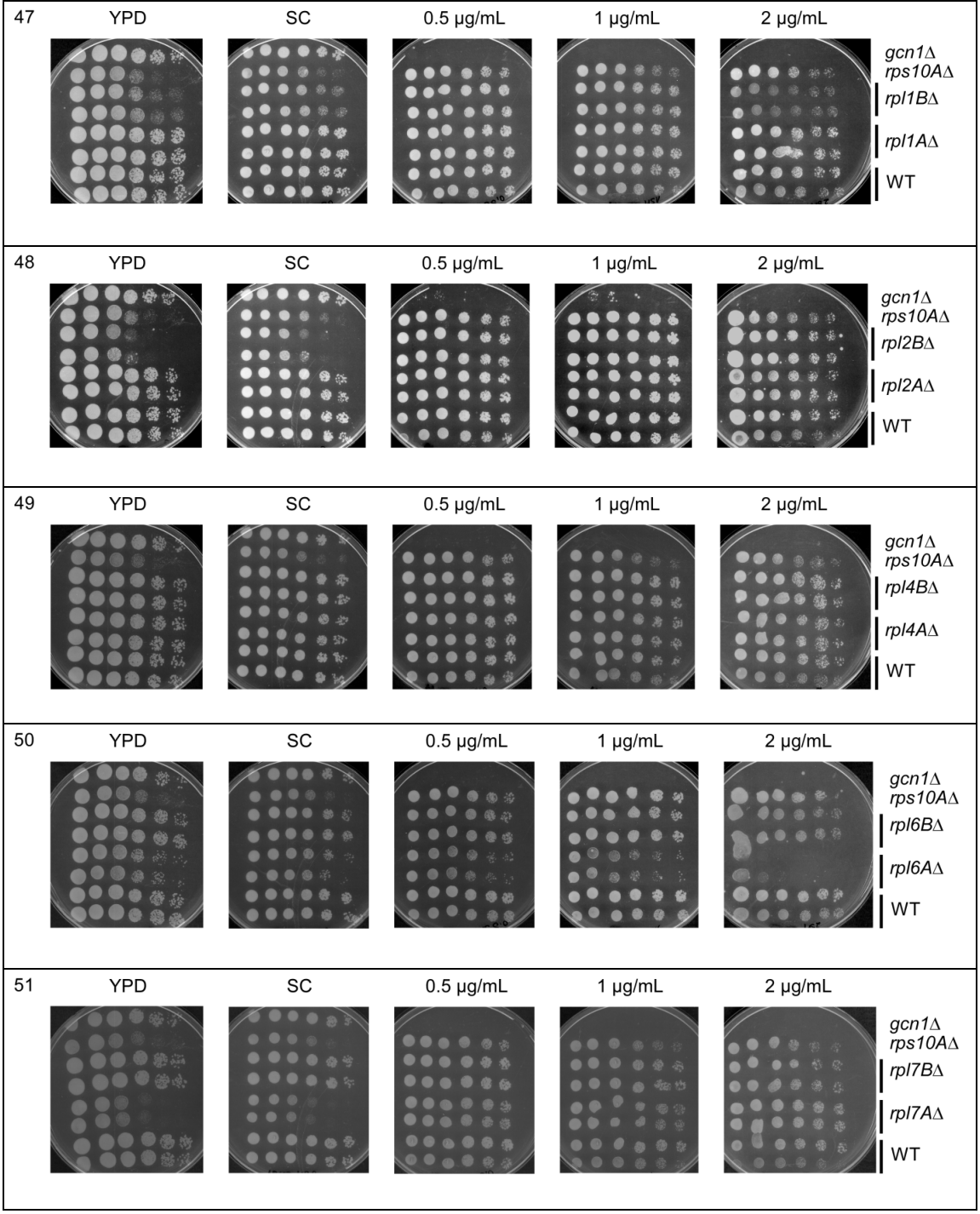

Test #	Control plates	Starvation plates

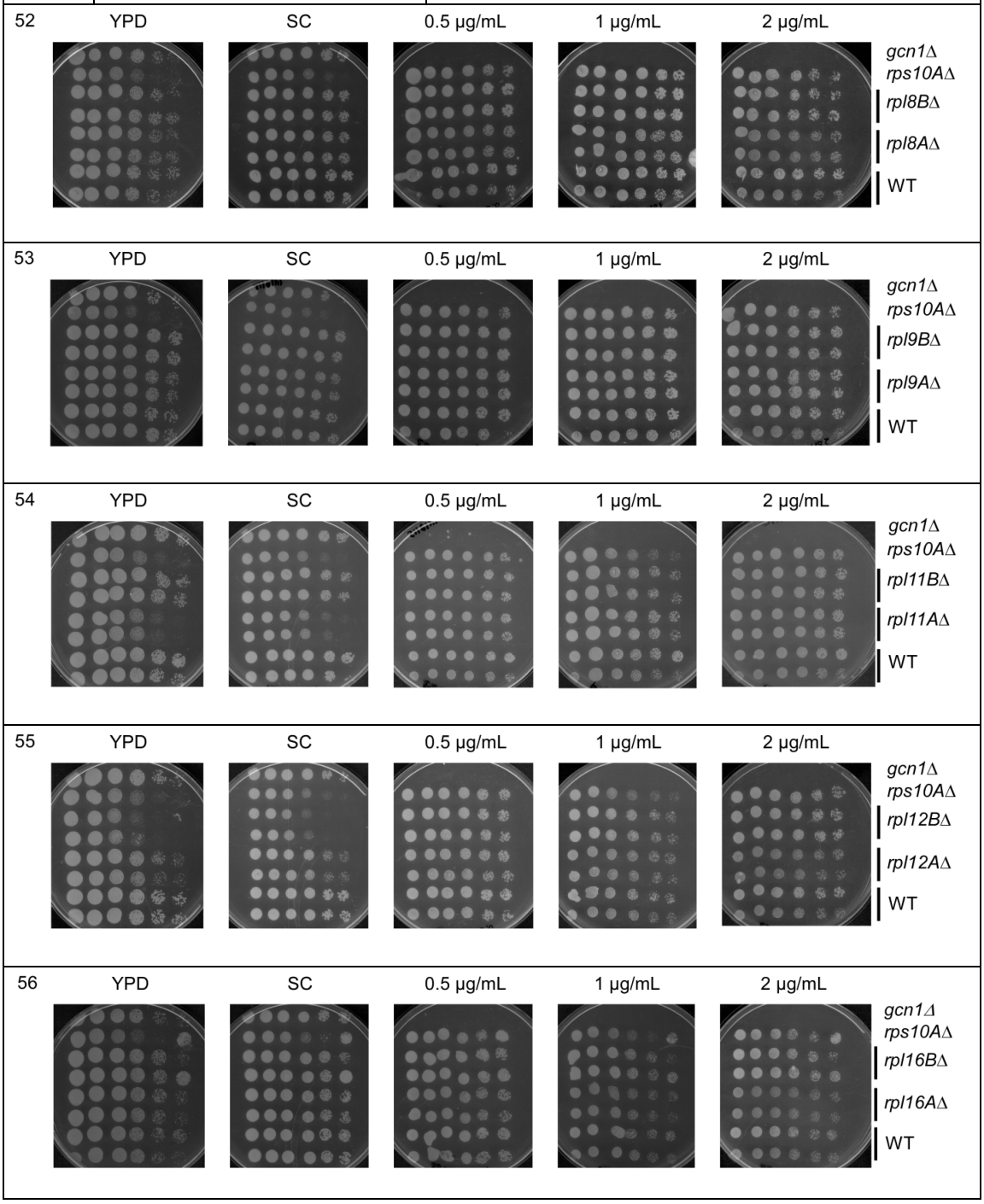

Test #	Control plates	Starvation plates

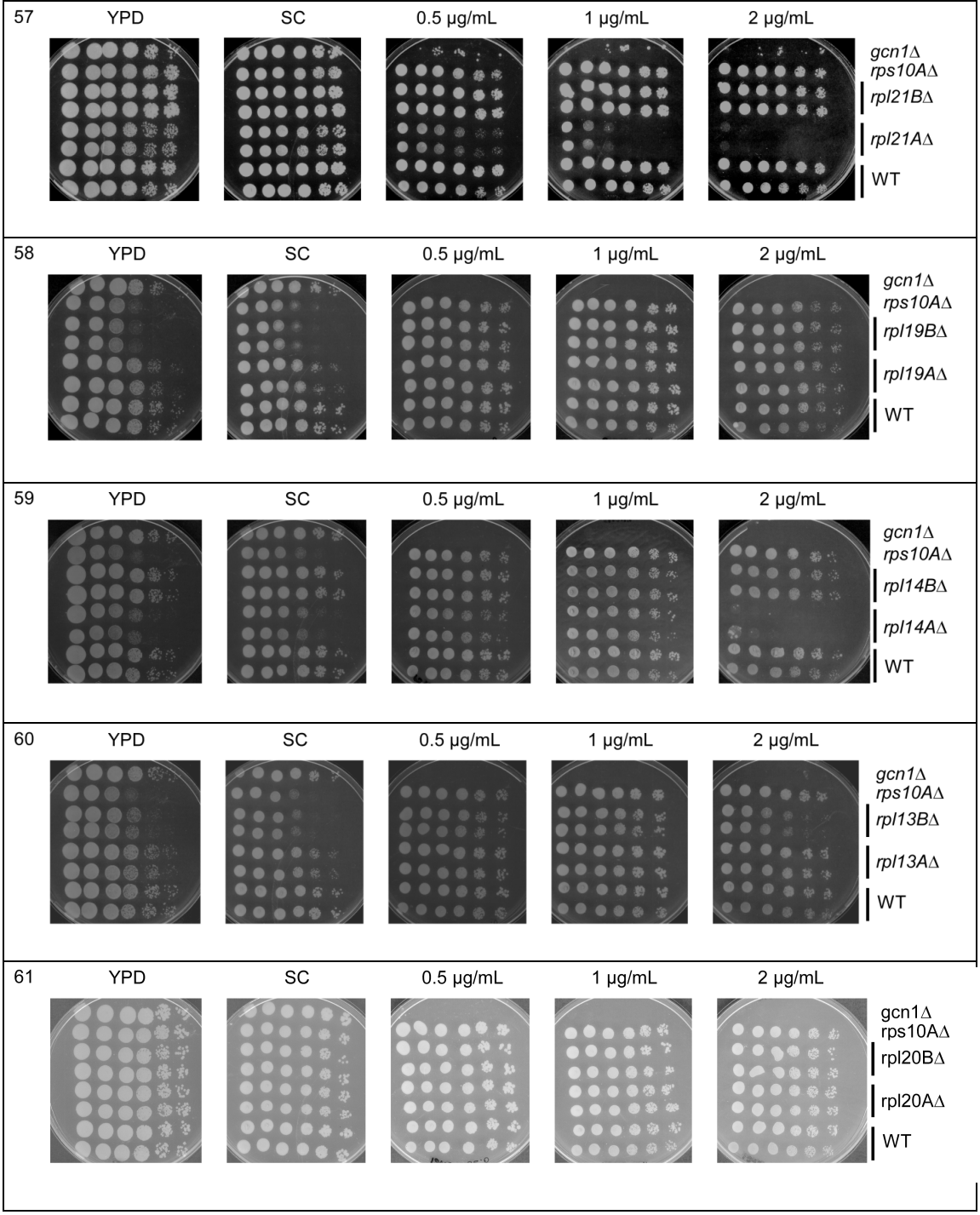

Test #	Control plates	Starvation plates

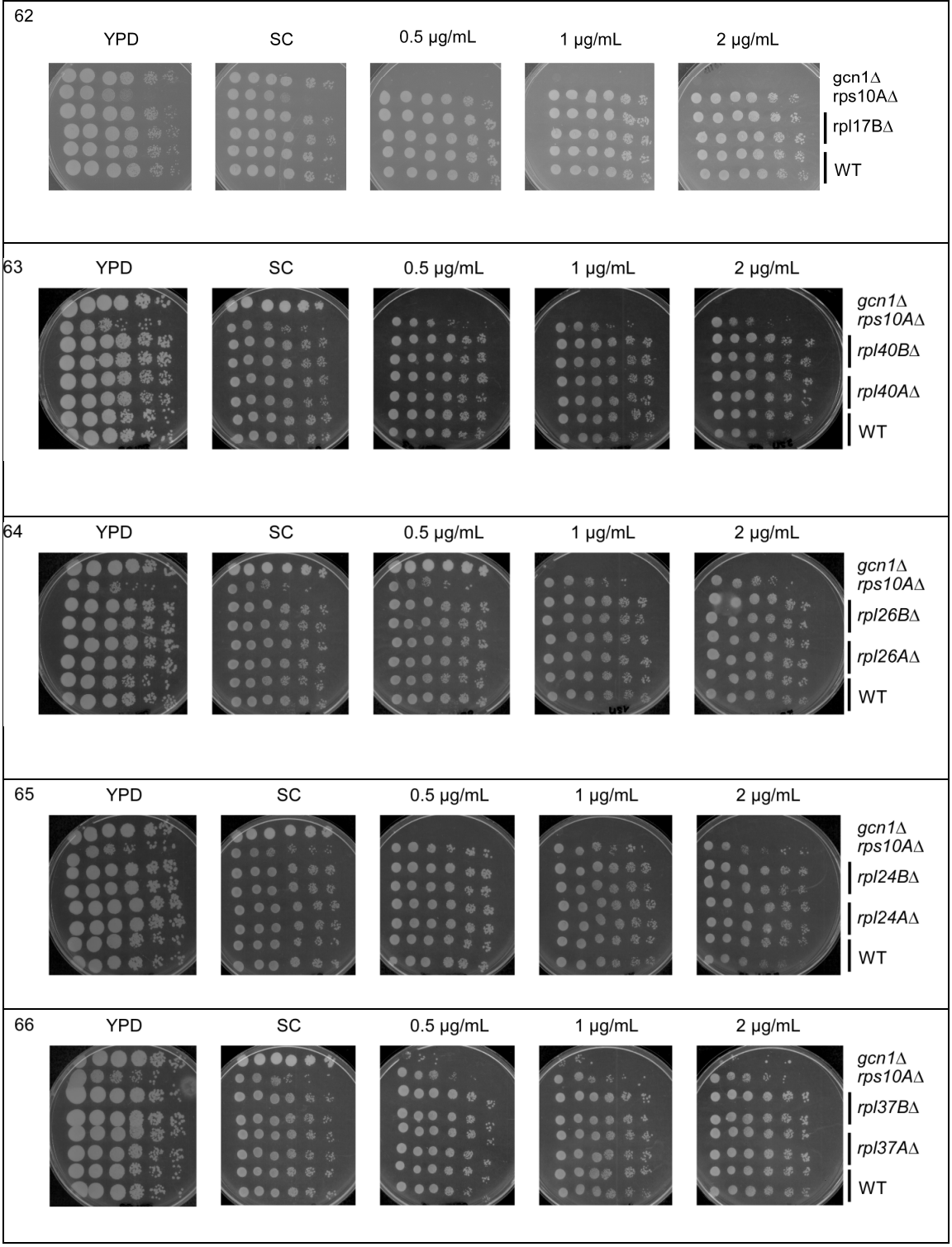

Test #	Control plates	Starvation plates

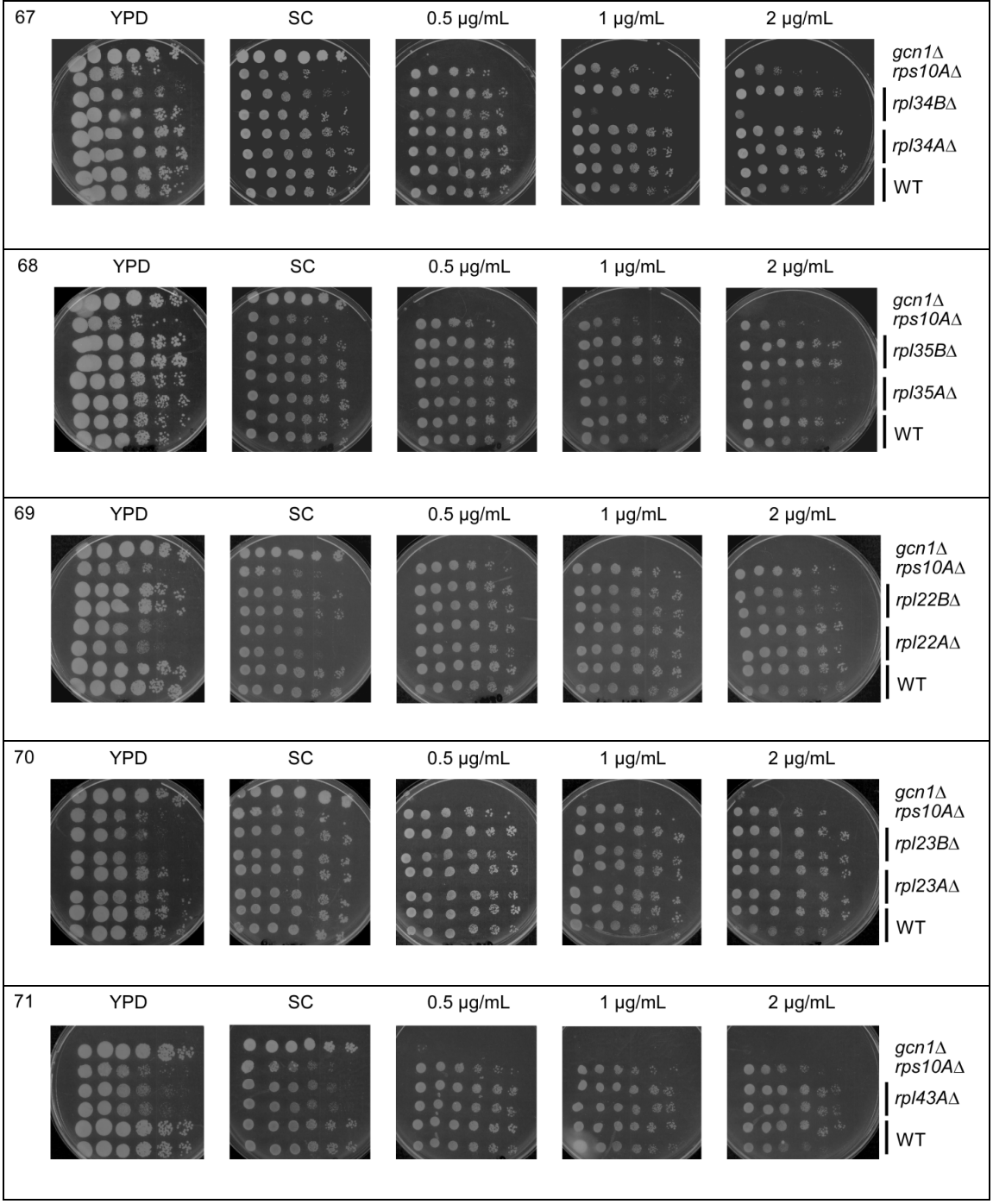

Test #	Control plates	Starvation plates

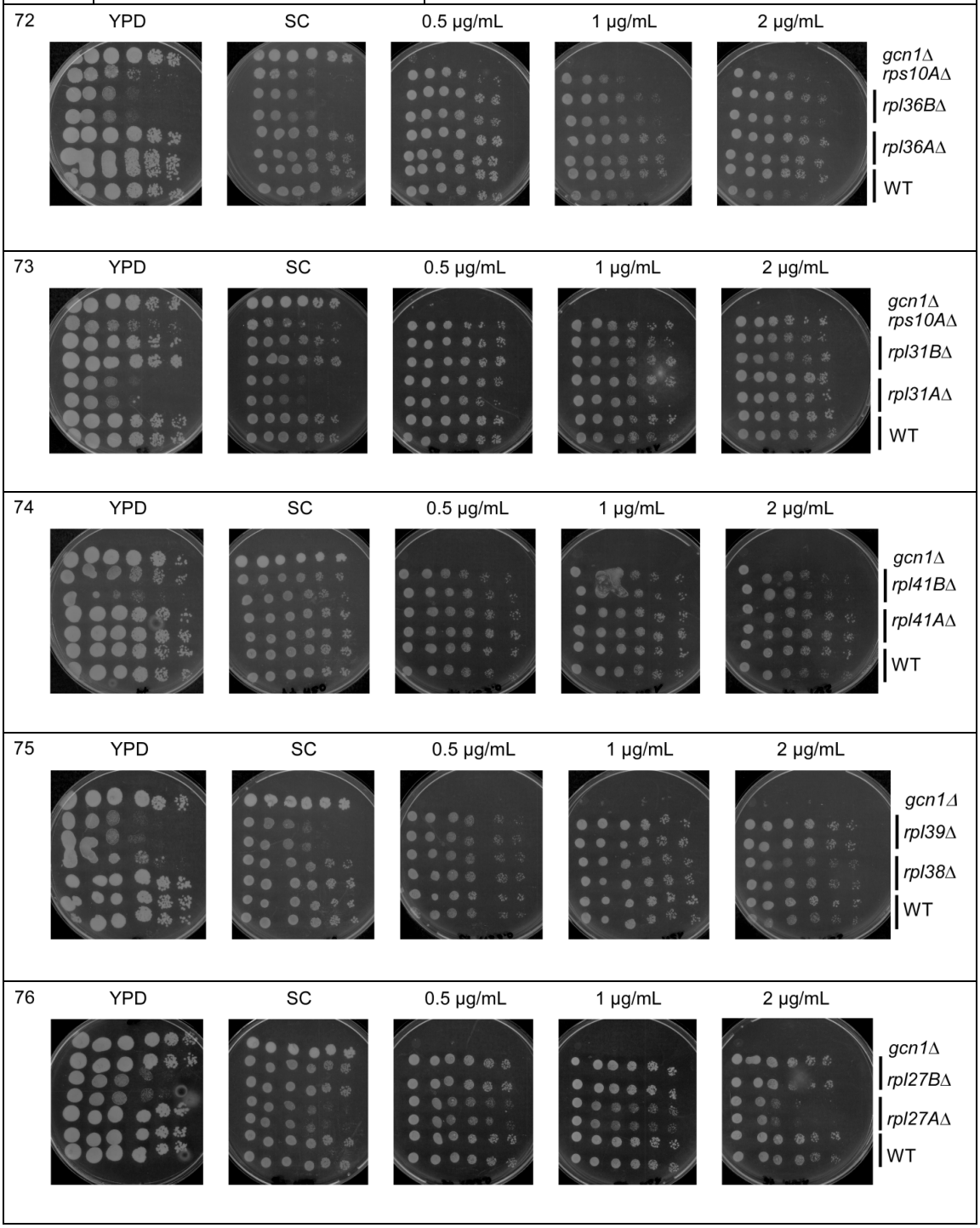

Test #	Control plates	Starvation plates
78	YPD	SC	0.5 µg/mL	1 µg/mL	2 µg/mL

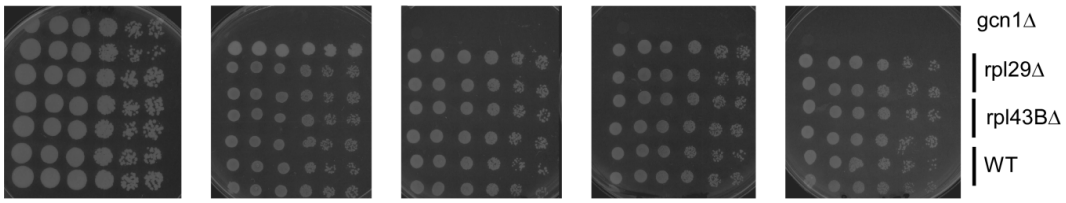

5.2 Section B

Table 12: Scoring of semi-quantitative growth assays shown in appendix, section A

Test Nr.	Auxotrophies	Strain	Starvation plates			
			SC	SM (0.5)	SM (1)	SM (2)
1	MET,lys	*rps18B* Δ	7.5	8.0	8.0	7.0
			7.5	7.5	8.0	7.0
	met,lys	*rps18A* Δ	8.0	7.0	7.0	5.0
			8.0	7.0	7.0	5.0
	MET,lys	BY4742	7.5	8.0	8.0	7.0
	met,LYS	BY4741	7.5	6.5	7.0	6.5
18	met,LYS	*rps25B* Δ	9.0	7.0	7.0	4.0
			8.5	7.0	7.0	4.0
	MET,lys	*rps25A* Δ	8.5	8.0	8.5	7.5
			9.0	8.0	8.5	7.5
	MET,lys	BY4742	9.0	8.0	8.5	7.5
	met,LYS	BY4741	8.5	6.5	8.0	4.0
21	MET,lys	*rps17B* Δ	8.0	9.0	9.0	6.6
			8.0	8.0	9.5	6.5
	MET,lys	*rps17A* Δ	5.0	4.0	5.0	3.0
			5.0	4.0	5.0	3.0
	MET,lys	BY4742	7.0	8.5	9.0	6.5
	met,LYS	BY4741	7.0	8.0	7.0	3.0
22	MET,lys	*rps19B* Δ	1.0	1.0	1.5	3.0
			1.0	1.0	1.5	3.0
	MET,lys	*rps19A* Δ	6.5	9.0	9.0	7.0
			6.5	8.5	8.5	7.0
	MET,lys	BY4742	7.5	9.0	8.5	7.5
	met,LYS	BY4741	7.0	7.5	7.0	5.5
23	MET,lys	*rps11B* Δ	5.0	6.5	8.5	6.0
			5.0	6.5	8.5	6.0
	MET,lys	*rps11A* Δ	4.0	6.0	6.0	4.0
			4.0	6.0	6.0	4.0
	MET,lys	BY4742	6.5	8.5	9.0	7.0
	met,LYS	BY4741	6.0	6.5	6.5	6.0

Table 13: Scoring of semi-quantitative growth assays shown in appendix, section A

Test Nr.	Auxotrophies	Strain	Starvation plates			
			SC	SM (0.5)	SM (1)	SM (2)
25	MET,lys	*rps22B* Δ	6.5	8.0	8.0	6.5
			6.5	8.0	8.0	6.5
	MET,lys	*rps22A* Δ	5.0	7.0	8.5	6.5
			5.0	6.0	8.5	6.5
	MET,lys	BY4742	6.5	8.0	9.0	6.5
	met,LYS	BY4741	6.5	7.5	8.0	5.0
29	MET,lys	*rps1B* Δ	5.0	9.0	8.5	7.0
			5.0	9.0	8.5	7.0
	MET,lys	*rps1A* Δ	7.0	9.0	8.5	7.0
			7.0	9.5	8.5	7.0
	MET,lys	BY4742	7.5	9.5	8.5	8.0
	met,LYS	BY4741	7.5	9.5	7.5	7.0
30	MET,lys	*rps6B* Δ	6.0	8.5	8.5	7.5
			6.0	9.0	9.0	7.5
	met,lys	*rps6A* Δ	5.0	7.0	5.0	5.0
			5.0	7.0	5.0	5.0
	MET,lys	BY4742	8.5	9.0	8.5	8.5
	met,LYS	BY4741	8.0	8.5	7.5	6.5
31	MET,LYS	*rps9B* Δ	6.0	7.0	4.0	4.0
			6.0	7.0	4.0	4.0
	MET,lys	*rps9A* Δ	9.0	9.0	8.5	8.5
			9.0	9.0	8.5	8.5
	MET,lys	BY4742	8.0	8.5	8.5	7.0
	met,LYS	BY4741	8.5	8.5	8.0	6.5
32	met,lys	rps24BΔ	8.0	9.0	8.5	7.0
			8.0	9.0	8.5	7.0
	MET,lys	rps24AΔ	4.0	7.0	5.0	3.0
			4.0	7.0	5.0	3.0
	MET,lys	BY4742	8.5	10.0	9.5	9.0
	met,LYS	BY4741	8.5	8.0	7.0	6.0
33	MET,LYS	*rps29B* Δ	10.0	9.0	8.5	6.5
			9.5	9.0	8.0	6.5
	MET,lys	*rps29A* Δ	10.0	10.0	9.0	8.0
			10.0	9.5	8.5	8.0
	MET,lys	BY4742	9.5	9.5	8.5	8.0
	met,LYS	BY4741	9.0	8.5	7.5	6.5
34	met,lys	*rps28B* Δ	7.0	8.5	3.0	1.0
			7.0	8.5	3.0	1.0
	MET,lys	BY4742	8.0	9.5	9.0	8.5
	met,LYS	BY4741	8.0	8.5	8.0	7.0

Table 14: Scoring of semi-quantitative growth assays shown in appendix, section A

Test Nr.	Auxotrophies	Strain	Starvation plates			
			SC	SM (0.5)	SM (1)	SM (2)
35	MET,lys	*rps4B* Δ	9.5	8.5	8.5	8.0
			9.0	8.5	8.5	8.0
	MET,lys	*rps4A* Δ	9.5	9.0	8.0	6.5
			9.5	9.0	8.0	6.5
	MET,lys	BY4742	9.5	9.0	8.5	8.0
	met,LYS	BY4741	9.5	8.0	7.0	6.0
36	MET,LYS	*rps0B* Δ	9.5	9.5	9.5	8.5
			9.5	9.5	9.0	8.5
	MET,lys	*rps0A* Δ	9.5	8.5	8.5	8.0
			9.5	8.5	8.0	8.0
	MET,lys	BY4742	10.0	9.0	9.5	9.5
	met,LYS	BY4741	8.0	8.5	9.0	8.0
37	MET,LYS	*rps7B* Δ	8.5	8.0	8.0	5.0
			8.0	8.5	9.0	8.0
	met,lys	*rps7A* Δ	7.0	8.5	8.5	7.5
			7.0	7.5	7.5	7.0
	MET,lys	BY4742	9.5	9.0	9.0	8.5
	met,LYS	BY4741	8.0	9.0	8.0	7.0
38	MET,lys	*rps8B* Δ	9.5	9.5	9.5	8.0
			10.0	10.0	9.5	8.0
	MET,lys	*rps8A* Δ	9.0	9.0	8.5	6.0
			9.0	9.0	8.5	6.0
	MET,lys	BY4742	9.0	9.0	9.0	7.0
	met,LYS	BY4741	9.0	8.0	7.0	6.0
39	met,LYS	*rps14B* Δ	8.5	8.5	8.0	7.0
			8.5	8.5	8.0	7.0
	MET,lys	*rps14A* Δ	9.0	9.0	9.5	9.5
			9.0	9.5	10.0	9.5
	MET,lys	BY4742	9.5	9.5	10.0	9.5
	met,LYS	BY4741	8.0	8.5	8.5	7.5
40	MET,lys	*rps16B* Δ	8.0	9.5	8.0	6.0
			8.0	9.5	8.0	6.0
	MET,LYS	*rps16A* Δ	7.5	8.5	6.0	5.0
			7.5	8.5	6.0	5.0
	MET,lys	BY4742	9.0	9.0	9.5	8.0
	met,LYS	BY4741	8.5	8.5	7.0	5.0
41	MET,lys	*rps21B* Δ	9.0	10.0	9.5	8.0
			9.0	9.5	9.5	8.5
	MET,lys	*rps21A* Δ	9.5	9.5	9.5	8.5
			8.5	9.5	9.5	8.5
	MET,lys	BY4742	8.5	9.0	9.0	8.0
	met,LYS	BY4741	8.5	8.5	7.0	7.0

Table 15: Scoring of semi-quantitative growth assays shown in appendix, section A

Test Nr.	Auxotrophies	Strain	Starvation plates			
			SC	SM (0.5)	SM (1)	SM (2)
42	MET,lys	*rps26B* Δ	9.0	9.0	9.5	9.5
			9.5	9.5	10.0	10.0
	MET,lys	*rps26A* Δ	8.0	8.5	5.0	2.0
			7.5	9.0	5.0	2.0
	MET,lys	BY4742	7.0	8.5	8.5	8.0
	met,LYS	BY4741	8.5	8.5	8.0	8.5
43	MET,lys	*rps23B* Δ	7.0	8.5	6.5	/
			7.0	9.5	6.5	/
	MET,lys	*rps23A* Δ	10.0	10.0	8.5	/
			9.0	9.0	8.5	/
	MET,lys	BY4742	8.5	8.5	7.5	/
	met,LYS	BY4741	8.5	8.5	7.5	/
44	MET,lys	*rps30A* Δ	8.5	8.0	4.5	5.0
			8.5	8.0	4.5	5.0
	MET,lys	BY4742	9.5	8.5	8.0	8.0
	met,LYS	BY4741	9.0	9.5	7.5	7.5
45	MET,lys	*rps27B* Δ	4.0	4.0	3.5	2.5
			4.0	4.0	3.5	2.5
	MET,lys	*rps27A* Δ	9.0	9.0	8.5	7.0
			9.0	9.0	8.5	7.0
	MET,lys	BY4742	8.5	8.5	8.0	7.0
	met,LYS	BY4741	9.5	8.5	7.0	6.0
46	met,LYS	*rpl18B* Δ	9.0	9.0	9.5	8.5
			8.0	5.0	4.0	1.0
	MET,lys	*rpl15A* Δ	8.5	9.0	9.5	9.0
			9.5	9.5	9.5	9.0
	MET,lys	BY4742	9.5	9.5	9.5	9.0
	met,LYS	BY4741	9.5	10.0	9.5	9.0
47	MET,lys	*rpl1B* Δ	7.0	10.0	9.0	6.0
			7.0	10.0	9.0	6.0
	MET,lys	*rpl1A* Δ	10.0	10.0	9.0	8.5
			9.5	10.0	9.0	8.5
	MET,lys	BY4742	9.0	10.0	9.0	8.0
	met,LYS	BY4741	9.0	10.0	9.0	8.0
48	MET,lys	*rpl2B* Δ	5.0	9.5	9.5	7.5
			5.0	9.5	9.5	8.0
	MET,lys	*rpl2A* Δ	9.0	9.5	9.5	7.0
			9.0	9.5	9.5	7.0
	MET,lys	BY4742	9.5	9.5	9.5	7.0
	met,LYS	BY4741	9.0	9.0	9.5	6.0

Table 16: Scoring of semi-quantitative growth assays shown in appendix, section A

Test Nr.	Auxotrophies	Strain	Starvation plates			
			SC	SM (0.5)	SM (1)	SM (2)
49	MET,lys	*rpl4B* Δ	9.5	10.0	9.0	8.5
			9.5	9.5	9.0	8.5
	MET,LYS	*rpl4A* Δ	9.5	9.5	8.5	8.0
			9.5	9.5	8.5	8.0
	MET,lys	BY4742	9.0	9.0	8.5	8.0
	met,LYS	BY4741	9.5	9.5	8.0	7.0
50	met,lys	*rpl6B* Δ	8.5	9.0	9.0	7.5
			9.0	9.5	9.5	8.5
	MET,lys	*rpl6A* Δ	8.0	7.0	7.0	0.0
			7.0	7.0	7.0	0.0
	MET,lys	BY4742	10.0	10.0	10.0	9.0
	met,LYS	BY4741	9.5	10.0	10.0	8.5
51	MET,lys	*rpl7B* Δ	8.5	9.5	8.5	8.0
			8.5	10.0	8.5	8.5
	MET,lys	*rpl7A* Δ	5.0	9.5	9.0	9.0
			5.0	10.0	9.0	9.0
	MET,lys	BY4742	9.5	10.0	9.0	8.5
	met,LYS	BY4741	9.0	9.5	8.0	6.0
52	MET,lys	*rpl8B* Δ	9.5	10.0	10.0	8.5
			9.5	9.5	10.0	8.5
	met,lys	*rpl8A* Δ	10.0	10.0	9.5	8.5
			10.0	9.5	9.5	8.5
	MET,lys	BY4742	9.5	9.5	9.5	8.5
	met,LYS	BY4741	9.5	8.5	9.0	8.0
53	MET,lys	*rpl9B* Δ	10.0	10.0	10.0	10.0
			9.5	10.0	10.0	9.5
	MET,lys	*rpl9A* Δ	9.0	10.0	9.5	9.5
			9.0	10.0	10.0	9.0
	MET,lys	BY4742	8.5	10.0	9.5	9.0
	met,LYS	BY4741	9.5	8.0	9.5	8.0
54	MET,LYS	*rpl11B* Δ	9.5	9.5	8.5	9.5
			9.5	9.5	8.5	9.5
	MET,lys	*rpl11A* Δ	6.0	9.5	9.5	10.0
			6.0	9.5	9.0	9.5
	MET,lys	BY4742	10.0	10.0	10.0	10.0
	met,LYS	BY4741	8.0	9.0	7.0	8.0
55	MET,lys	*rpl12B* Δ	5.0	10.0	7.0	9.5
			5.0	9.5	7.0	9.5
	met,lys	*rpl12A* Δ	6.5	10.0	7.0	8.5
			6.5	9.0	7.0	7.5
	MET,lys	BY4742	9.0	10.0	7.5	8.5
	met,LYS	BY4741	8.5	8.5	7.0	7.0

Table 17: Scoring of semi-quantitative growth assays shown in appendix, section A

Test Nr.	Auxotrophies	Strain	Starvation plates			
			SC	SM (0.5)	SM (1)	SM (2)
56	MET,lys	*rpl16B* Δ	9.0	9.5	7.0	8.0
			10.0	10.0	8.0	9.0
	met,lys	*rpl16A* Δ	9.5	9.5	7.0	7.0
			9.5	9.0	7.0	7.0
	MET,lys	BY4742	10.0	10.0	7.5	8.0
	met,LYS	BY4741	9.5	9.5	7.0	7.0
57	met,LYS	*rpl21B* Δ	10.0	10.0	10.0	9.0
			10.0	9.5	10.0	9.0
	MET,lys	*rpl21A* Δ	9.5	5.0	1.5	0.0
			9.5	5.0	1.5	0.0
	MET,lys	BY4742	10.0	10.0	10.0	9.5
	met,LYS	BY4741	9.5	9.0	9.5	8.0
58	MET,lys	*rpl19B* Δ	5.0	9.0	9.0	7.0
			5.0	9.0	9.5	7.0
	MET,LYS	*rpl19A* Δ	6.5	9.5	9.5	7.0
			6.0	9.5	9.0	7.0
	MET,lys	BY4742	8.0	8.5	9.0	7.0
	met,LYS	BY4741	8.0	8.5	8.0	6.5
59	met,lys	*rpl14B* Δ	9.0	9.0	8.5	7.5
			9.0	9.0	9.0	7.5
	MET,lys	*rpl14A* Δ	5.0	7.0	7.5	0.0
			5.0	7.0	7.0	0.0
	MET,lys	BY4742	8.0	9.0	9.0	8.0
	met,LYS	BY4741	8.0	9.0	8.0	7.0

Table 18: Scoring of semi-quantitative growth assays shown in appendix, section A

Test Nr.	Auxotrophies	Strain	Starvation plates			
			SC	SM (0.5)	SM (1)	SM (2)
60	MET,lys	*rpl13B* Δ	5.0	8.0	8.5	6.0
			5.0	8.0	8.5	6.0
	MET,lys	*rpl13A* Δ	7.5	9.5	9.5	8.5
			7.5	9.0	9.5	8.5
	MET,lys	BY4742	8.5	9.0	9.0	8.5
	met,LYS	BY4741	8.5	9.0	9.5	8.0
61	MET,lys	*rpl20B* Δ	9.0	9.0	8.5	8.0
			9.5	9.0	9.0	9.0
	MET,lys	*rpl20A* Δ	9.5	9.5	9.0	9.5
			9.0	9.5	9.5	9.5
	MET,lys	BY4742	9.0	9.0	8.5	8.5
	met,LYS	BY4741	9.5	9.5	8.0	8.0
62	MET,lys	*rpl17B* Δ	8.5	9.5	9.0	9.0
			8.5	9.0	9.5	9.0
	MET,lys	BY4742	8.5	9.0	9.0	8.5
	met,LYS	BY4741	8.5	8.5	9.0	8.5
63	MET,LYS	*rpl40B* Δ	8.5	9.0	9.5	8.5
			9.0	9.0	9.5	8.5
	MET,LYS	*rpl40A* Δ	9.0	9.5	9.0	8.5
			8.0	8.5	8.5	8.0
	MET,lys	BY4742	8.5	9.0	9.0	8.5
	met,LYS	BY4741	8.0	8.0	7.5	6.0
64	MET,lys	*rpl26B* Δ	9.0	9.0	8.5	8.5
			9.5	8.5	8.0	8.0
	MET,lys	*rpl26A* Δ	8.5	8.5	8.0	8.5
			9.0	8.5	8.5	9.0
	MET,lys	BY4742	8.5	8.0	8.0	8.0
	met,LYS	BY4741	9.0	8.0	8.5	7.0

Table 19: Scoring of semi-quantitative growth assays shown in appendix, section A

Test Nr.	Auxotrophies	Strain	Starvation plates			
			SC	SM (0.5)	SM (1)	SM (2)
65	MET,lys	*rpl24B* Δ	9.5	9.5	9.5	9.0
			9.0	9.0	8.5	8.5
	MET,lys	*rpl24A* Δ	8.5	9.5	9.0	9.0
			8.5	9.5	8.5	9.0
	MET,lys	BY4742	8.0	8.5	8.5	7.5
	met,LYS	BY4741	8.5	9.0	7.5	5.0
66	MET,lys	*rpl37B* Δ	8.0	8.5	8.5	8.5
			8.0	8.0	8.0	9.0
	MET,lys	*rpl37A* Δ	8.0	8.0	8.5	9.0
			8.0	8.0	8.5	8.5
	MET,lys	BY4742	8.0	8.0	8.5	8.5
	met,LYS	BY4741	8.0	7.0	7.0	8.0
67	MET,LYS	*rpl34B* Δ	5.0	8.0	8.5	8.0
			6.0	7.5	1.0	0.0
	MET,lys	*rpl34A* Δ	8.5	9.5	8.5	8.0
			8.5	8.5	8.0	8.5
	MET,lys	BY4742	8.0	8.5	8.5	8.0
	met,LYS	BY4741	8.0	8.0	8.0	5.0
68	MET,lys	*rpl35B* Δ	8.5	9.0	8.0	8.5
			9.0	9.5	8.0	9.0
	MET,lys	*rpl35A* Δ	8.5	9.0	4.0	3.0
			8.5	8.5	4.0	3.0
	MET,lys	BY4742	8.0	8.5	8.0	7.5
	met,LYS	BY4741	8.0	8.5	5.0	5.0
69	met,lys	*rpl22B* Δ	7.5	8.5	8.0	7.0
			7.5	8.0	8.0	7.0
	MET,lys	*rpl22A* Δ	5.0	8.0	8.0	9.0
			5.0	8.0	8.0	8.0
	MET,lys	BY4742	8.5	8.5	8.5	8.0
	met,LYS	BY4741	8.5	8.5	8.5	5.0
70	MET,lys	*rpl23B* Δ	8.5	8.5	9.0	8.0
			8.5	8.0	8.5	8.0
	MET,lys	*rpl23A* Δ	8.5	8.0	8.0	8.0
			8.5	8.5	8.0	8.0
	MET,lys	BY4742	8.5	8.5	8.0	8.0
	met,LYS	BY4741	8.5	8.0	7.0	5.0

Table 20: Scoring of semi-quantitative growth assays shown in appendix, section A

Test Nr.	Auxotrophies	Strain	Starvation plates			
			SC	SM (0.5)	SM (1)	SM (2)
	MET,lys	*rpl43A* Δ	5.0	9.0	9.0	7.0
			5.0	8.5	9.0	7.0
	MET,lys	BY4742	8.5	8.5	8.5	7.0
71	met,LYS	BY4741	8.5	8.5	6.0	4.0
	MET,lys	*rpl36B* Δ	5.0	9.0	6.0	6.5
			5.0	8.5	6.0	6.0
	MET,lys	*rpl36A* Δ	9.0	9.5	8.5	8.0
			8.5	9.0	8.5	8.0
	MET,lys	BY4742	8.5	9.0	8.5	8.0
72	met,LYS	BY4741	8.5	8.5	4.0	5.0
	met,lys	*rpl31B* Δ	8.0	9.0	8.0	7.0
			9.5	9.5	9.0	7.0
	?	*rpl31A* Δ	4.0	8.5	9.0	9.5
			4.0	7.0	7.5	8.0
	MET,lys	BY4742	8.5	9.5	8.0	9.0
73	met,LYS	BY4741	9.0	9.0	7.5	8.0
	MET,LYS	*rpl41B* Δ	8.0	7.5	7.0	6.5
			8.0	7.5	7.0	6.5
	MET,LYS	*rpl41A* Δ	8.5	8.0	8.5	8.0
			9.0	9.0	9.0	8.5
	MET,lys	BY4742	9.0	8.0	8.0	7.5
74	met,LYS	BY4741	8.5	8.0	7.5	5.0

Table 21: Scoring of semi-quantitative growth assays shown in appendix, section A

Test Nr.	Auxotrophies	Strain	Starvation plates			
			SC	SM (0.5)	SM (1)	SM (2)
75	MET,LYS	*rpl39* Δ	4.0	6.5	8.0	7.5
			5.0	7.0	8.5	7.0
	MET,lys	*rpl38* Δ	8.0	7.0	8.0	6.0
			9.0	7.5	8.5	7.0
	MET,lys	BY4742	7.5	7.5	8.5	7.0
	met,LYS	BY4741	8.0	7.5	8.0	6.5
76	MET,LYS	*rpl27B* Δ	7.0	7.0	7.5	6.0
			7.5	7.0	8.0	6.5
	met,lys	*rpl27A* Δ	8.0	8.5	8.0	8.0
			8.5	8.5	8.5	8.0
	MET,lys	BY4742	8.0	8.0	7.5	7.0
	met,LYS	BY4741	9.0	8.0	8.0	6.0
78	MET,lys	*rpl29* Δ	7.5	8.5	8.5	7.0
			8.5	8.5	8.5	7.0
	MET,lys	*rpl43B* Δ	8.0	8.5	8.5	8.0
			8.5	8.5	8.5	8.5
	MET,lys	BY4742	8.0	8.5	8.5	8.5
	met,LYS	BY4741	10.0	9.0	9.0	8.0

5.3 Section C

Table 22: Final SM scores of *rps*Δ strains after dividing the numerical scores of each SM plate by that of the control plate and after dividing the ratio of the *rps*Δ strains by that of the WT strain.

Strain	SM (0.5)	SM (1)	SM (2)
rps0A Δ	1.111	1.025	0.942
rps0B Δ	0.994	0.914	0.886
rps1A Δ	1.421	1.500	1.313
rps1B Δ	1.043	1.071	0.938
rps2 Δ	essential		
rps3 Δ	essential		
rps4A Δ	0.971	1.028	1.028
rps4B Δ	1.000	0.941	0.813
rps5 Δ	essential		
rps6A Δ	1.377	1.458	1.250
rps6B Δ	1.318	1.067	1.231
rps7A Δ	1.057	1.090	0.888
rps7B Δ	1.016	1.143	1.184
rps8A Δ	1.000	0.975	0.935
rps8B Δ	1.000	0.944	0.857
rps9A Δ	1.098	0.627	0.762
rps9B Δ	0.941	0.889	1.079
rps10A Δ	reference		
rps10B Δ	not determined		
rps11A Δ	0.994	1.228	1.114
rps11B Δ	1.147	1.083	0.929
rps12 Δ	sick		
rps13 Δ	essential		
rps14A Δ	0.941	0.886	0.878
rps14B Δ	1.028	1.029	1.056
rps15 Δ	essential		
rps16A Δ	1.188	0.947	0.844
rps16B Δ	1.133	0.971	1.133
rps17A Δ	0.875	0.899	0.882
rps17B Δ	0.659	0.778	0.646
rps18A Δ	0.969	1.000	1.000
rps18B Δ	1.010	0.938	0.721
rps19A Δ	0.833	1.324	3.000
rps19B Δ	1.122	1.188	1.077
rps20 Δ	essential		
rps21A Δ	1.023	0.997	0.974
rps21B Δ	1.000	1.000	1.007
rps22A Δ	1.000	0.889	1.000
rps22B Δ	1.056	1.228	1.300
rps23A Δ	1.286	1.052	/
rps23B Δ	1.000	1.017	/
rps24A Δ	1.195	1.290	1.240
rps24B Δ	1.488	1.118	0.708
rps25A Δ	1.047	0.851	0.972
rps25B Δ	1.029	1.029	1.029
rps26A Δ	0.824	0.868	0.922
rps26B Δ	0.932	0.532	0.226
rps27A Δ	1.000	0.930	0.759
rps27B Δ	1.000	1.488	0.944
rps28B Δ	1.143	0.429	0.163
rps29A Δ	0.924	0.946	0.792
rps29B Δ	0.975	0.978	0.950
rps30A Δ	1.052	0.629	0.699
rps30B Δ	essential		
rps31 Δ	essential		

Table 23: Final SM scores of *rpl*Δ strains after dividing the numerical scores of each SM plate by that of the control plate and after dividing the ratio of the *rpl*Δ strains by that of the WT strain.

Strain	SM (0.5)	SM (1)	SM (2)
rpl1B Δ	1.286	1.286	0.964
rpl1A Δ	0.924	0.924	0.981
rpl2B Δ	1.900	1.900	2.104
rpl2A Δ	1.056	1.056	1.056
rpl3 Δ	essential		
rpl4B Δ	1.026	1.003	1.007
rpl4A Δ	1.000	0.947	0.947
rpl5 Δ	essential		
rpl6B Δ	1.004	1.004	1.021
rpl6A Δ	0.938	0.938	0.000
rpl7B Δ	1.090	1.056	1.085
rpl7A Δ	1.853	1.900	2.012
rpl8B Δ	1.026	1.053	1.000
rpl8A Δ	1.090	1.003	1.009
rpl9B Δ	0.872	0.918	0.944
rpl9A Δ	0.944	0.969	0.971
rpl10 Δ	essential		
rpl11B Δ	0.900	1.074	1.059
rpl11A Δ	1.425	1.850	1.721
rpl12B Δ	1.755	1.680	2.012
rpl12A Δ	1.462	1.308	1.495
rpl13B Δ	1.511	1.606	1.200
rpl13A Δ	1.165	1.196	1.133
rpl14B Δ	0.889	0.972	0.952
rpl14A Δ	1.244	1.289	0.000
rpl15A Δ	essential		
rpl15B Δ	1.029	1.059	1.059
rpl16B Δ	1.028	1.052	1.118
rpl16A Δ	0.974	1.000	1.000
rpl17B Δ	1.088	1.088	1.115
rpl18A Δ	essential		
rpl18B Δ	0.772	0.778	0.564
rpl19B Δ	1.694	1.644	1.600
rpl19A Δ	1.433	1.316	1.282
rpl20B Δ	0.974	1.002	0.972
rpl20A Δ	1.028	1.060	1.088

Table 24: Final SM scores of *rpl*Δ strains after dividing the numerical scores of each SM plate by that of the control plate and after dividing the ratio of the *rpl*Δ strains by that of the WT strain.

Strain	SM (0.5)	SM (1)	SM (2)
rpl21B Δ	1.029	1.000	1.069
rpl21A Δ	0.526	0.158	0.000
rpl22B Δ	1.100	1.067	1.587
rpl22A Δ	1.600	1.600	1.806
rpl23B Δ	0.971	1.094	1.000
rpl23A Δ	0.971	1.000	1.000
rpl24B Δ	0.941	0.915	1.009
rpl24A Δ	1.052	0.969	1.129
rpl25 Δ	essential		
rpl26B Δ	1.007	0.949	0.949
rpl26A Δ	1.033	1.002	1.063
rpl27B Δ	0.967	1.140	0.985
rpl27A Δ	1.160	1.125	1.456
rpl28 Δ	essential		
rpl29 Δ	1.004	1.004	0.827
rpl30 Δ	essential		
rpl31B Δ	1.063	1.168	0.907
rpl31A Δ	1.734	2.191	2.066
rpl32 Δ	essential		
rpl33A Δ	essential		
rpl33B Δ	essential		
rpl34B Δ	1.341	0.878	0.800
rpl34A Δ	0.997	0.913	0.971
rpl35B Δ	0.995	0.915	1.067
rpl35A Δ	0.969	0.471	0.376
rpl36B Δ	1.653	1.200	1.328
rpl36A Δ	0.998	0.972	0.972
rpl37B Δ	1.031	0.971	1.029
rpl37A Δ	1.000	1.000	1.029
rpl39 Δ	1.513	1.632	1.754
rpl38 Δ	0.854	0.858	0.818
rpl40B Δ	0.972	1.026	0.972
rpl40A Δ	1.000	0.974	0.972
rpl41B Δ	1.055	0.984	0.975
rpl41A Δ	1.092	1.125	1.131
rpl42 Δ	essential		
rpl43A Δ	1.658	1.906	1.575
rpl43B Δ	0.97058824	0.97058824	0.94117647

5.4 Section D

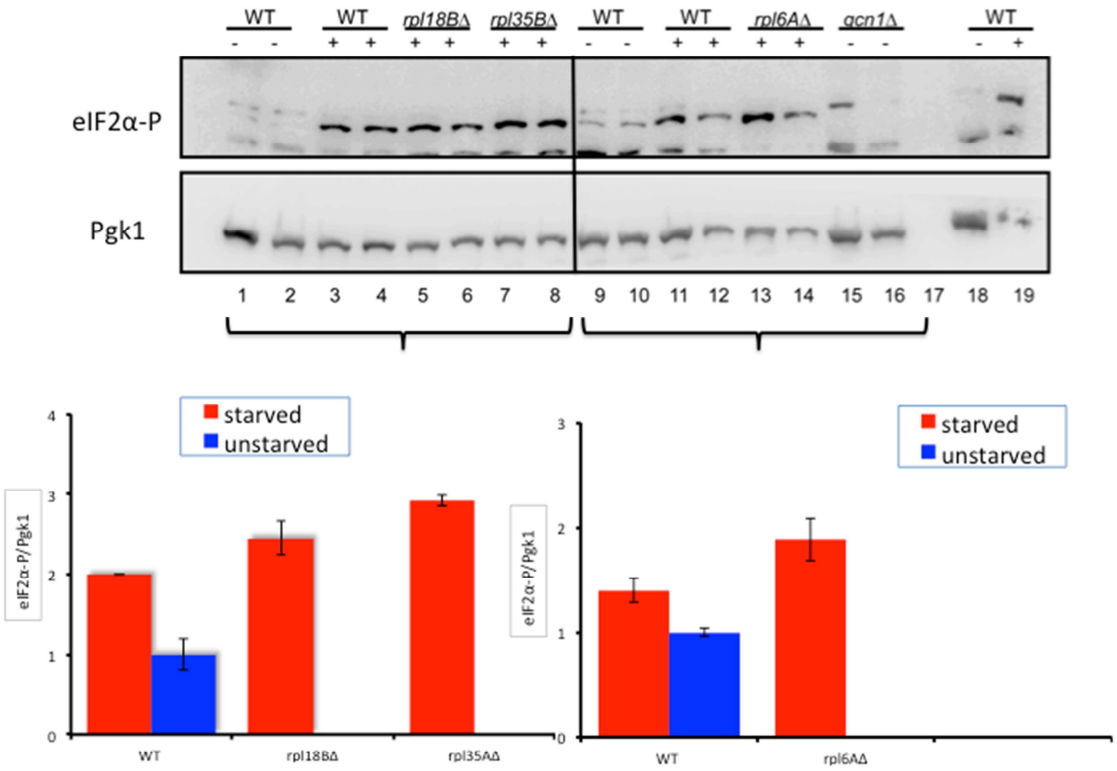

Figure 23: Western blot and analysis of three *rpl*Δ strains that have SM^S but do not have reduction in eIF2α-P level.

The intensity of the eIF2α phosphorylation signal was quantified by densitometry using the Multi Gauge V3.1 software (Fujifilm). eIF2α phosphorylation levels of unstarved (-, blue) samples and amino acid starved (+, red) is shown relative to that of the WT under unstarved conditions. The increase in phosphorylation level of the starved WT sample compared to unstarved WT sample indicates a proper starvation accomplishment. The standard error bars of two independent colonies are indicated.

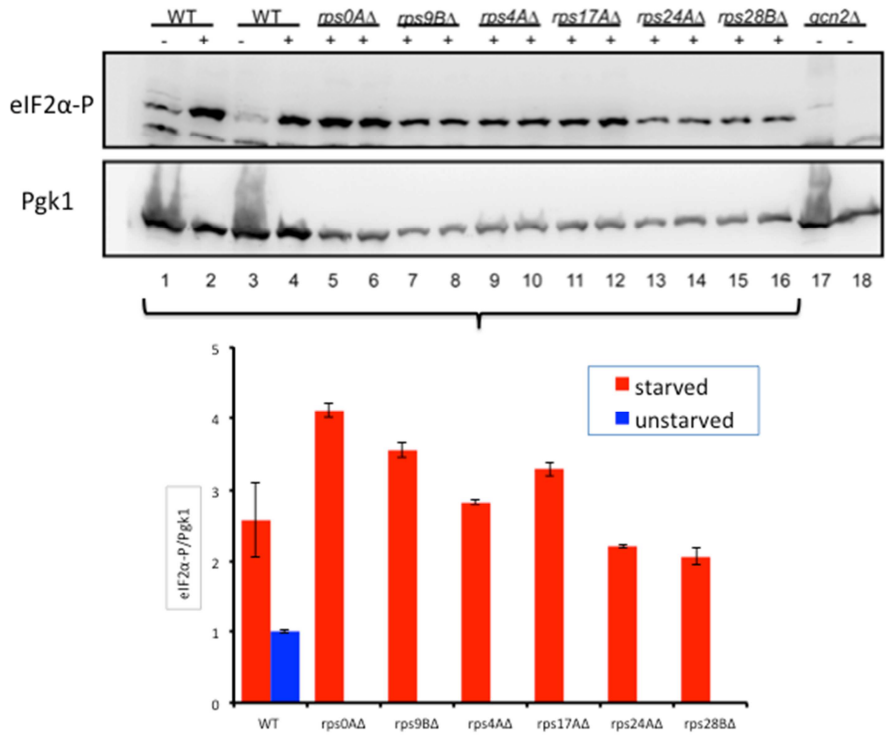

Figure 24: Western blot and analysis of six *rps*Δ strains that have SM^S but do not have reduction in eIF2α-P level with the exception of *rps28B*Δ. This strain might have a slight reduction (chapter3.2,Figure 14).

The intensity of the eIF2α phosphorylation signal was quantified by densitometry using the Multi Gauge V3.1 software (Fujifilm). eIF2α phosphorylation levels of unstarved (-, blue) samples and amino acid starved (+, red) is shown relative to that of the WT under unstarved conditions. The increase in phosphorylation level of the starved WT sample compared to unstarved WT sample indicates a proper starvation accomplishment. The standard error bars of two independent colonies are indicated.

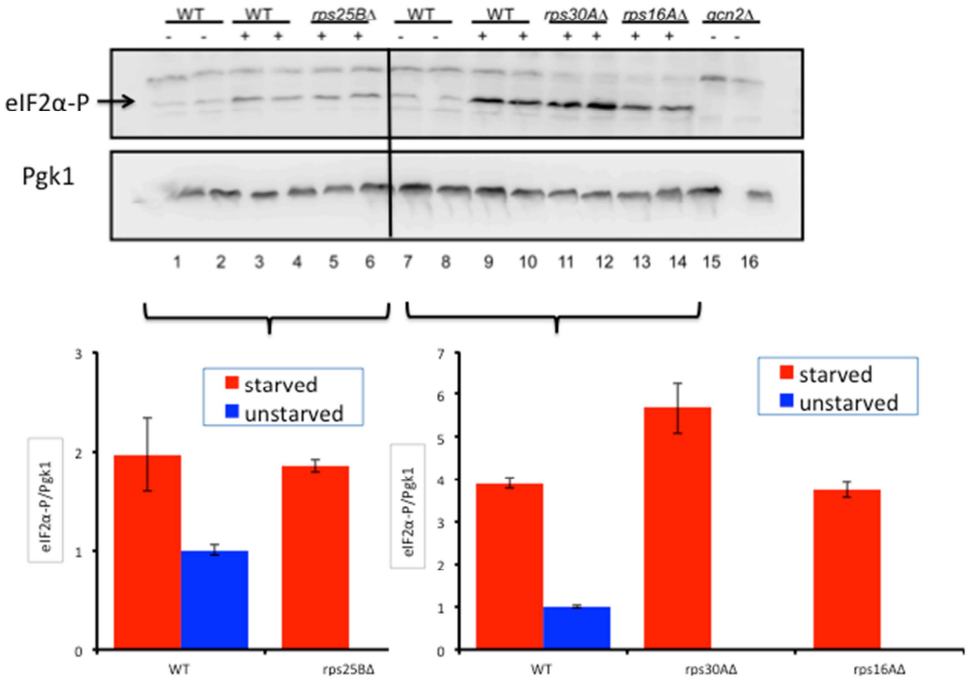

Figure 25: Western blot and analysis of three *rps*Δ strains that have SM^S but do not have reduction in eIF2α-P level.

The intensity of the eIF2α phosphorylation signal was quantified by densitometry using the Multi Gauge V3.1 software (Fujifilm). eIF2α phosphorylation levels of unstarved (-, blue) samples and amino acid starved (+, red) is shown relative to that of the WT under unstarved conditions. The increase in phosphorylation level of the starved WT sample compared to unstarved WT sample indicates a proper starvation accomplishment. The standard error bars of two independent colonies are indicated.

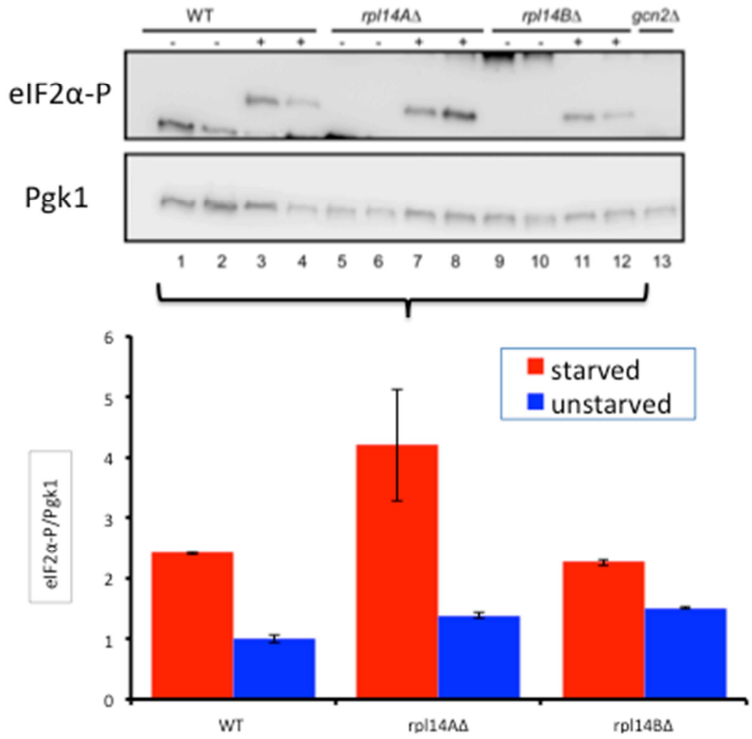

Figure 26: Western blot and analysis of *rps14 A+BΔ* strains that have SM^S but do not have reduction in eIF2α-P level.

The intensity of the eIF2α phosphorylation signal was quantified by densitometry using the Multi Gauge V3.1 software (Fujifilm). eIF2α phosphorylation levels of unstarved (-, blue) samples and amino acid starved (+, red) is shown relative to that of the WT under unstarved conditions. The increase in phosphorylation level of the starved WT sample compared to unstarved WT sample indicates a proper starvation accomplishment. The standard error bars of two independent colonies are indicated.

6. Reference

Abastado, J. P., Miller, P. F., Jackson, B. M., & Hinnebusch, A. G. (1991). Suppression of ribosomal reinitiation at upstream open reading frames in amino acid-starved cells forms the basis for GCN4 translational control. *Mol Cell Biol, 11*(1), 486-496.

Agirrezabala, X., Ferna´ndez, I. S., Kelley, A. C., Carto´n, D. G., Ramakrishnan, V., & Valle, M. (2013). The ribosome triggers the stringent response by RelA via a highly distorted tRNA. *EMBO reports, 14*, 811–816. doi: 10.1038

Almeida, B., Ohlmeier, S., Almeida, A. J., Madeo, F., Leão, C., Rodrigues, F., & Ludovico, P. (2009). Yeast protein expression profile during acetic acid-induced apoptosis indicates causal involvement of the TOR pathway. *Proteomics, 9*(3), 720-732.

Andersen, C. B., Becker, T., Blau, M., Anand, M., Halic, M., Balar, B., . . . Beckmann, R. (2006). Structure of eEF3 and the mechanism of transfer RNA release from the E-site. *Nature, 443*(7112), 663-668. doi: 10.1038/nature05126

Andrade, M. A., & Bork, P. (1995). HEAT repeats in the Huntington's disease protein. *Nature genetics, 11*(2), 115-116.

Armache, J.-P., Jarasch, A., Anger, A. M., Villa, E., Becker, T., Bhushan, S., . . . Franckenberg, S. (2010). Localization of eukaryote-specific ribosomal proteins in a 5.5-Å cryo-EM map of the 80S eukaryotic ribosome. *Proceedings of the National Academy of Sciences, 107*(46), 19754-19759.

Becker, T. (2005). *Strukturn von eF3 und Sc61 als aktive ribosomale Liganden.* (doctor rerum naturalium), Humboldt-Universitaet, Berlin.

Ben-Shem, A., Garreau de Loubresse, N., Melnikov, S., Jenner, L., Yusupova, G., & Yusupov, M. (2011). The structure of the eukaryotic ribosome at 3.0 A resolution. *Science, 334*(6062), 1524-1529. doi: 10.1126/science.1212642

Berlanga, J. J., Santoyo, J., & de Haro, C. (1999). Characterization of a mammalian homolog of the GCN2 eukaryotic initiation factor 2 alpha kinase. *European Journal of Biochemistry, 265*(2), 754-762. doi: 10.1046/j.1432-1327.1999.00780.x

Berlanga, J. J., Ventoso, I., Harding, H. P., Deng, J., Ron, D., Sonenberg, N., . . . de Haro, C. (2006). Antiviral effect of the mammalian translation initiation factor 2 alpha kinase GCN2 against RNA viruses. *Embo Journal, 25*(8), 1730-1740. doi: 10.1038/sj.emboj.7601073

Costa-Mattioli, M., Gobert, D., Harding, H., Herdy, B., Azzi, M., Bruno, M., . . . Sonenberg, N. (2005). Translational control of hippocampal synaptic plasticity and memory by the eIF2 alpha kinase GCN2. *Nature, 436*(7054), 1166-1170. doi: 10.1038/nature03897

Costa-Mattioli, M., Gobert, D., Stern, E., Gamache, K., Colina, R., Cuello, C., . . . Sonenberg, N. (2007). eIF2 alpha phosphorylation bidirectionally regulates the switch from short- to long-term synaptic plasticity and memory. *Cell, 129*(1), 195-206. doi: 10.1016/j.cell.2007.01.050

Cridge, A. G., Visweswaraiah, J., Ramesh, R., & Sattlegger, E. (2014). Semi-quantitative colony immunoassay for determining and optimizing protein expression in Saccharomyces cerevisiae and Escherichia coli. *Anal Biochem, 447*, 82-89. doi: 10.1016/j.ab.2013.10.020

de Aldana, C. V., Marton, M., & Hinnebusch, A. (1995). GCN20, a novel ATP binding cassette protein, and GCN1 reside in a complex that mediates activation of the eIF-2 alpha kinase GCN2 in amino acid-starved cells. *The EMBO journal, 14*(13), 3184.

De Haro, C., Mendez, R., & Santoyo, J. (1996). The eIF-2alpha kinases and the control of protein synthesis. *The FASEB journal, 10*(12), 1378-1387.

Delforge, J., Messenguy, F., & Wiame, J. M. (1975). Regulation of Arginine-Biosynthesis in Saccharomyces-Cerevisiae - Specificity of Argr- Mutations and General Control of Amino-Acid Biosynthesis. *European Journal of Biochemistry, 57*(1), 231-239. doi: 10.1111/j.1432-1033.1975.tb02295.x

Deng, J., Harding, H. P., Raught, B., Gingras, A. C., Berlanga, J. J., Scheuner, D., . . . Sonenberg, N. (2002). Activation of GCN2 in UV-irradiated cells inhibits translation. *Current Biology, 12*(15), 1279-1286. doi: 10.1016/S0960-9822(02)01037-0

Dever, T. E., Feng, L., Wek, R. C., Cigan, A. M., Donahue, T. F., & Hinnebusch, A. G. (1992). Phosphorylation of Initiation Factor-2-Alpha by Protein-Kinase Gcn2 Mediates Gene-Specific Translational Control of Gcn4 in Yeast. *Cell, 68*(3), 585-596.

Dong, J. S., Qiu, H. F., Garcia-Barrio, M., Anderson, J., & Hinnebusch, A. G. (2000). Uncharged tRNA activates GCN2 by displacing the protein kinase moiety from a bipartite tRNA-Binding domain. *Molecular Cell, 6*(2), 269-279.

English, B. P., Hauryliuk, V., Sanamrad, A., Tankov, S., Dekker, N. H., & Elf, J. (2011). Single-molecule investigations of the stringent response machinery in living bacterial cells. *Proc Natl Acad Sci U S A, 108*(31), E365-373. doi: 10.1073/pnas.1102255108

Filipovska, A., & Rackham, O. (2013). Specialization from synthesis: How ribosome diversity can customize protein function. *FEBS Letters, 587*(8), 1189-1197. doi: http://dx.doi.org/10.1016/j.febslet.2013.02.032

Galkin, O., Bentley, A. A., Gupta, S., Compton, B. A., Mazumder, B., Kinzy, T. G., . . . Komar, A. A. (2007). Roles of the negatively charged N-terminal extension of Saccharomyces cerevisiae ribosomal protein S5 revealed by characterization of a yeast strain containing human ribosomal protein S5. *RNA, 13*(12), 2116-2128. doi: 10.1261/rna.688207

Garcia-Barrio, M., Dong, J. S., Ufano, S., & Hinnebusch, A. G. (2000). Association of GCN1-GCN20 regulatory complex with the N-terminus of eIF2 alpha kinase GCN2 is required for GCN2 activation. *Embo Journal, 19*(8), 1887-1899.

Gavin, A. C., Aloy, P., Grandi, P., Krause, R., Boesche, M., Marzioch, M., . . . Superti-Furga, G. (2006). Proteome survey reveals modularity of the yeast cell machinery. *Nature, 440*(7084), 631-636. doi: 10.1038/nature04532

Ghaemmaghami, S., Huh, W.-K., Bower, K., Howson, R. W., Belle, A., Dephoure, N., . . . Weissman, J. S. (2003). Global analysis of protein expression in yeast. *Nature, 425*(6959), 737-741.

Goldman, E., & Jakubowski, H. (1990). Uncharged tRNA, protein synthesis, and the bacterial stringent response. *Molecular Microbiology, 4*(12), 2035-2040. doi: 10.1111/j.1365-2958.1990.tb00563.x

Grallert, B., & Boye, E. (2007). The Gcn2 kinase as a cell cycle regulator. *CELL CYCLE-LANDES BIOSCIENCE-, 6*(22), 2768.

Hinnebusch, A. G. (2005). Translational regulation of GCN4 and the general amino acid control of yeast. *Annual Review of Microbiology, 59*, 407-450. doi: 10.1146/annurev.micro.59.031805.133833

Hinnebusch, A. G., & Natarajan, K. (2002). Gcn4p, a master regulator of gene expression, is controlled at multiple levels by diverse signals of starvation and stress. *Eukaryotic Cell, 1*(1), 22-32. doi: 10.1128/Ec.1.1.22-32.2002

Horiguchi, G., Van Lijsebettens, M., Candela, H., Micol, J. L., & Tsukaya, H. (2012). Ribosomes and translation in plant developmental control. *Plant Science, 191*, 24-34.

Juan-Vidales, F., Sanchez Madrid, F., Saenz-Robles, M. T., & Ballesta, J. P. (1983). Purification and characterization of two ribosomal proteins of Saccharomyces cerevisiae.

Homologies with proteins from eukaryotic species and with bacterial protein EC L11. *Eur J Biochem, 136*(2), 275-281.

Kerr, I. D. (2004). Sequence analysis of twin ATP binding cassette proteins involved in translational control, antibiotic resistance, and ribonuclease L inhibition. *Biochem Biophys Res Commun, 315*(1), 166-173. doi: 10.1016/j.bbrc.2004.01.044

Kiel, M. C., Aoki, H., & Ganoza, M. C. (1999). Identification of a ribosomal ATPase in Escherichia coli cells. *Biochimie, 81*(12), 1097-1108.

Kim, T.-Y., Ha, C. W., & Huh, W.-K. (2009). Differential subcellular localization of ribosomal protein L7 paralogs in Saccharomyces cerevisiae. *Molecules and cells, 27*(5), 539-546.

Knutsson Jenvert, R.-M., & Holmberg Schiavone, L. (2005). Characterization of the tRNA and ribosome-dependent pppGpp-synthesis by recombinant stringent factor from Escherichia coli. *FEBS Journal, 272*(3), 685-695. doi: 10.1111/j.1742-4658.2004.04502.x

Komili, S., Farny, N. G., Roth, F. P., & Silver, P. A. (2007). Functional specificity among ribosomal proteins regulates gene expression. *Cell, 131*(3), 557-571.

Kressler, D., Hurt, E., & Bassler, J. (2010). Driving ribosome assembly. *Biochimica Et Biophysica Acta-Molecular Cell Research, 1803*(6), 673-683. doi: 10.1016/j.bbamcr.2009.10.009

LaRossa, R. A., & Schloss, J. V. (1984). The sulfonylurea herbicide sulfometuron methyl is an extremely potent and selective inhibitor of acetolactate synthase in Salmonella typhimurium. *J Biol Chem, 259*(14), 8753-8757.

Lindström, M. S. (2009). Emerging functions of ribosomal proteins in gene-specific transcription and translation. *Biochemical and biophysical research communications, 379*(2), 167-170.

Malygin, A. A., & Karpova, G. G. (2010). Site-specific cleavage of the 40S ribosomal subunit reveals eukaryote-specific ribosomal protein S28 in the subunit head. *FEBS Lett, 584*(21), 4396-4400. doi: 10.1016/j.febslet.2010.10.013

Martin-Marcos, P., Hinnebusch, A. G., & Tamame, M. (2007). Ribosomal protein L33 is required for ribosome biogenesis, subunit joining, and repression of GCN4 translation. *Molecular and Cellular Biology, 27*(17), 5968-5985. doi: 10.1128/Mcb.00019-07

Marton, M., Crouch, D., & Hinnebusch, A. (1993). GCN1, a translational activator of GCN4 in Saccharomyces cerevisiae, is required for phosphorylation of eukaryotic translation initiation factor 2 by protein kinase GCN2. *Molecular and cellular biology, 13*(6), 3541-3556.

Marton, M. J., de Aldana, C. V., Qiu, H., Chakraburtty, K., & Hinnebusch, A. G. (1997). Evidence that GCN1 and GCN20, translational regulators of GCN4, function on elongating ribosomes in activation of eIF2alpha kinase GCN2. *Molecular and cellular biology, 17*(8), 4474-4489.

Munn, D. H., Sharma, M. D., Baban, B., Harding, H. P., Zhang, Y., Ron, D., & Mellor, A. L. (2005). GCN2 kinase in T cells mediates proliferative arrest and anergy induction in response to indoleamine 2, 3-dioxygenase. *Immunity, 22*(5), 633-642.

Murchie, M.-J., & Leader, D. P. (1978). Codon-specific interaction of uncharged transfer-RNA with eukaryotic ribosomes. *Biochimica et Biophysica Acta (BBA) - Nucleic Acids and Protein Synthesis, 520*(1), 233-236. doi: http://dx.doi.org/10.1016/0005-2787(78)90024-2

Pavitt, G. D., Ramaiah, K. V. A., Kimball, S. R., & Hinnebusch, A. G. (1998). eIF2 independently binds two distinct eIF2B subcomplexes that catalyze and regulate guanine-nucleotide exchange. *Genes & Development, 12*(4), 514-526.

Planta, R. J., & Mager, W. H. (1998). The list of cytoplasmic ribosomal proteins of Saccharomyces cerevisiae. *Yeast, 14*(5), 471-477.

Pnueli, L., & Arava, Y. (2007). Genome-wide polysomal analysis of a yeast strain with mutated ribosomal protein S9. *BMC genomics, 8*(1), 285.

Ramirez, M., Wek, R. C., & Hinnebusch, A. G. (1991). Ribosome Association of Gcn2 Protein-Kinase, a Translational Activator of the Gcn4 Gene of Saccharomyces-Cerevisiae. *Molecular and Cellular Biology, 11*(6), 3027-3036.

Ramsdale, M., Selway, L., Stead, D., Walker, J., Yin, Z., Nicholls, S. M., . . . Brown, A. J. (2008). MNL1 Regulates Weak Acid–induced Stress Responses of the Fungal Pathogen Candida albicans. *Molecular biology of the cell, 19*(10), 4393-4403.

Ruggero, D., & Pandolfi, P. P. (2003). Does the ribosome translate cancer? *Nature Reviews Cancer, 3*(3), 179-192.

Sattlegger, E., & Hinnebusch, A. G. (2000). Separate domains in GCN1 for binding protein kinase GCN2 and ribosomes are required for GCN2 activation in amino acid-starved cells. *Embo Journal, 19*(23), 6622-6633. doi: 10.1093/emboj/19.23.6622

Sattlegger, E., & Hinnebusch, A. G. (2005). Polyribosome binding by GCN1 is required for full activation of eukaryotic translation initiation factor 2 alpha kinase GCN2 during amino acid starvation. *Journal of Biological Chemistry, 280*(16), 16514-16521. doi: 10.1074/jbc.M414566200

Shenoy, N., Kessel, R., Bhagat, T. D., Bhattacharyya, S., Yu, Y., McMahon, C., & Verma, A. (2012). Alterations in the ribosomal machinery in cancer and hematologic disorders. *J Hematol Oncol, 5*, 32. doi: 10.1186/1756-8722-5-32

Shi, Y. G., Vattem, K. M., Sood, R., An, J., Liang, J. D., Stramm, L., & Wek, R. C. (1998). Identification and characterization of pancreatic eukaryotic initiation factor 2 alpha-subunit kinase, PEK, involved in translational control. *Molecular and Cellular Biology, 18*(12), 7499-7509.

Spahn, C. M., Beckmann, R., Eswar, N., Penczek, P. A., Sali, A., Blobel, G., & Frank, J. (2001). Structure of the 80S ribosome from Saccharomyces cerevisiae--tRNA-ribosome and subunit-subunit interactions. *Cell, 107*(3), 373-386.

Steffen, K. K., MacKay, V. L., Kerr, E. O., Tsuchiya, M., Hu, D., Fox, L. A., . . . Kaeberlein, M. (2008). Yeast life span extension by depletion of 60s ribosomal subunits is mediated by Gcn4. *Cell, 133*(2), 292-302. doi: 10.1016/j.cell.2008.02.037

Steffen, K. K., McCormick, M. A., Pham, K. M., MacKay, V. L., Delaney, J. R., Murakami, C. J., . . . Kennedy, B. K. (2012). Ribosome deficiency protects against ER stress in Saccharomyces cerevisiae. *Genetics, 191*(1), 107-118.

Trianaalonso, F. J., Chakraburtty, K., & Nierhaus, K. H. (1995). The Elongation- Factor- 3 unique in higher fungi and essential for protein- biosynthesis is an E-site factor *Journal of Biological Chemistry, 270*(35), 20473-20478.

Tzamarias, D., Roussou, I., & Thireos, G. (1989). Coupling of GCN4 messenger-RNA translational activation with decreased rates of polypeptide-chain initiation *Cell, 57*(6), 947-954. doi: 10.1016/0092-8674(89)90333-4

Tzamarias, D., & Thireos, G. (1988). Evidence that the GCN2 protein kinase regulates reinitiation by yeast ribosomes. *The EMBO journal, 7*(11), 3547.

Visweswaraiah, J., Lee, S. J., Hinnebusch, A. G., & Sattlegger, E. (2012). Overexpression of Eukaryotic Translation Elongation Factor 3 Impairs Gcn2 Protein Activation. *Journal of Biological Chemistry, 287*(45). doi: 10.1074/jbc.M112.368266

Wek, R. C., Ramirez, M., Jackson, B. M., & Hinnebusch, A. G. (1990). Identification of Positive-Acting Domains in Gcn2 Protein-Kinase Required for Translational Activation of Gcn4 Expression. *Molecular and Cellular Biology, 10*(6), 2820-2831.

Wek, S. A., Zhu, S., & Wek, R. C. (1995). The histidyl-tRNA synthetase-related sequence in the eIF-2 alpha protein kinase GCN2 interacts with tRNA and is required for activation in response to starvation for different amino acids. *Molecular and cellular biology, 15*(8), 4497-4506.

Wendrich, T. M., Blaha, G., Wilson, D. N., Marahiel, M. A., & Nierhaus, K. H. (2002). Dissection of the mechanism for the stringent factor RelA. *Mol Cell, 10*(4), 779-788.

Wilson, D. N., & Cate, J. H. D. (2012). The structure and function of the eukaryotic ribosome. *Cold Spring Harbor Perspectives in Biology, 4*(5).

Wolfe, K. H., & Shields, D. C. (1997). Molecular evidence for an ancient duplication of the entire yeast genome. *Nature, 387*(6634), 708-713. doi: 10.1038/42711

Ye, J., Kumanova, M., Hart, L. S., Sloane, K., Zhang, H., De Panis, D. N., . . . Koumenis, C. (2010). The GCN2-ATF4 pathway is critical for tumour cell survival and proliferation in response to nutrient deprivation. *The EMBO journal, 29*(12), 2082-2096.

Zimmermann, R. A. (2003). The double life of ribosomal proteins. *Cell, 115*(2), 130-132.